HAZARD MAPPING OF THE PHILIPPINES USING LIDAR (PHIL-LIDAR 1)

LiDAR Surveys and Flood Mapping of Sulat River

University of the Philippines Training Center
for Applied Geodesy and Photogrammetry
Visayas State University

APRIL 2017

Published by the UP Training Center for Applied Geodesy and Photogrammetry (TCAGP)
College of Engineering
University of the Philippines – Diliman
Quezon City
1101 PHILIPPINES

This research project is supported by the Department of Science and Technology (DOST) as part of its Grants-in-Aid Program and is to be cited as:

E.C. Paringit, and F. Morales Jr. (Eds.). (2017), LiDAR Surveys and Flood Mapping of Sulat River. Quezon City: University of the Philippines Training Center for Applied Geodesy and Photogrammetry – 117pp

For questions/queries regarding this report, contact:

Engr. Florentino Morales, Jr.
Project Leader, PHIL-LiDAR 1 Program
Visayas State University
Baybay, Leyte, Philippines 6521
E-mail: ffmorales_jr@yahoo.com

Enrico C. Paringit, Dr. Eng.
Program Leader, DREAM Program
University of the Philippines Diliman
Quezon City, Philippines 1101
E-mail: ecparingit@up.edu.ph

National Library of the Philippines
ISBN: 978-621-430-217-8

TABLE OF CONTENTS

LIST OF TABLES

LIST OF FIGURES

LIST OF ACRONYMS AND ABBREVIATIONS

AAC	Asian Aerospace Corporation
Ab	abutment
ALTM	Airborne LiDAR Terrain Mapper
ARG	automatic rain gauge
AWLS	Automated Water Level Sensor
BA	Bridge Approach
BM	benchmark
CAD	Computer-Aided Design
CN	Curve Number
CSRS	Chief Science Research Specialist
DAC	Data Acquisition Component
DEM	Digital Elevation Model
DENR	Department of Environment and Natural Resources
DOST	Department of Science and Technology
DPPC	Data Pre-Processing Component
DREAM	Disaster Risk and Exposure Assessment for Mitigation [Program]
DRRM	Disaster Risk Reduction and Management
DSM	Digital Surface Model
DTM	Digital Terrain Model
DVBC	Data Validation and Bathymetry Component
FMC	Flood Modeling Component
FOV	Field of View
GiA	Grants-in-Aid
GCP	Ground Control Point
GNSS	Global Navigation Satellite System
GPS	Global Positioning System
HEC-HMS	Hydrologic Engineering Center - Hydrologic Modeling System
HEC-RAS	Hydrologic Engineering Center - River Analysis System
HC	High Chord
IDW	Inverse Distance Weighted [interpolation method]
IMU	Inertial Measurement Unit
kts	knots
LAS	LiDAR Data Exchange File format
LC	Low Chord
LGU	local government unit
LiDAR	Light Detection and Ranging
LMS	LiDAR Mapping Suite
m AGL	meters Above Ground Level
MMS	Mobile Mapping Suite
MSL	mean sea level
NAMRIA	National Mapping and Resource Information Authority
NSTC	Northern Subtropical Convergence
PAF	Philippine Air Force
PAGASA	Philippine Atmospheric Geophysical and Astronomical Services Administration
PDOP	Positional Dilution of Precision
PPK	Post-Processed Kinematic [technique]
PRF	Pulse Repetition Frequency
PTM	Philippine Transverse Mercator
QC	Quality Check
QT	Quick Terrain [Modeler]
RA	Research Associate
RIDF	Rainfall-Intensity-Duration-Frequency
RMSE	Root Mean Square Error
SAR	Synthetic Aperture Radar
SCS	Soil Conservation Service
SRTM	Shuttle Radar Topography Mission
SRS	Science Research Specialist
SSG	Special Service Group
TBC	Thermal Barrier Coatings
UP-TCAGP	University of the Philippines – Training Center for Applied Geodesy and Photogrammetry
UTM	Universal Transverse Mercator
VSU	Visayas State University
WGS	World Geodetic System

CHAPTER 1: OVERVIEW OF THE PROGRAM AND SULAT RIVER

Engr. Florentino Morales Jr. and Enrico C. Paringit, Dr. Eng.

1.1 Background of the Phil-LIDAR 1 Program

The University of the Philippines Training Center for Applied Geodesy and Photogrammetry (UP-TCAGP) launched a research program entitled "Nationwide Hazard Mapping using LiDAR in 2014" or Phil-LiDAR 1, supported by the Department of Science and Technology (DOST) Grants-in-Aid (GiA) Program. The program was primarily aimed at acquiring a national elevation and resource dataset at sufficient resolution to produce information necessary to support the different phases of disaster management. Particularly, it targeted to operationalize the development of flood hazard models that would produce updated and detailed flood hazard maps for the major river systems in the country.

Also, the program was aimed at producing an up-to-date and detailed national elevation dataset suitable for 1:5,000 scale mapping, with 50 cm and 20 cm horizontal and vertical accuracies, respectively. These accuracies were achieved through the use of the state-of-the-art Light Detection and Ranging (LiDAR) airborne technology procured by the project through DOST. The methods applied in this report are thoroughly described in a separate publication entitled "FLOOD MAPPING OF RIVERS IN THE PHILIPPINES USING AIRBORNE LIDAR: METHODS (Paringit, et. al. 2017) available separately.

The implementing partner university for the Phil-LiDAR 1 Program is the Visayas State University (VSU). VSU is in charge of processing LiDAR data and conducting data validation reconnaissance, cross section, bathymetric survey, validation, river flow measurements, flood height and extent data gathering, flood modeling, and flood map generation for the 28 river basins in the Easter Visayas Region. The university is located in Baybay City in the province of Leyte.

1.2 Overview of the Sulat River Basin

Sulat River Basin covers the municipalities of Sulat, San Julian and small portions of Hinabangan and Taft in the province of Eastern Samar. The DENR River Basin Control Office identified the basin to have a drainage area of 129 km^2 and an estimated 245 million cubic meter (MCM) annual run-off (RBCO, 2015).

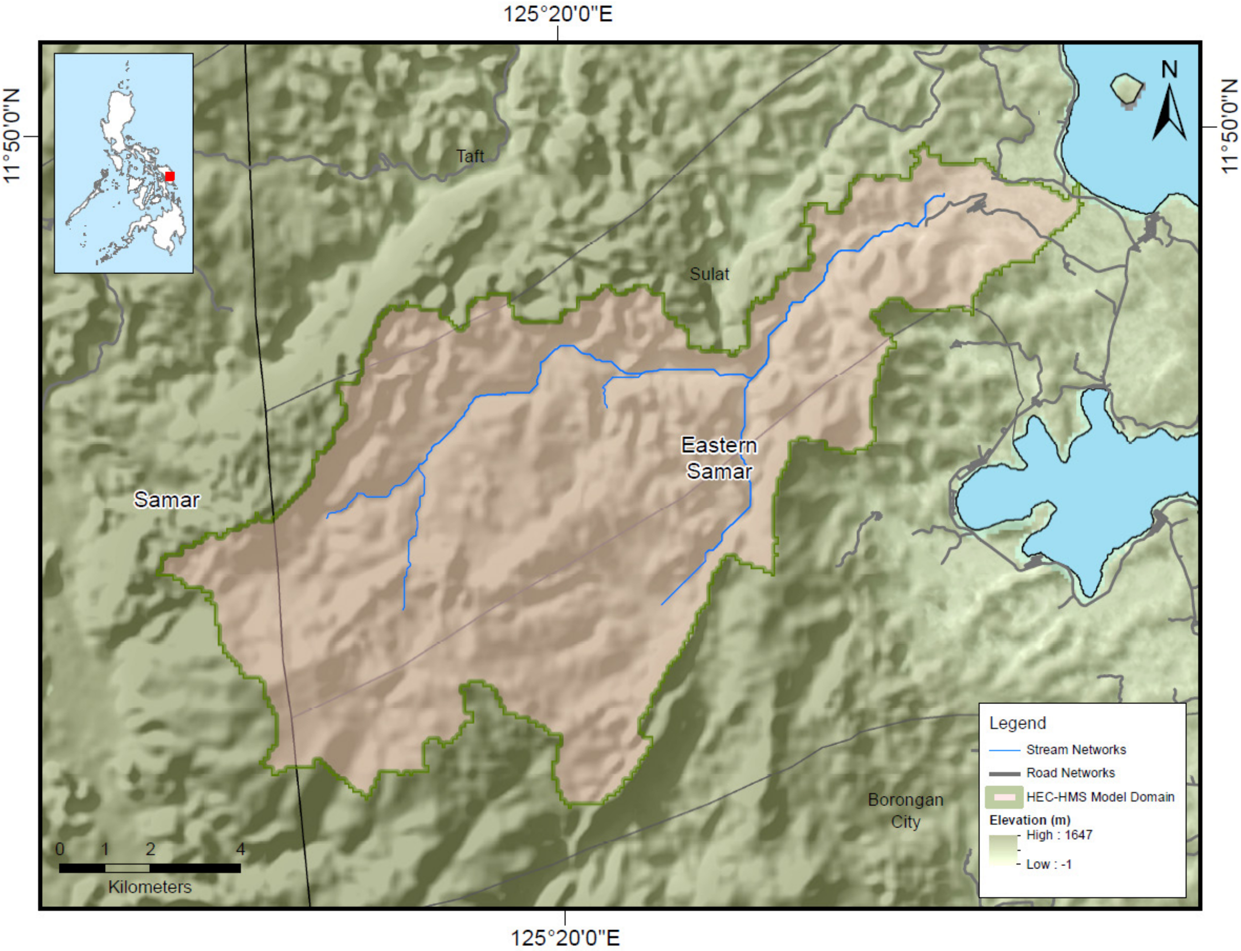

Figure 1. Map of Sulat River Basin (in brown).

Its main stem, Sulat River, is part of the 19 river systems in the Eastern Visayas Region. According to the 2015 national census of NSO, a total of 5,343 persons are residing within the immediate vicinity of the river which is distributed among seven (7) barangays from the municipality of Sulat, Eastern Samar (NSO, 2015). The primary source of revenue of Eastern Samar is fishery and agriculture which includes production of coconut, copra, corn, rice, sugar and vegetables. There is also a big tourism potential in the province centered in Guiauan, Calicoan and Homonhon Islands. (http://philgis.org/province-page/eastern-samar, 2017). On December 06, 2014, Typhoon Ruby, internationally known as *Hagupit*, made landfall in Eastern Samar. The aftermath of the typhoon caused massive destruction in the province with 8 casualties. In the municipality of Sulat, a total of 18 barangays with 4,214 families were directly affected by the typhoon. (http://ndrrmc.gov.ph/attachments/article/1356/FINAL_REPORT_re_Effects_of_Typhoon_RUBY_(HAGUPIT)_04_-_10DEC2014.pdf, 2017).

CHAPTER 2: LIDAR DATA ACQUISITION OF THE SULAT FLOODPLAIN

Engr. Louie P. Balicanta, Engr. Christopher Cruz, Lovely Gracia Acuña, Engr. Gerome Hipolito, Engr. Christopher L. Joaquin, Ms. Mary Catherine Elizabeth M. Baliguas

The methods applied in this chapter were based on the DREAM methods manual (Ang, et. al., 2014) and further enhanced and updated in Paringit, et. al. (2017).

2.1 Flight Plans

To initiate the LiDAR acquisition survey of the Sulat floodplain, the Data Acquisition Component (DAC) created flight plans within the delineated priority area for Sulat Floodplain in Eastern Samar. These flight missions were planned for 17 lines and ran for at most four and a half hours (4.5) including take-off, landing and turning time. The flight planning parameters for the LiDAR system are outlined in Table 1. Figure 2 shows the flight plan for Sulat floodplain survey.

Table 1. Flight planning parameters for the Aquarius LiDAR system.

Block Name	Flying Height (m AGL)	Overlap (%)	Field of View (θ)	Pulse Repetition Frequency (PRF) (KHz)	Scan Frequency (Hz)	Average Speed (kts)	Average Turn Time (Minutes)
BLK33J	500	20	44	50	45	120	5

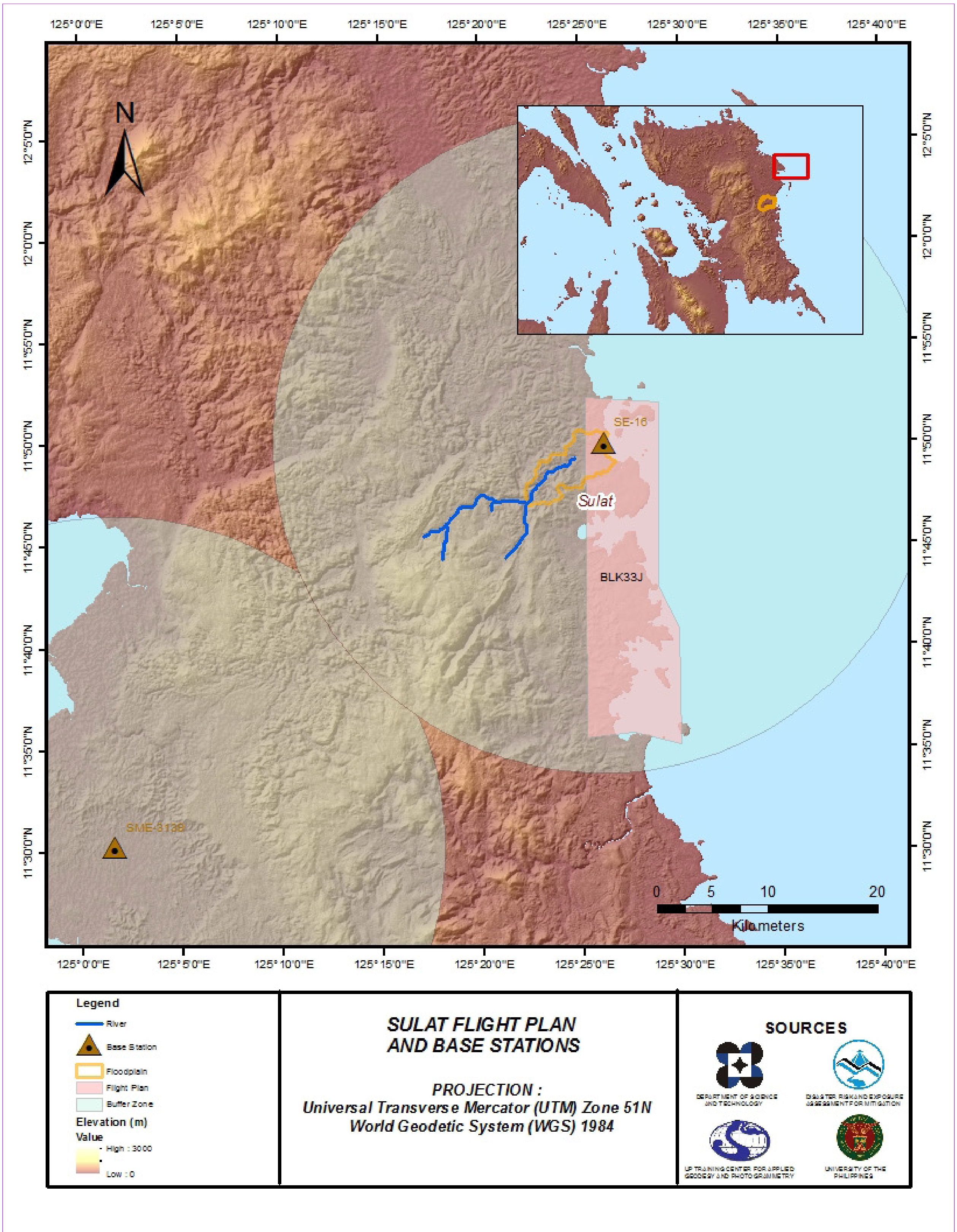

Figure 2. Flight plans and base stations used for Sulat floodplain using Aquarius LiDAR system.

2.2 Ground Base Stations

The project team was able to recover one (1) NAMRIA horizontal ground control point: SME-3139 which is of fourth (4th) order accuracy. One (1) NAMRIA benchmark was recovered, SE-16, which was used as vertical reference point and was also established as ground control point.

The certifications for the base stations are found in ANNEX 2 while the baseline processing reports for the established control points are found in ANNEX 3. These were used as base stations during flight operations for the entire duration of the survey on June 9, 2014. Base stations were observed using dual frequency GPS receivers, TRIMBLE SPS 852 and SPS 985. Flight plans and location of base stations used during the aerial LiDAR acquisition in Sulat floodplain are shown in Figure 2.

The succeeding sections depict the sets of reference points, control stations and established points, and the ground control points for the entire Sulat Floodplain LiDAR Survey. Figure 3 to Figure 4 show the recovered NAMRIA reference points within the area of the floodplain, while Table 2 to Table 3 show the details about the following NAMRIA control stations and established points. Table 4, on the other hand, shows the list of all ground control points occupied during the acquisition together with the corresponding dates of utilization.

Figure 3. GPS set-up over SME-3139 located along the highway in Brgy. Sto. Nino, Sulat, Eastern Samar (a) and NAMRIA reference point SME-3139 (b) as recovered by the field team.

Table 2. Details of the recovered NAMRIA horizontal control point SME-3139 used as base station for the LiDAR acquisition.

Station Name	SME-3139	
Order of Accuracy	4th Order	
Relative Error (horizontal positioning)	1:10,000	
Geographic Coordinates, Philippine Reference of 1992 Datum (PRS 92)	Latitude Longitude Ellipsoidal Height	11° 30’ 17.85657” North 125° 1’ 29.837339” East 26.13400 meters
Grid Coordinates, Philippine Transverse Mercator Zone 5 (PTM Zone 5 PRS 92)	Easting Northing	502722.403 meters 1272180.079 meters
Geographic Coordinates, World Geodetic System 1984 Datum (WGS 84)	Latitude Longitude Ellipsoidal Height	11° 30’ 13.52495” North 125° 1’ 34.96980” East 87.78700 meters
Grid Coordinates, Universal Transverse Mercator Zone 51 North (UTM 51N PRS1992)	Easting Northing	720874.14 meters 1272513.40 meters

(a)

(b)

Figure 4. GPS set-up over SE-16 located in front of the flagpole of Gregorio Moralizon Elementary School II (a) and NAMRIA reference point DVE-19 (b) as recovered by the field team.

Table 3. Details of the recovered NAMRIA horizontal control point SE-16 used as base station for the LiDAR acquisition.

Station Name	SE-16	
Order of Accuracy	4th order	
Relative Error (horizontal positioning)	1:10,000	
Geographic Coordinates, Philippine Reference of 1992 Datum (PRS 92)	Latitude Longitude Ellipsoidal Height	11° 50' 03.05106" North 125° 26' 03.03429" East 0.472 meters
Geographic Coordinates, World Geodetic System 1984 Datum (WGS 84)	Latitude Longitude Ellipsoidal Height	11° 49' 58.67117" North 125° 26' 08.13400" East 62.301 meters
Grid Coordinates, Universal Transverse Mercator Zone 51 North (UTM 51N PRS1992)	Easting Northing	765219.942 meters 1309292.154 meters

Table 4. Ground control points used during the LiDAR data acquisition.

Date Surveyed	Flight Number	Mission Name	Ground Control Points
June 9, 2014	1558A	3BLK33J160A	SE-16,SME-3139
June 9, 2014	1560A	3BLK33JS160B	SE-16,SME-3139

2.3 Flight Missions

A total of two (2) missions were conducted to complete the LiDAR data acquisition in Sulat floodplain, for a total of seven hours and ninety-four minutes (7+94) of flying time for RP-9122 (See ANNEX 6). All missions were acquired using Aquarius LiDAR system. As shown below, the total area of actual coverage per mission and the corresponding flying hours are depicted in Table 5, while the actual parameters used during the LiDAR data acquisition are presented in Table 6.

Table 5. Flight missions for LiDAR data acquisition in Sulat floodplain.

Date Surveyed	Flight Number	Flight Plan Area (km²)	Surveyed Area (km²)	Area Surveyed within the Floodplain (km²)	Area Surveyed outside the Floodplain (km²)	No. of Images (Frames)	Flying Hours	
							Hr	Min
June 9, 2014	1558A	225.57	117.98	8.17	19.59	98	4	41
June 9, 2014	1560A	225.57	127.54	NA	27.76	1294	3	53
TOTAL		**451.14**	**245.52**	**8.17**	**47.35**	**1392**	**7**	**94**

Table 6. Actual parameters used during LiDAR data acquisition.

Date Surveyed	Flight Number	Flying Height (AGL) (m)	Overlap (%)	Field of View	PRF (kHz)	Scan Frequency (Hz)	Speed of Plane (Kts)
1558A	500	30	44	50	45	120	5
1560A	500	20	44	50	45	120	5

2.4 Survey Coverage

This certain LiDAR acquisition survey covered the Sulat floodplain (See ANNEX 7). It is located in the province of Eastern Samar with majority of the floodplain situated within the municipality of Sulat. The list of municipalities and cities surveyed, with at least one (1) square kilometer coverage, is shown in Table 7. Figure 5, on the other hand, shows the actual coverage of the LiDAR acquisition for the Sulat floodplain.

Table 7. List of municipalities and cities surveyed during Sulat floodplain LiDAR survey.

Province	Municipality/City	Area of Municipality/ City (km²)	Total Area Surveyed (km²)	Percentage of Area Surveyed
Eastern Samar	Sulat	150.05	39.95	26.63%
	San Julian	127.43	22.72	17.83%
	Borongan City	596.08	69.2	11.61%
	Sulat	230.27	1.95	0.85%
Total		**1,103.83**	**133.82**	**12.12%**

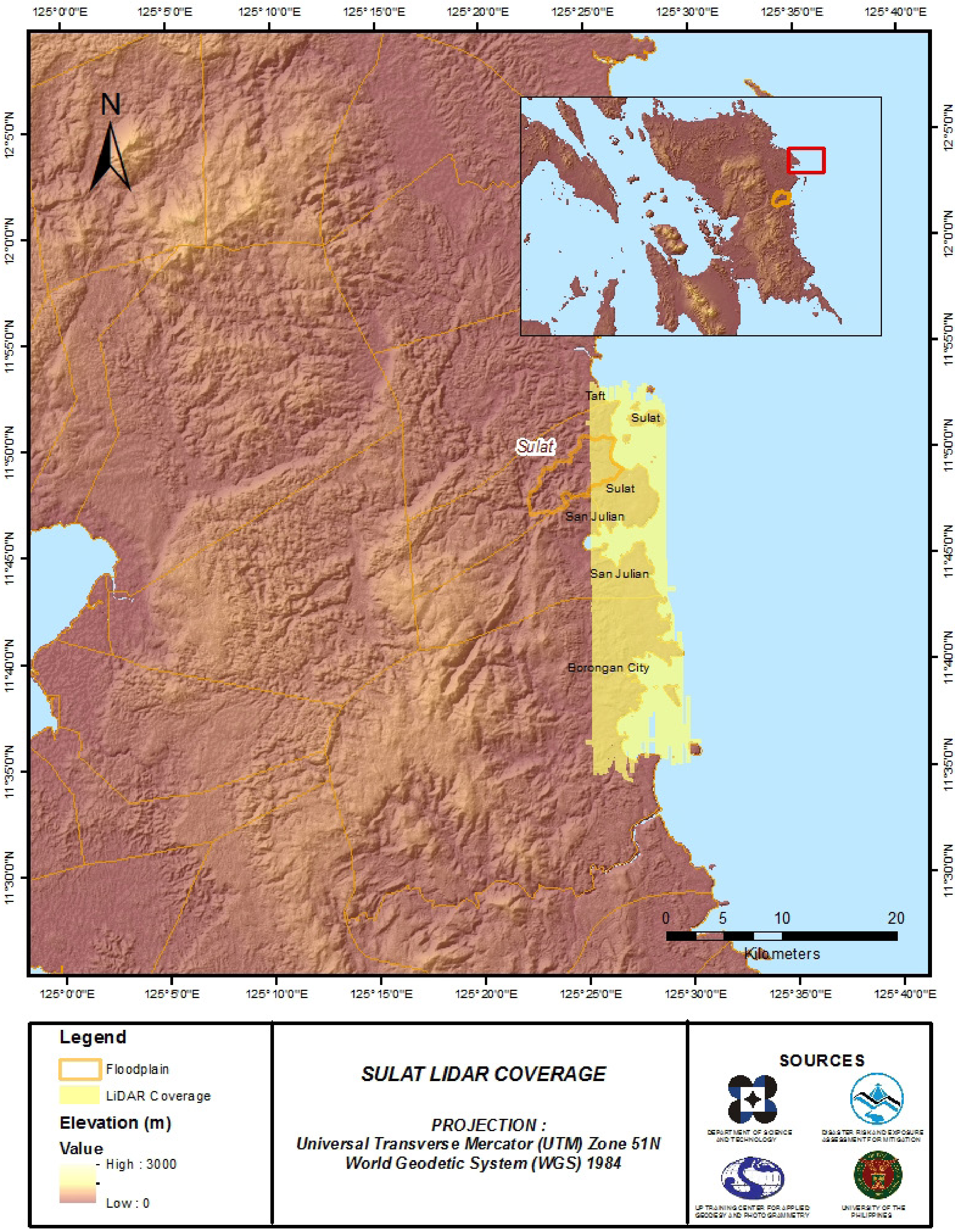

Figure 5. Actual LiDAR survey coverage for Sulat floodplain.

CHAPTER 3: LIDAR DATA PROCESSING OF THE SULAT FLOODPLAIN

Engr. Ma. Rosario Concepcion O. Ang, Engr. John Louie D. Fabila, Engr. Sarah Jane D. Samalburo , Engr. Gladys Mae Apat, Engr. Harmond F. Santos , Engr. Ma. Ailyn L. Olanda, Engr. Erica Erin E. Elazegui, Jovy Anne S. Narisma, Engr. Karl Adrian P. Vergara

The methods applied in this chapter were based on the DREAM methods manual (Ang, et. al., 2014) and further enhanced and updated in Paringit, et. al. (2017).

3.1 Overview of the LIDAR Data Pre-Processing

The data transmitted by the Data Acquisition Component are checked for completeness based on the list of raw files required to proceed with the pre-processing of the LiDAR data. Upon acceptance of the LiDAR field data, georeferencing of the flight trajectory is done in order to obtain the exact location of the LiDAR sensor when the laser was shot. Point cloud georectification is performed to incorporate correct position and orientation for each point acquired. The georectified LiDAR point clouds are subject for quality checking to ensure that the required accuracies of the program, which are the minimum point density, vertical and horizontal accuracies, are met. The point clouds are then classified into various classes before generating Digital Elevation Models such as Digital Terrain Model and Digital Surface Model.

Using the elevation of points gathered in the field, the LiDAR-derived digital models are calibrated. Portions of the river that are barely penetrated by the LiDAR system are replaced by the actual river geometry measured from the field by the Data Validation and Bathymetry Component. LiDAR acquired temporally are then mosaicked to completely cover the target river systems in the Philippines. Orthorectification of images acquired simultaneously with the LiDAR data is done through the help of the georectified point clouds and the metadata containing the time the image was captured.

These processes are summarized in the flowchart shown in Figure 6.

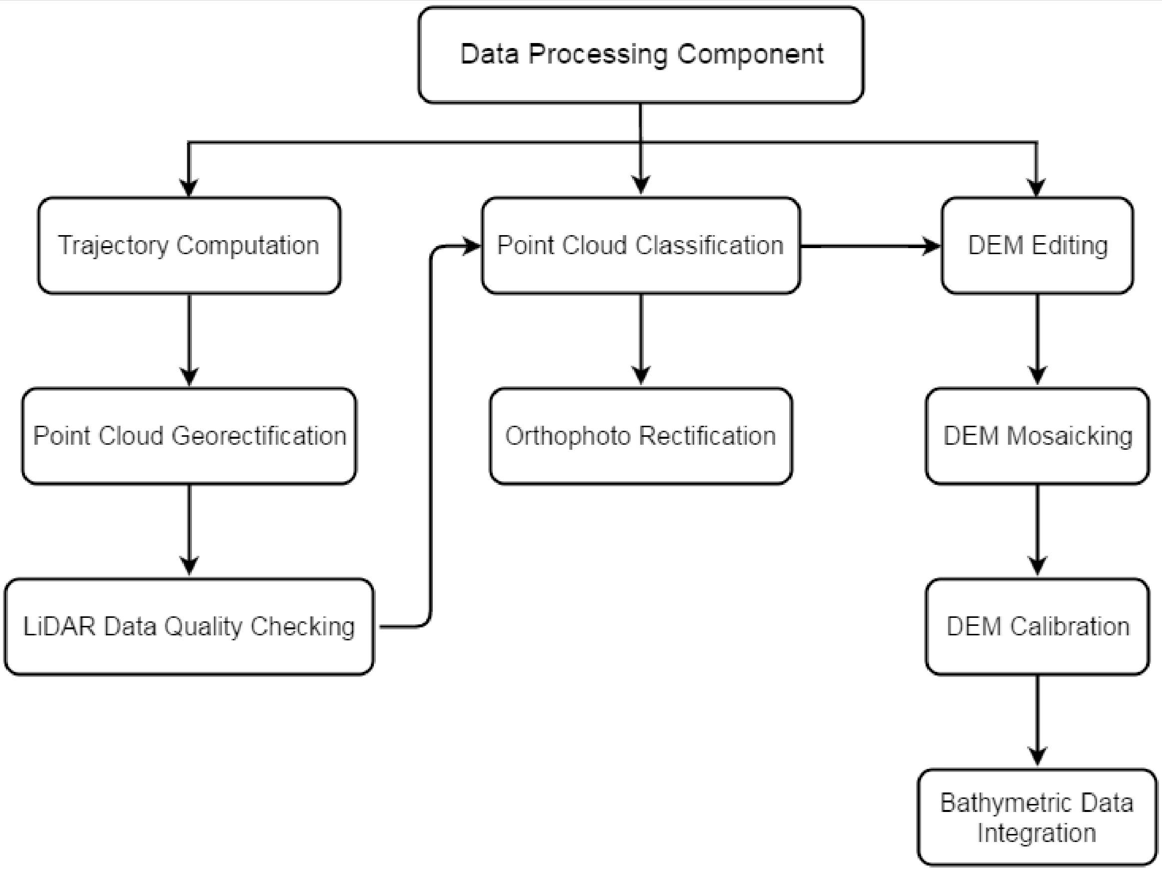

Figure 6. Schematic diagram for the data pre-processing.

3.2 Transmittal of Acquired LiDAR Data

Data transfer sheets for all the LiDAR missions of the Sulat Floodplain can be found in ANNEX 5. The missions flown during the conduct of the survey in June 2014 utilized the Airborne LiDAR Terrain Mapper (ALTM™ Optech Inc.) Aquarius system over Sulat, Eastern Samar.

The Data Acquisition Component (DAC) transferred a total of 26.30 Gigabytes of Range data, 0.50 Gigabytes of POS data, 32.20 Megabytes of GPS base station data, and 167.90 Gigabytes of raw image data to the data server on June 19, 2014 which was verified for accuracy and completeness by the DPPC. The whole dataset for the Sulat Floodplain was fully transferred on June 19, 2014, as indicated on the Data Transfer Sheets for the Sulat floodplain.

3.3 Trajectory Computation

The Smoothed Performance Metric parameters of the computed trajectory for Flight 1560A, one of the Sulat flights, which is the North, East, and Down position RMSE values are shown in Figure 7. The x-axis corresponds to the time of the flight, which was measured by the number of seconds from the midnight of the start of the GPS week, which fell on the date and time of June 9, 2014, 00:00AM. The y-axis, on the other hand, represents the RMSE value for that particular position.

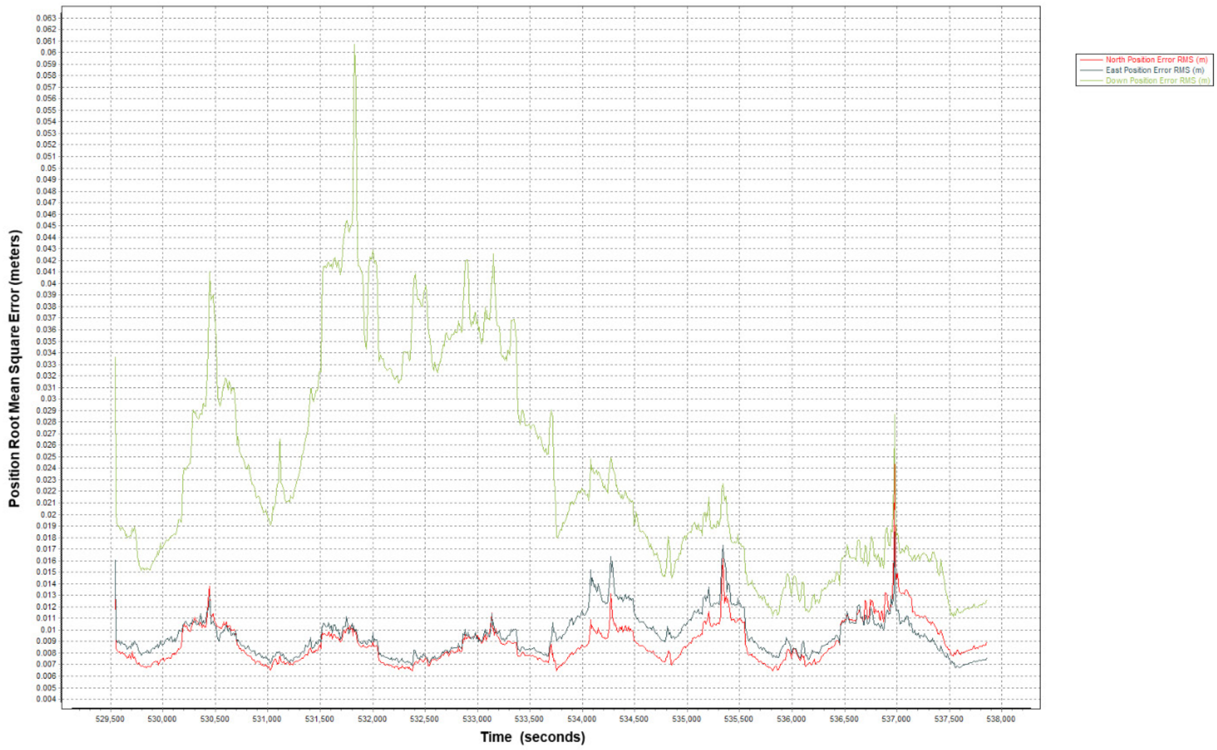

Figure 7. Smoothed Performance Metric Parameters of Sulat Flight 1560A.

The time of flight was from 529500 seconds to 537800 seconds, which corresponds to afternoon of June 9, 2014. The initial spike that is seen on the data corresponds to the time that the aircraft was getting into position to start the acquisition, and the POS system starts computing for the position and orientation of the aircraft.

Redundant measurements from the POS system quickly minimized the RMSE value of the positions. The periodic increase in RMSE values from an otherwise smoothly curving RMSE values correspond to the turn-around period of the aircraft, when the aircraft makes a turn to start a new flight line. Figure 8 shows that the North position RMSE peaks at 2.40 centimeters, the East position RMSE peaks at 1.60 centimeters, and the Down position RMSE peaks at 5.90 centimeters, which are within the prescribed accuracies described in the methodology.

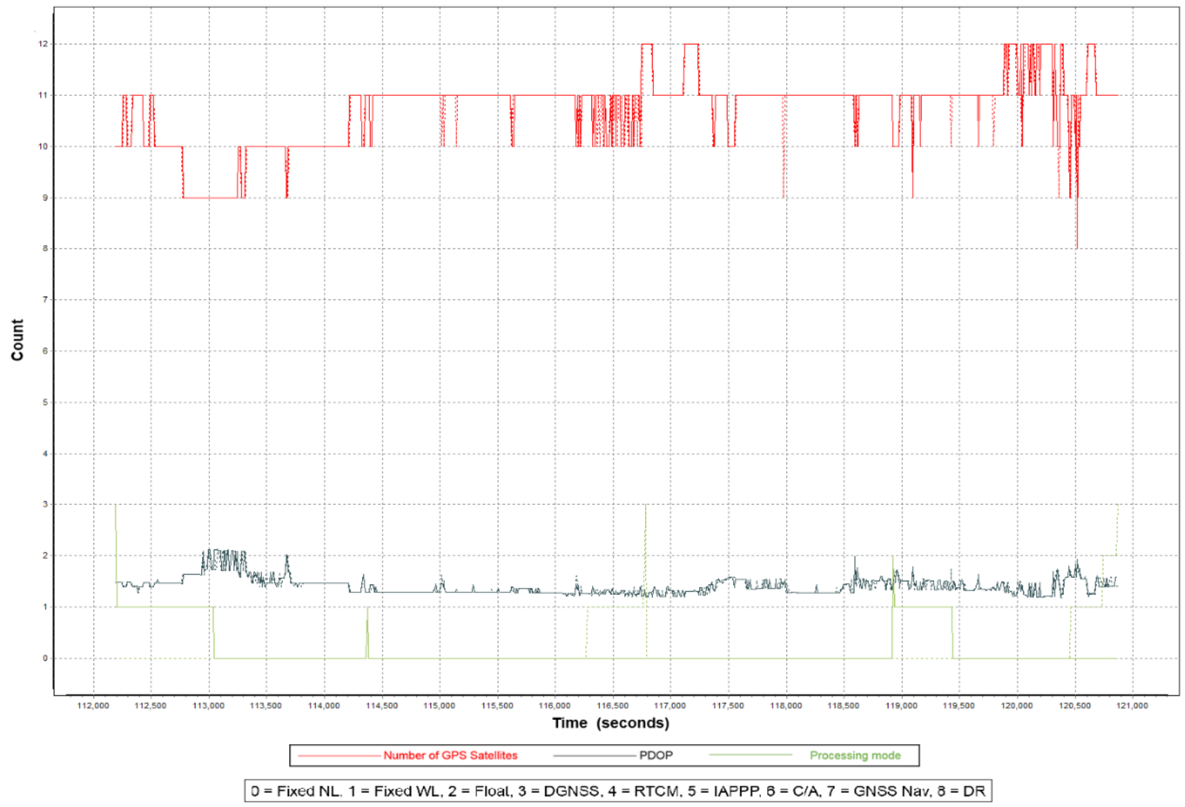

Figure 8. Solution Status Parameters of Sulat Flight 1560A.

The Solution Status parameters, which indicate the number of GPS satellites; Positional Dilution of Precision (PDOP); and the GPS processing mode used for Sulat Flight 1560A are shown in Figure 8. For the Solution Status parameters, the figure above signifies that the number of satellites utilized and tracked during the acquisition were between 10 and 12, not going lower than 6. Similarly, the PDOP value did not go above the value of 3, which indicates optimal GPS geometry. The processing mode also stayed at the value of 0 for the majority of the survey stayed at the value of 0 for majority of the survey with some peaks up to 1 attributed to the turns performed by the aircraft. The value of 0 corresponds to a Fixed, Narrow-Lane Mode, which is the optimum carrier-cycle integer ambiguity resolution technique available for the POSPAC MMS. Fundamentally, all of the parameters adhered to the accuracy requirements for optimal trajectory solutions, as indicated in the methodology. The computed best estimated trajectory for all Sulat flights is shown in Figure 9.

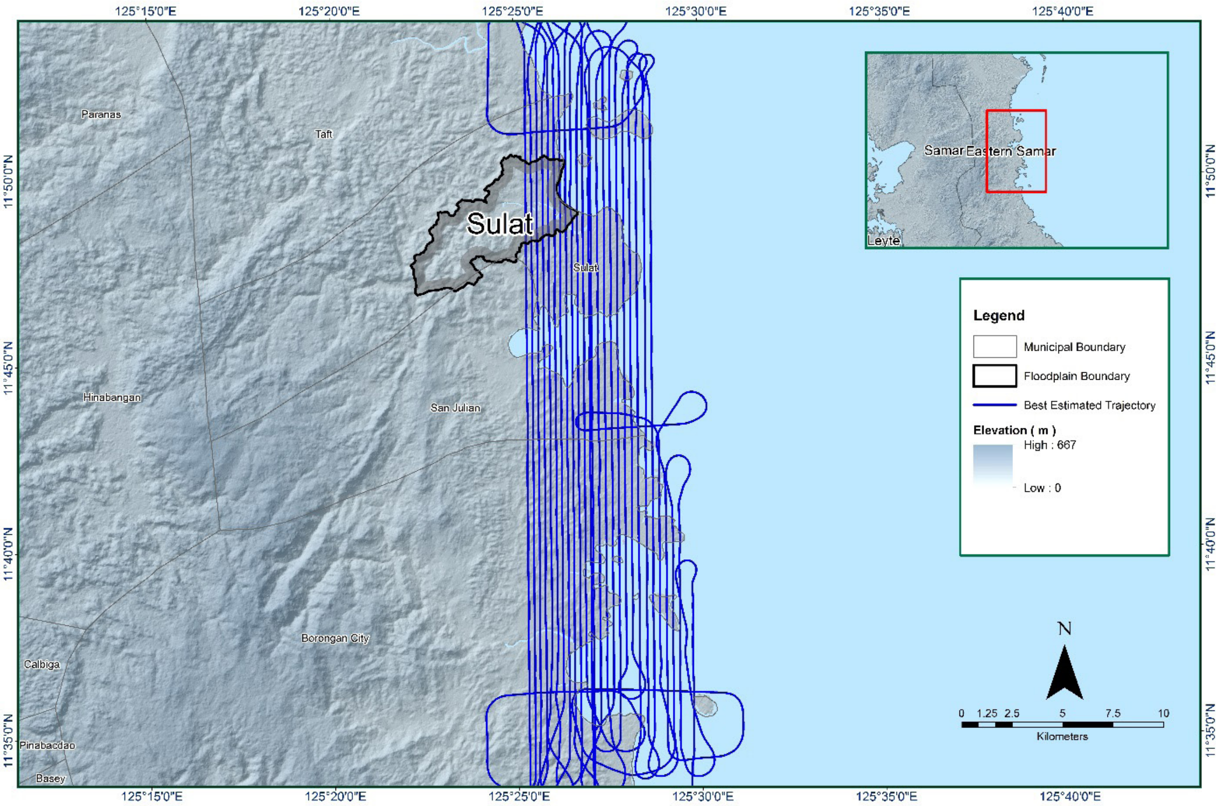

Figure 9. Best Estimated Trajectory of the LiDAR missions conducted over the Sulat Floodplain.

3.4 LiDAR Point Cloud Computation

The produced LAS contains 28 flight lines, with each flight line contains one channel, since the Aquarius system contains only one channel. The summary of the self-calibration results obtained from LiDAR processing in the LiDAR Mapping Suite (LMS) software for all flights over the Sulat floodplain are given in Table 8. Self-calibration Results values for Sulat flights..

Table 8. Self-calibration Results values for Sulat flights.

Parameter	Acceptable Value	Computed Value
Boresight Correction stdev)	<0.001degrees	0.000327
IMU Attitude Correction Roll and Pitch Corrections stdev)	<0.001degrees	0.000898
GPS Position Z-correction stdev)	<0.01meters	0.0098

The optimum accuracy values for all Sulat flights were also calculated, which are based on the computed standard deviations of the corrections of the orientation parameters. The standard deviation values for individual blocks are presented in the Mission Summary Reports (ANNEX 8).

3.5 LiDAR Quality Checking

The boundary of the processed LiDAR data on top of the SAR Elevation Data over the Sulat Floodplain is shown in Figure 10. The map shows gaps in the LiDAR coverage that are attributed to cloud coverage.

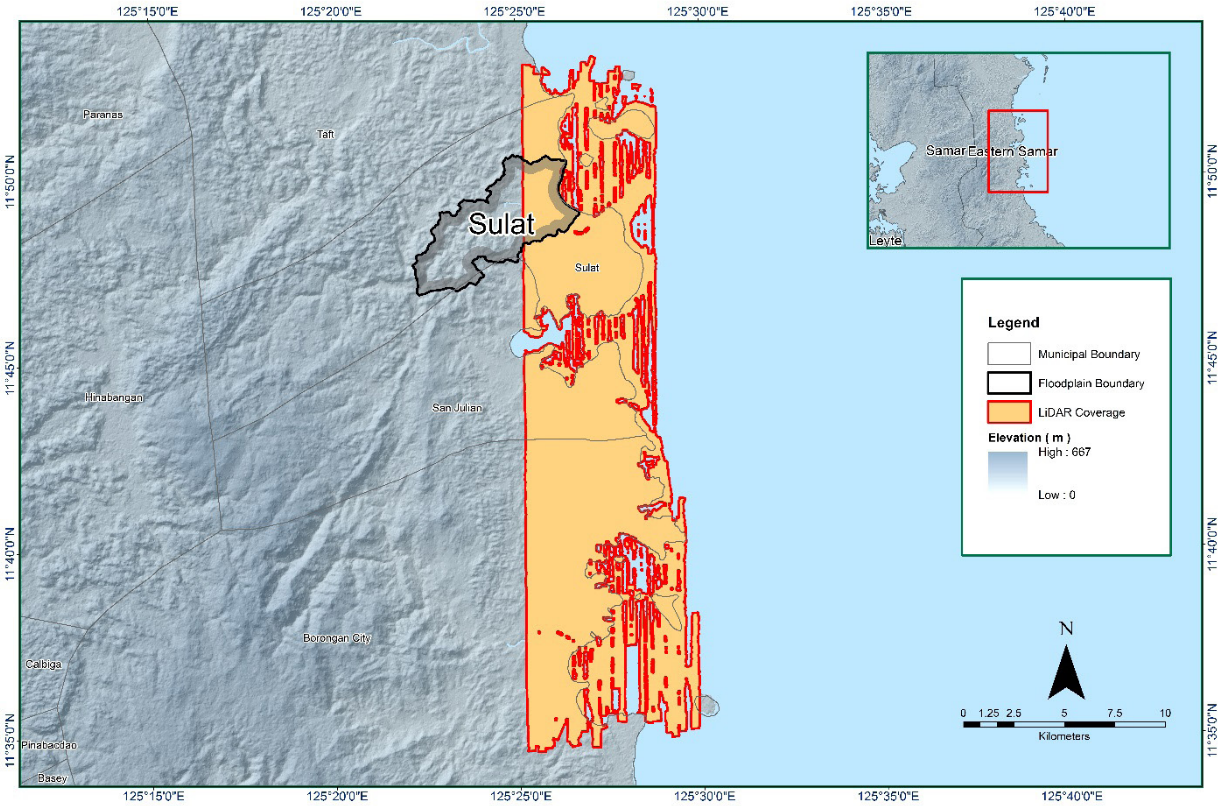

Figure 10. Boundaries of the processed LiDAR data over the Sulat Floodplain.

A total area of 174.99 square kilometers (sq. kms.) were covered by the Sulat flight missions as a result of two (2) flight acquisitions, which were grouped and merged into one (1) block accordingly, as portrayed in Table 9.

Table 9. List of LiDAR blocks for the Sulat floodplain.

LiDAR Blocks	Flight Numbers	Area (sq. km)
Samar_Leyte_Blk33J	1558A	174.99
	1560A	
TOTAL		**174.99 sq.km**

The overlap data for the merged LiDAR blocks, showing the number of channels that pass through a particular location is shown in Figure 11. Since the Aquarius system employs one channel, we would expect an average value of 1 (blue) for areas where there is limited overlap, and a value of 2 (yellow) or more (red) for areas with three or more overlapping flight lines.

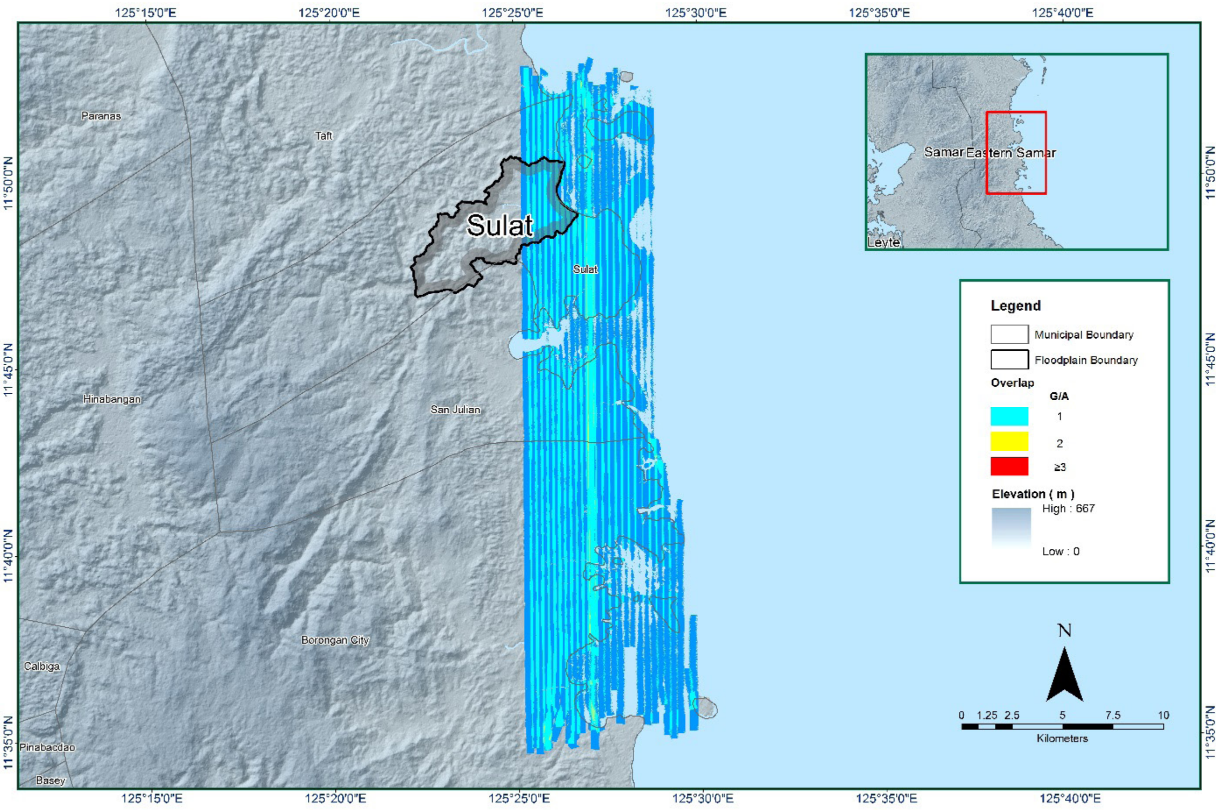

Figure 11. Image of data overlap for Sulat floodplain.

The overlap statistics per block for the Sulat floodplain can be found in the Mission Summary Reports (ANNEX 8). One pixel corresponds to 25.0 square meters on the ground. For this area, the percent overlap is 36.01%, which passed the 25% requirement.

The pulse density map for the merged LiDAR data, with the red parts showing the portions of the data that satisfy the two (2) points per square meter criterion is shown in Figure 12. As seen in the figure below, it was determined that all LiDAR data for the Sulat Floodplain Survey satisfy the point density requirement, as the average density for the entire survey area is 2.71 points per square meter.

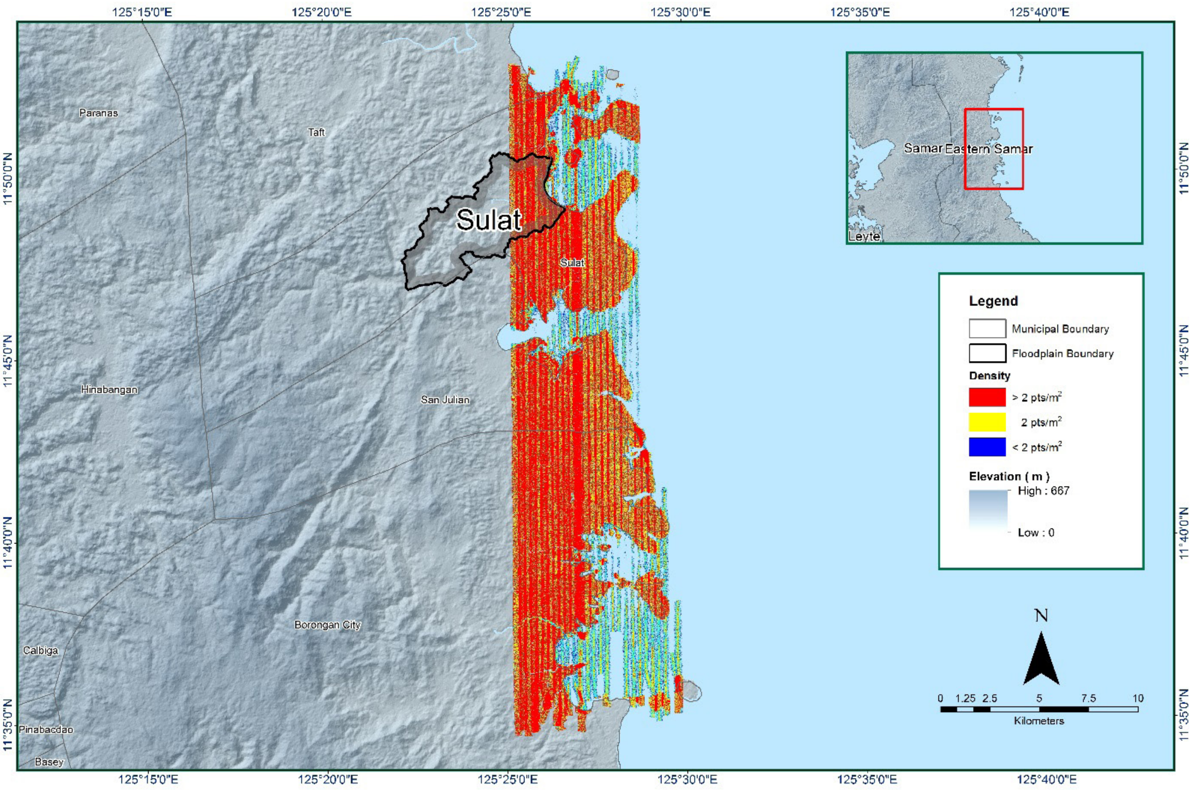

Figure 12. Pulse density map of the merged LiDAR data for Sulat floodplain..

The elevation difference between overlaps of adjacent flight lines is shown in Figure 13. The default color range is blue to red, where bright blue areas correspond to portions where elevations of a previous flight line are higher by more than 0.20m, as identified by its acquisition time; which is relative to the elevations of its adjacent flight line. Similarly, bright red areas indicate portions where elevations of a previous flight line are lower by more than 0.20m, relative to the elevations of its adjacent flight line. Areas highlighted in bright red or bright blue necessitate further investigation using the Quick Terrain Modeler software.

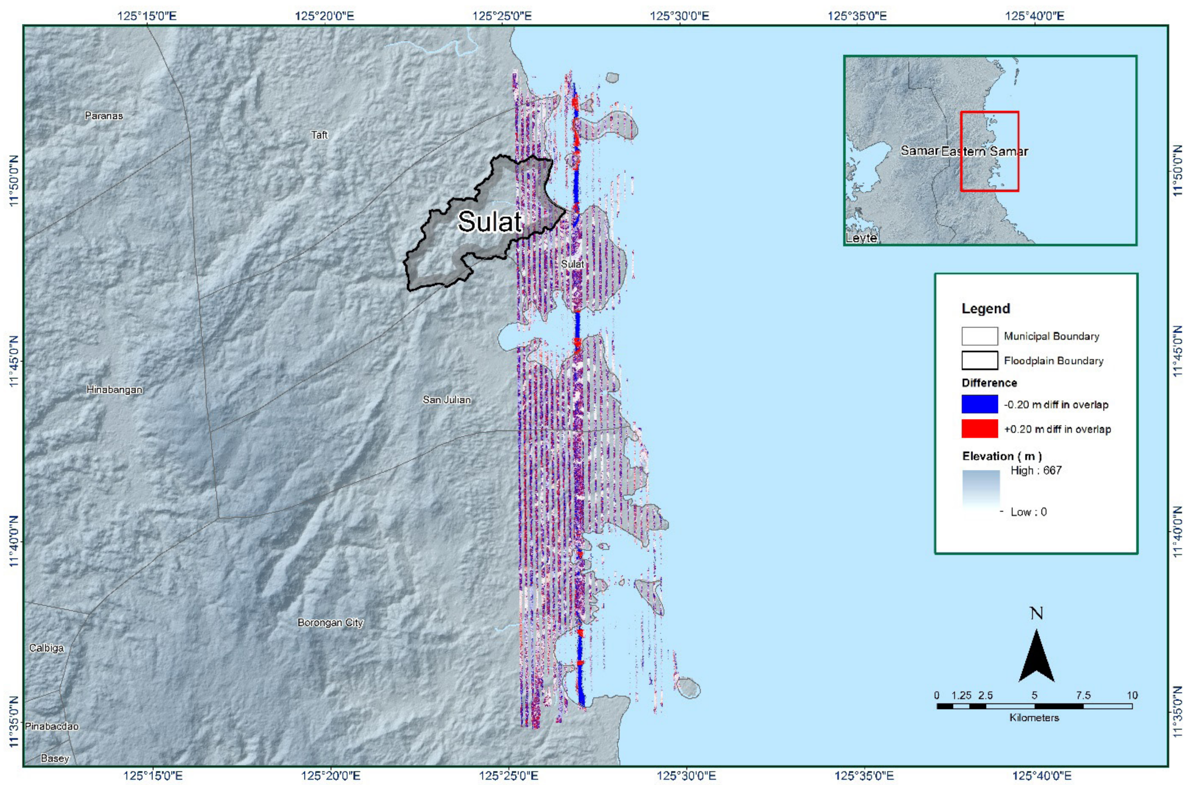

Figure 13. Elevation difference Map between flight lines for the Sulat Floodplain Survey.

A screen-capture of the processed LAS data from Sulat flight 1560A loaded in QT Modeler is shown in Figure 14. The upper left image shows the elevations of the points from two overlapping flight strips traversed by the profile, illustrated by a dashed red line. The x-axis corresponds to the length of the profile. It is evident that there are differences in elevation, but the differences do not exceed the 20-centimeter mark. This profiling was repeated until the quality of the LiDAR data generated satisfactory results. No reprocessing was done for this LiDAR dataset.

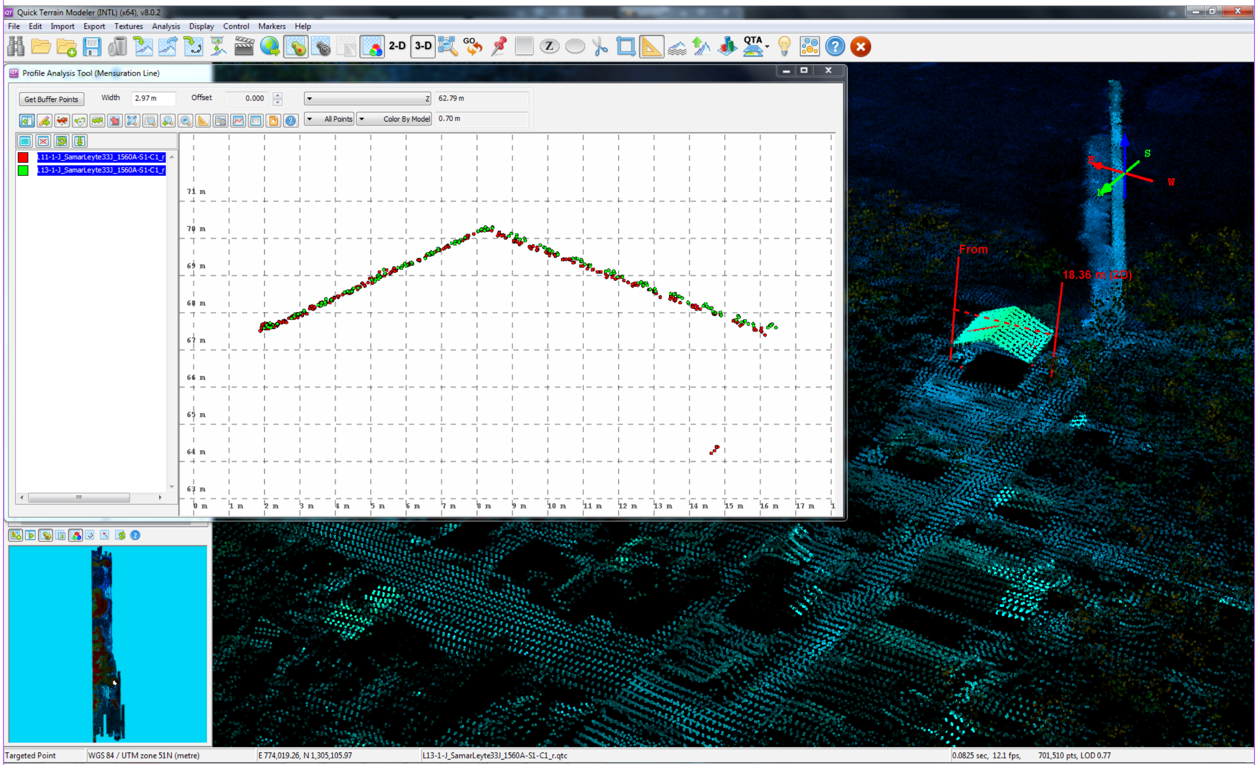

Figure 14. Quality checking for Sulat flight 1560A using the Profile Tool of QT Modeler.

3.6 LiDAR Point Cloud Classification and Rasterization

Table 10. Sulat classification results in TerraScan.

Pertinent Class	Total Number of Points
Ground	110,486,647
Low Vegetation	51,277,620
Medium Vegetation	61,095,498
High Vegetation	151,119,077
Building	2,518,830

The tile system that TerraScan employed for the LiDAR data as well as the final classification image for a block of the Sulat floodplain is shown in Figure 15. A total of 291 tiles with 1 km. X 1 km. (one kilometer by one kilometer) size were produced. Correspondingly, Table 11 summarizes the number of points classified to the pertinent categories. The point cloud has a maximum and minimum height of 248.48 meters and 49.30 meters respectively.

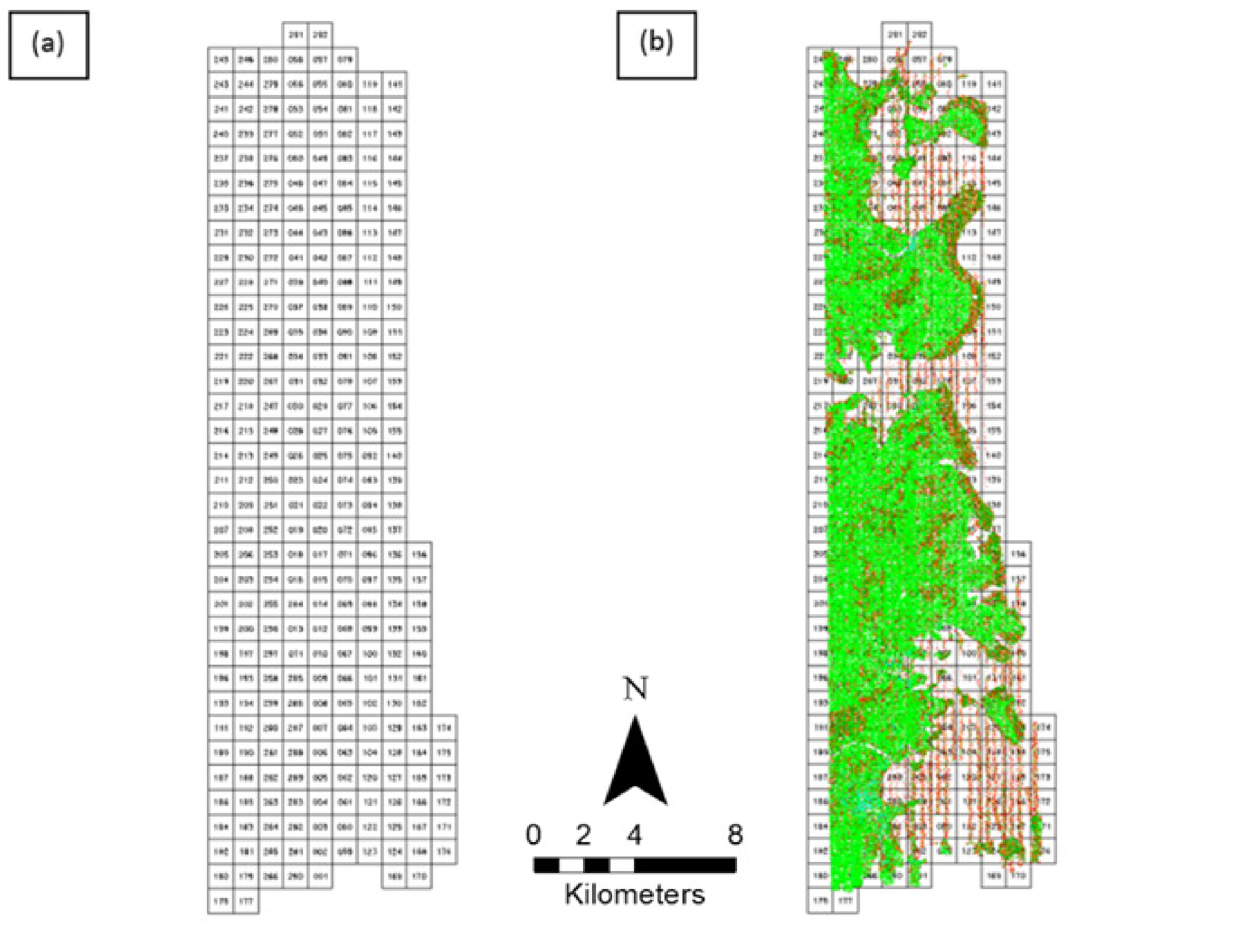

Figure 15. Tiles for Sulat floodplain (a) and classification results (b) in TerraScan.

An isometric view of an area before and after running the classification routines is shown in Figure 16. The ground points are highlighted in orange, while the vegetation is in different shades of green, and the buildings are in cyan. It can be seen that residential structures adjacent or even below the canopy are classified correctly, due to the density of the LiDAR data.

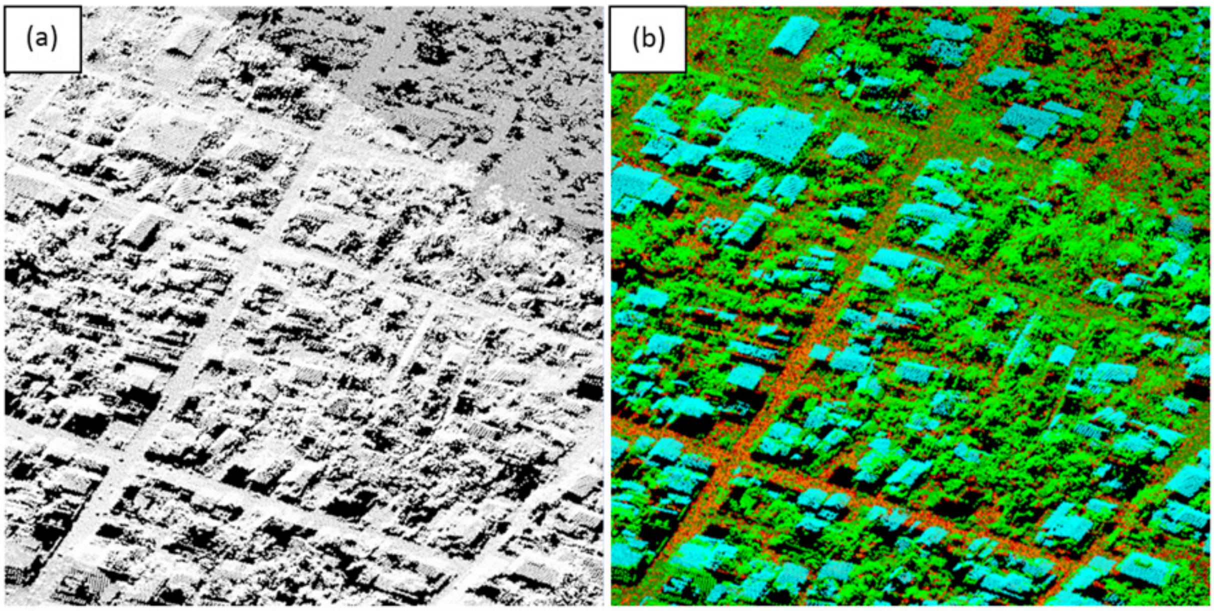

Figure 16. Point cloud before (a) and after (b) classification.

The production of the last return (V_ASCII) and secondary (T_ ASCII) DTM as well as the first (S_ ASCII) and last (D_ ASCII) return DSM of the area in top view display are show in Figure 17. It shows that DTMs are the representation of the bare earth, while on the DSMs, all features are present, such as buildings and vegetation.

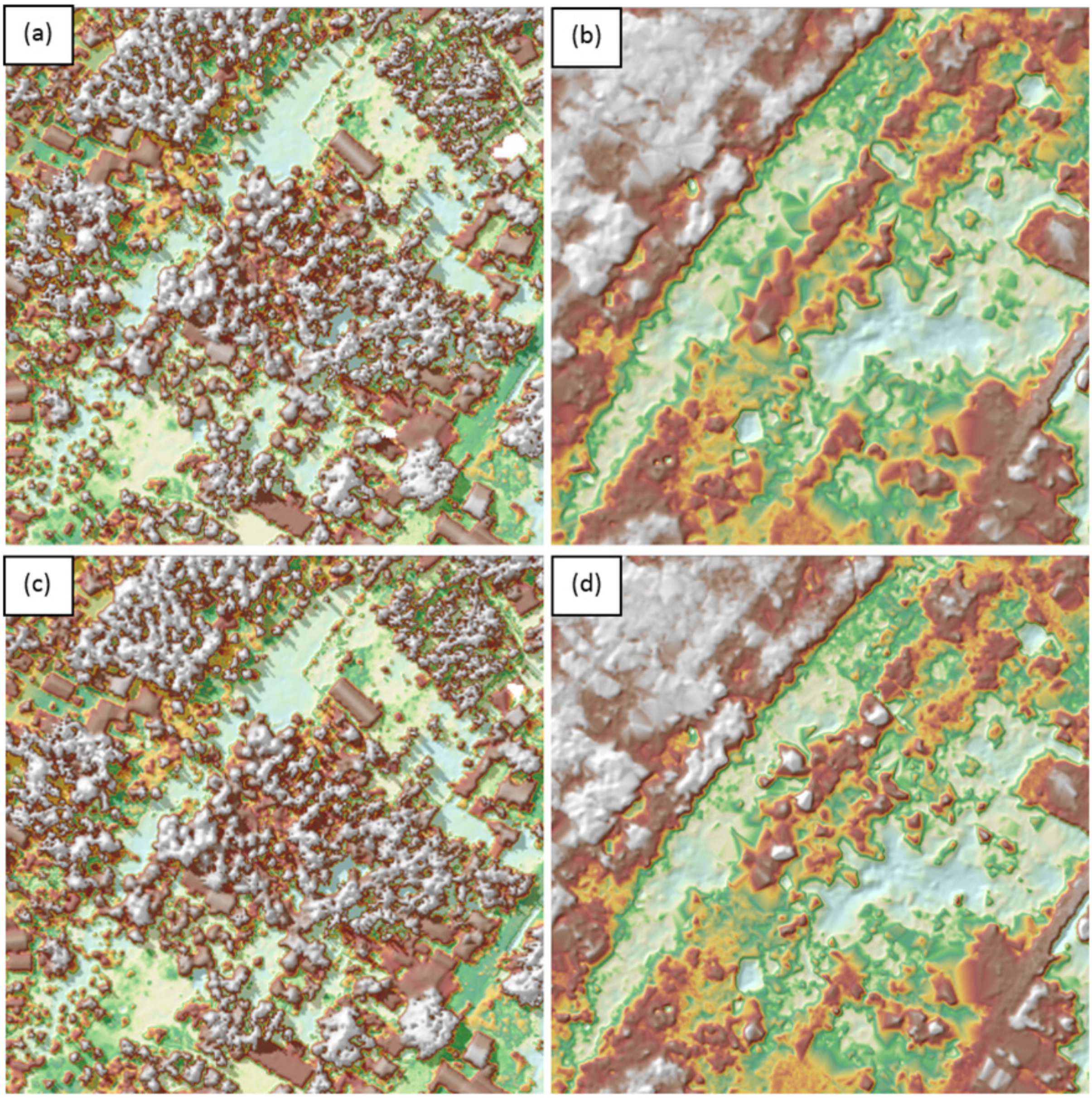

Figure 17. The production of last return DSM (a) and DTM (b), first return DSM (c) and secondary DTM (d) in some portion of Sulat floodplain.

3.7 LiDAR Image Processing and Orthophotograph Rectification

The 292 1km by 1km tiles area covered by Sulat floodplain is shown in Figure 18. After tie point selection to fix photo misalignments, color points were added to smoothen out visual inconsistencies along the seamlines where photos overlap. The Sulat floodplain has a total of 219.66 sq.km orthophotogaph coverage comprised of 2,657 images. A zoomed in version of sample orthophotographs named in reference to its tile number is shown in Figure 19.

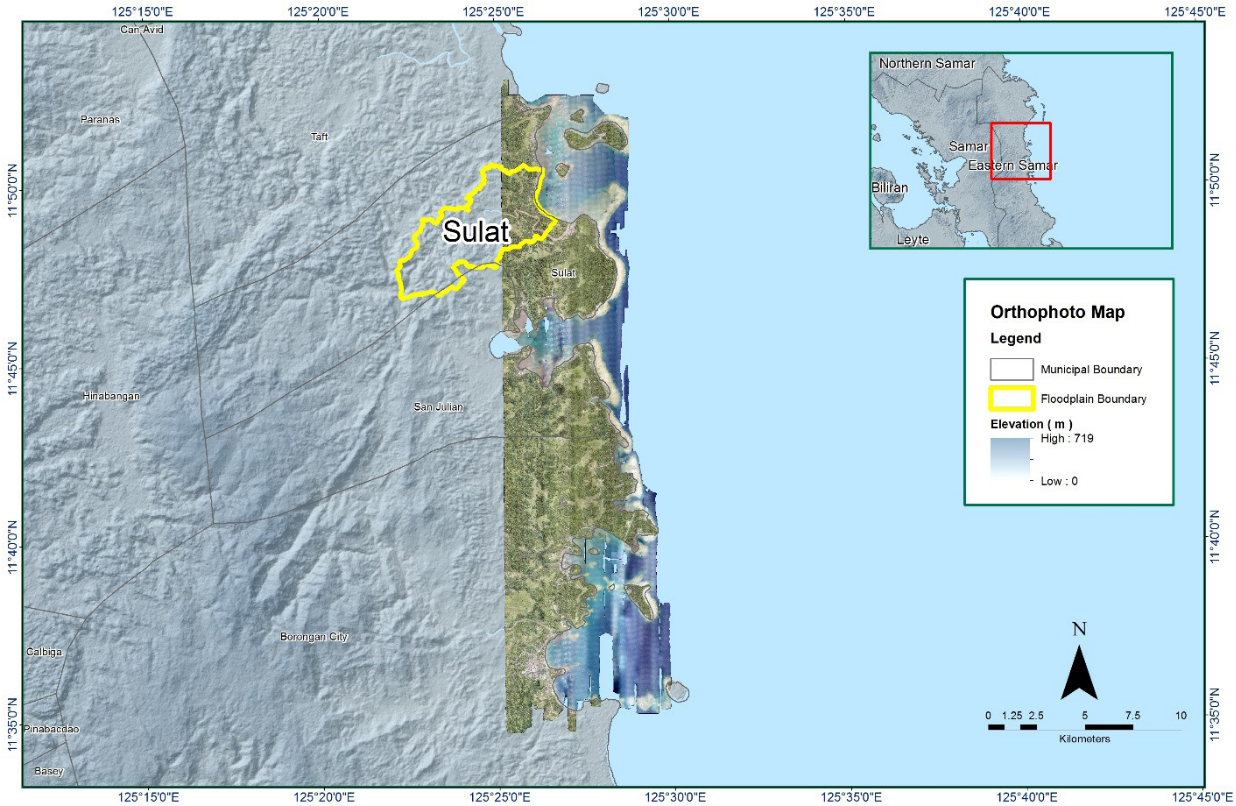

Figure 18. Sulat floodplain with the available orthographs.

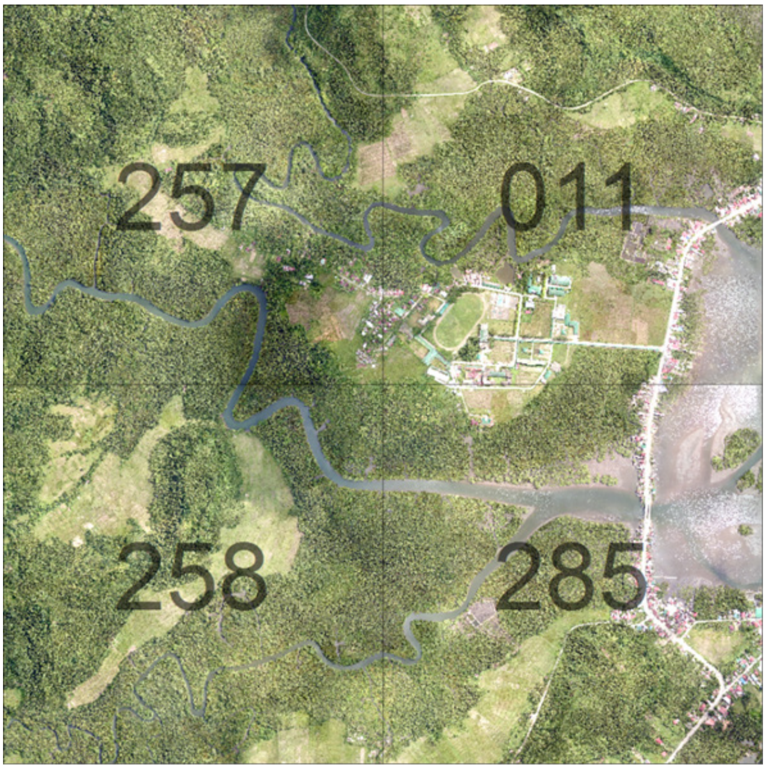

Figure 19. Sample orthophotograph tiles for Sulat floodplain.

3.8 DEM Editing and Hydro-Correction

One (1) mission block was processed for the Sulat Floodplain Survey. The block is from the Samar_Leyte mission with a total area of 174.99 square kilometers. Table 11 shows the name and corresponding area of each block in square kilometers.

Table 11. LiDAR blocks with its corresponding areas.

LiDAR Blocks	Area (sq.km)
Samar_Leyte_Blk33J	174.99
TOTAL	**174.99 sq.km**

Figure 20 shows portions of a DTM before and after manual editing. As evident in the figure, the bridge (Figure 20a) has obstructed the flow of water along the river. To correct the river hydrologically, the bridge was removed through manual editing (Figure 20b). The paddy field (Figure 20c) has been misclassified and removed during classification process and has to be retrieved to complete the surface (Figure 20d) to allow the correct flow of water.

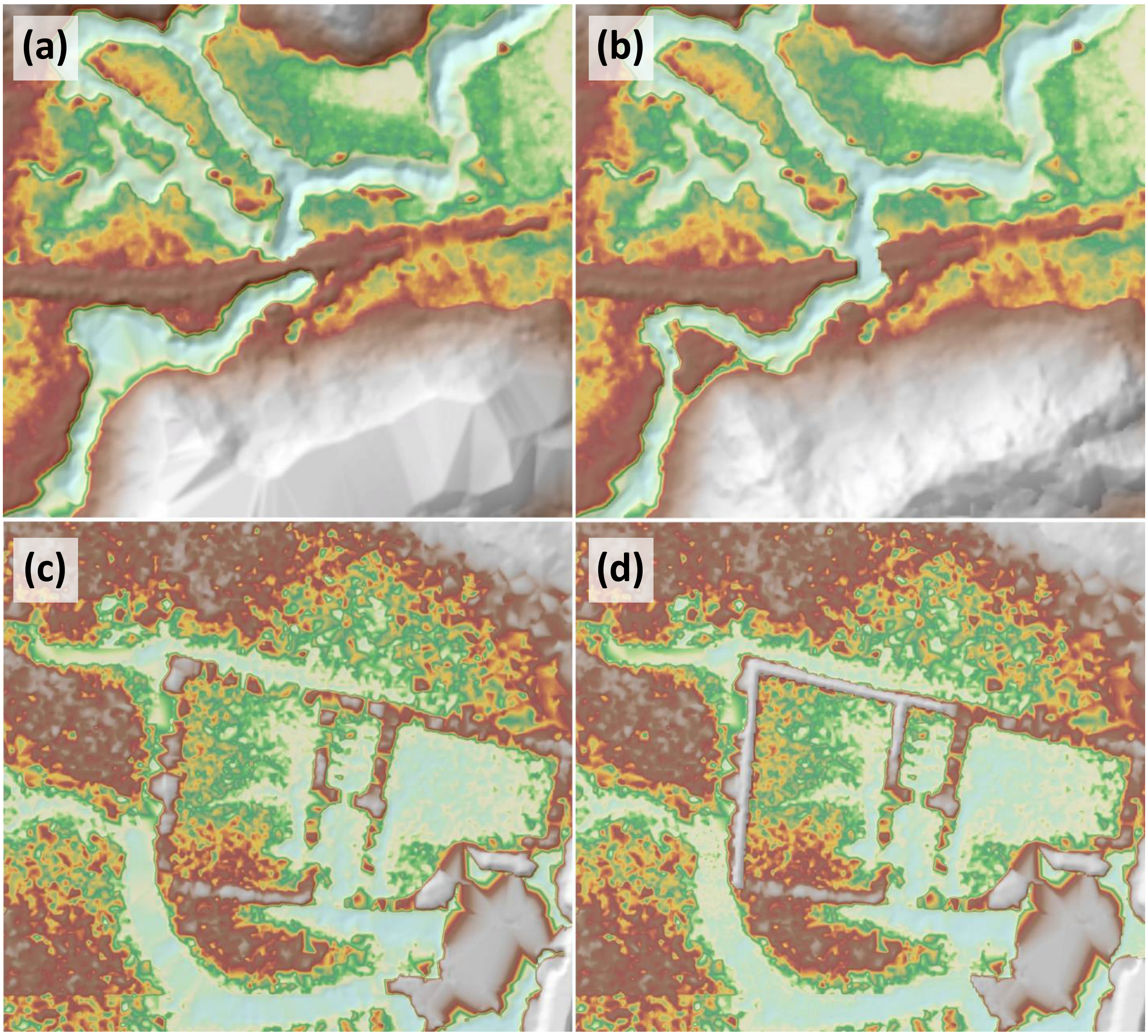

Figure 20. Portions in the DTM of the Sulat Floodplain – a bridge before (a) and after (b) manual editing; a paddy field before (c) and after (d) data retrieval.

3.9 Mosaicking of Blocks

No assumed reference block was used in mosaicking because the identified reference for shifting was an existing calibrated Tacloban DEM overlapping with the blocks to be mosaicked. Table 12 shows the shift values applied to each LiDAR block during mosaicking.

Mosaicked LiDAR DTM for Sulat Floodplain is shown in Figure 21. It can be seen that the entire Sulat floodplain is 14.04% covered by LiDAR data while portions with no LiDAR data were patched with the available IFSAR data.

Table 12. Shift values of each LiDAR block of Sulat Floodplain.

Mission Blocks	Shift Values (meters)		
	x	y	z
Samar_Leyte_Blk33J	-1.00	2.00	-1.00

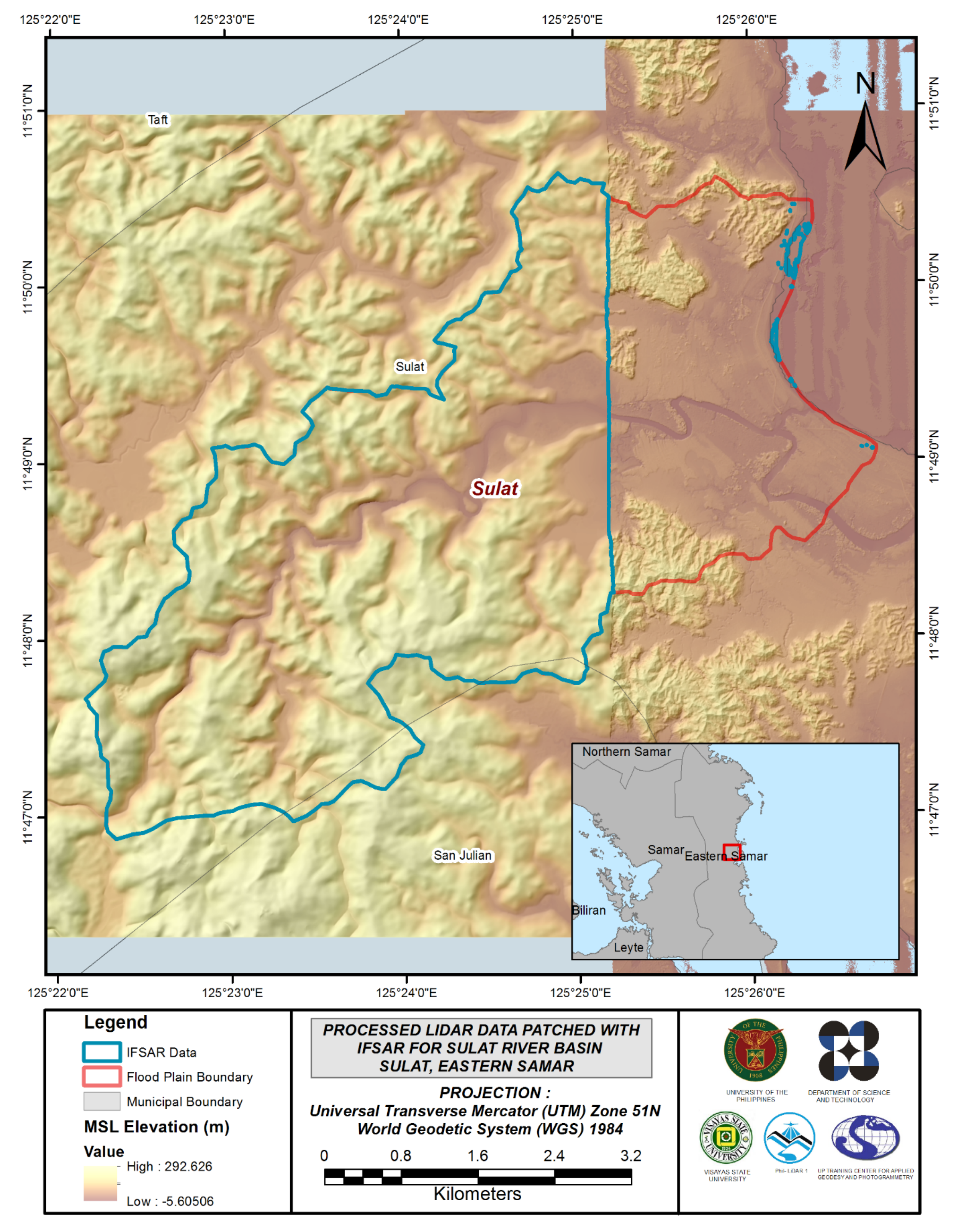

Figure 21. Map of processed LiDAR data for the Sulat Floodplain.

3.10 Calibration and Validation of Mosaicked LiDAR DEM

The extent of the validation survey done by the Data Validation and Bathymetry Component (DVBC) in Sulat to collect points with which the LiDAR dataset is validated is shown in Figure 22, with the validation survey points highlighted in green. A total of 101 survey points were gathered for the Sulat floodplain. However, the point dataset was not used for the calibration of the LiDAR data for Sulat because during the mosaicking process, each LiDAR block was referred to the calibrated Tacloban DEM. Therefore the mosaicked DEM of Sulat can already be considered as a calibrated DEM.

A good correlation between the uncalibrated Tacloban LiDAR DTM and the ground survey elevation values is shown in Figure 23. Statistical values were computed from extracted LiDAR values using the selected points to assess the quality of the data and obtain the value for vertical adjustment. The computed height difference between the LiDAR DTM and calibration points is 0.14 meters, with a standard deviation of 0.13 meters. The calibration of the Tacloban LiDAR data was accomplished by subtracting the height difference value of 0.14 meters to the Tacloban mosaicked LiDAR data. Table 13 shows the statistical values of the compared elevation values between the Tacloban LiDAR data and the calibration data. These values were also applicable to the Sulat DEM.

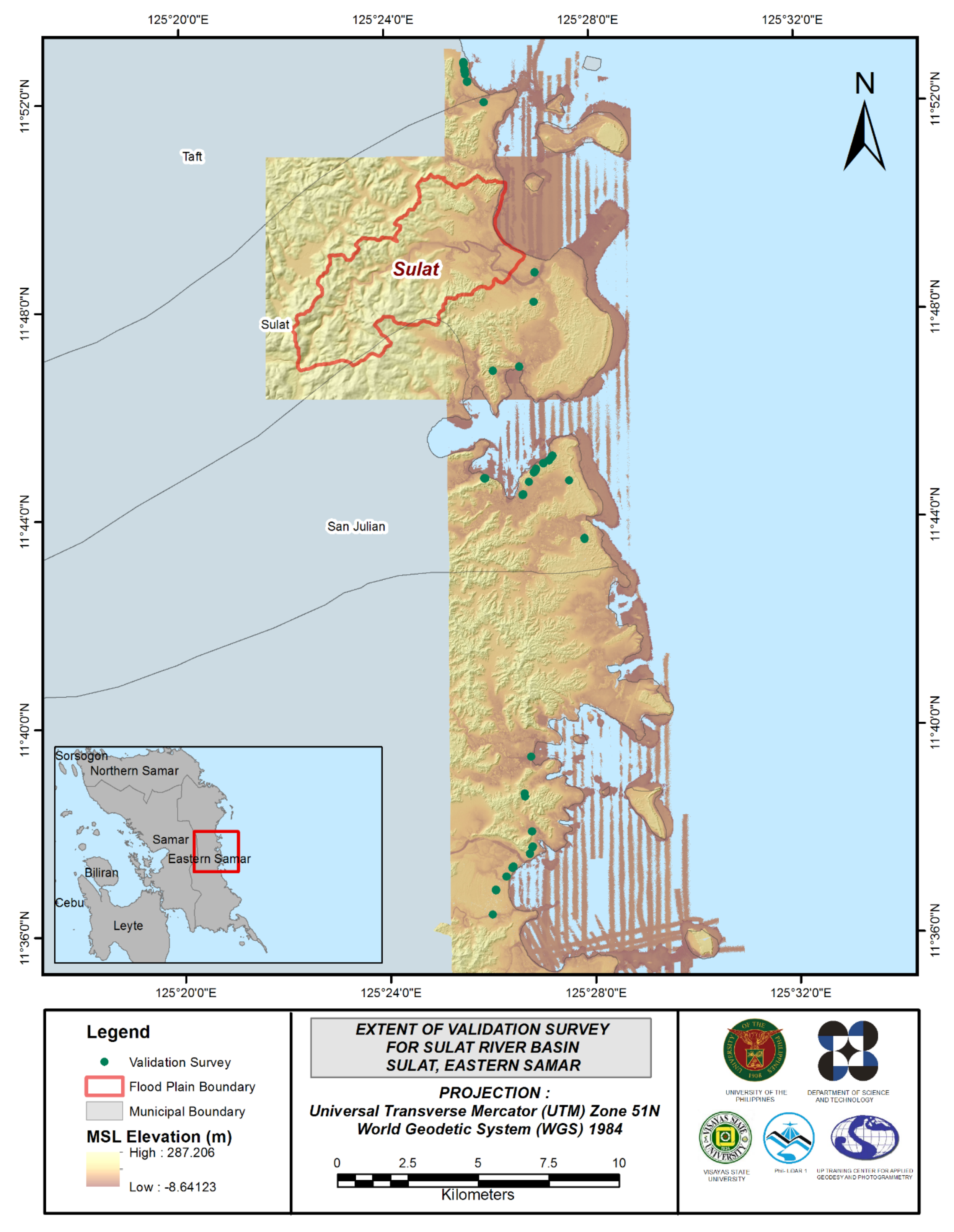

Figure 22. Map of Sulat Floodplain with validation survey points in green.

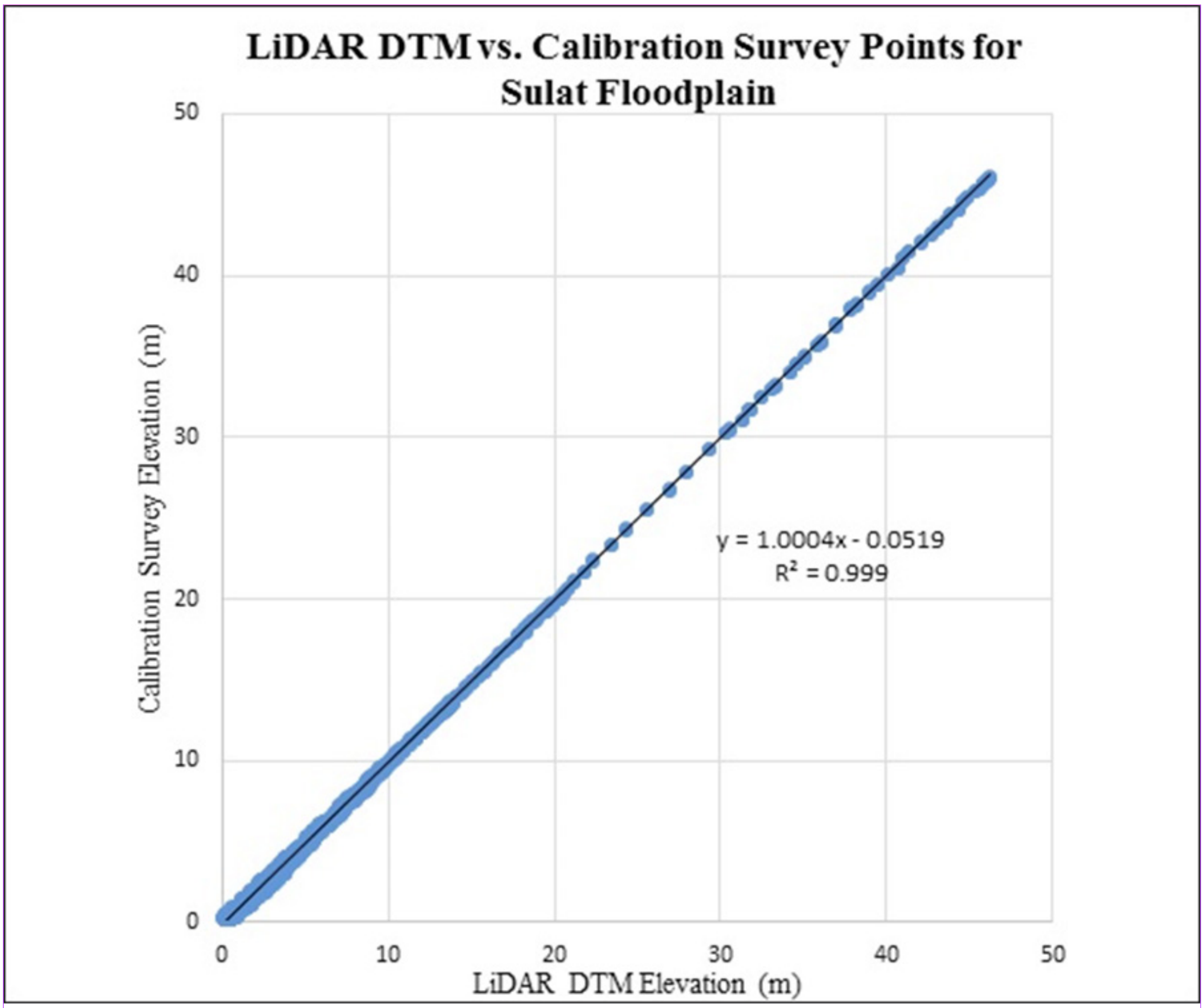

Figure 23. Correlation plot between calibration survey points and LiDAR data.

Table 13. Calibration Statistical Measures.

Calibration Statistical Measures	Value (meters)
Height Difference	0.14
Standard Deviation	0.13
Average	-0.05
Minimum	-0.32
Maximum	0.22

All survey points were used to validate the calibrated Sulat DTM. A good correlation between the calibrated mosaicked LiDAR elevation and the ground survey elevation values, which point toward the quality of the LiDAR DTM is shown in Figure 24. The computed RMSE value between the calibrated LiDAR DTM and the validation elevation values is at 0.20 meters with a standard deviation of 0.05 meters, as shown in Table 14.

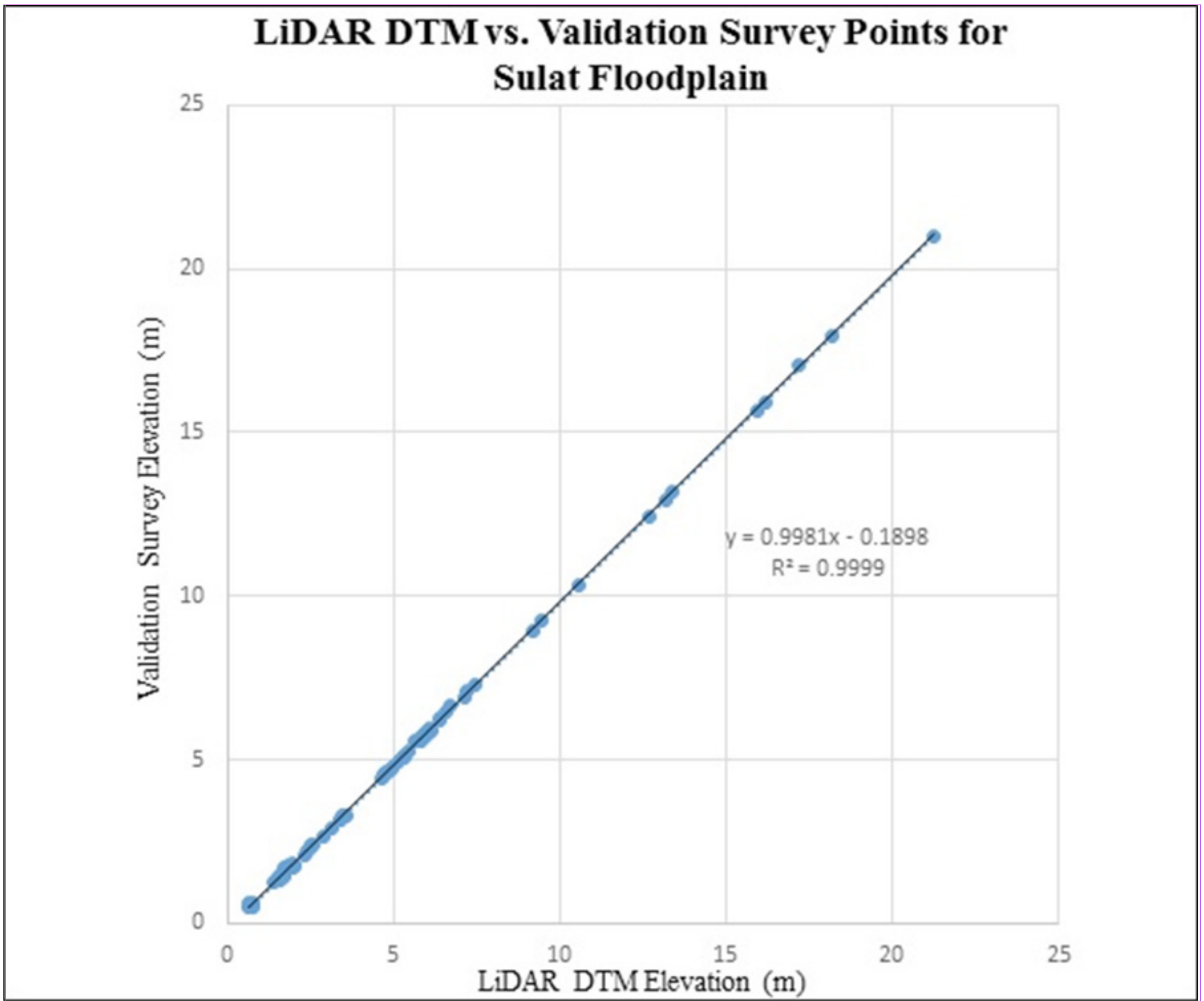

Figure 24. Correlation plot between the validation survey points and the LiDAR data.

Table 14. Validation Statistical Measures

Validation Statistical Measures	Value (meters)
RMSE	0.20
Standard Deviation	0.05
Average	0.20
Minimum	0.10
Maximum	0.30

3.11 Integration of Bathymetric Data into the LiDAR Digital Terrain Model

For bathy integration, centerline and zigzag data were available for Sulat with a total of 5,184 bathymetric survey points. The resulting raster surface produced was done by Kernel Interpolation with Barriers interpolation method. After burning the bathymetric data to the calibrated DTM, assessment of the interpolated surface is represented by the computed RMSE value of 0.50 meters. The extent of the bathymetric survey done by the Data Validation and Bathymetry Component (DVBC) in Sulat integrated with the processed LiDAR DEM is shown in Figure 25.

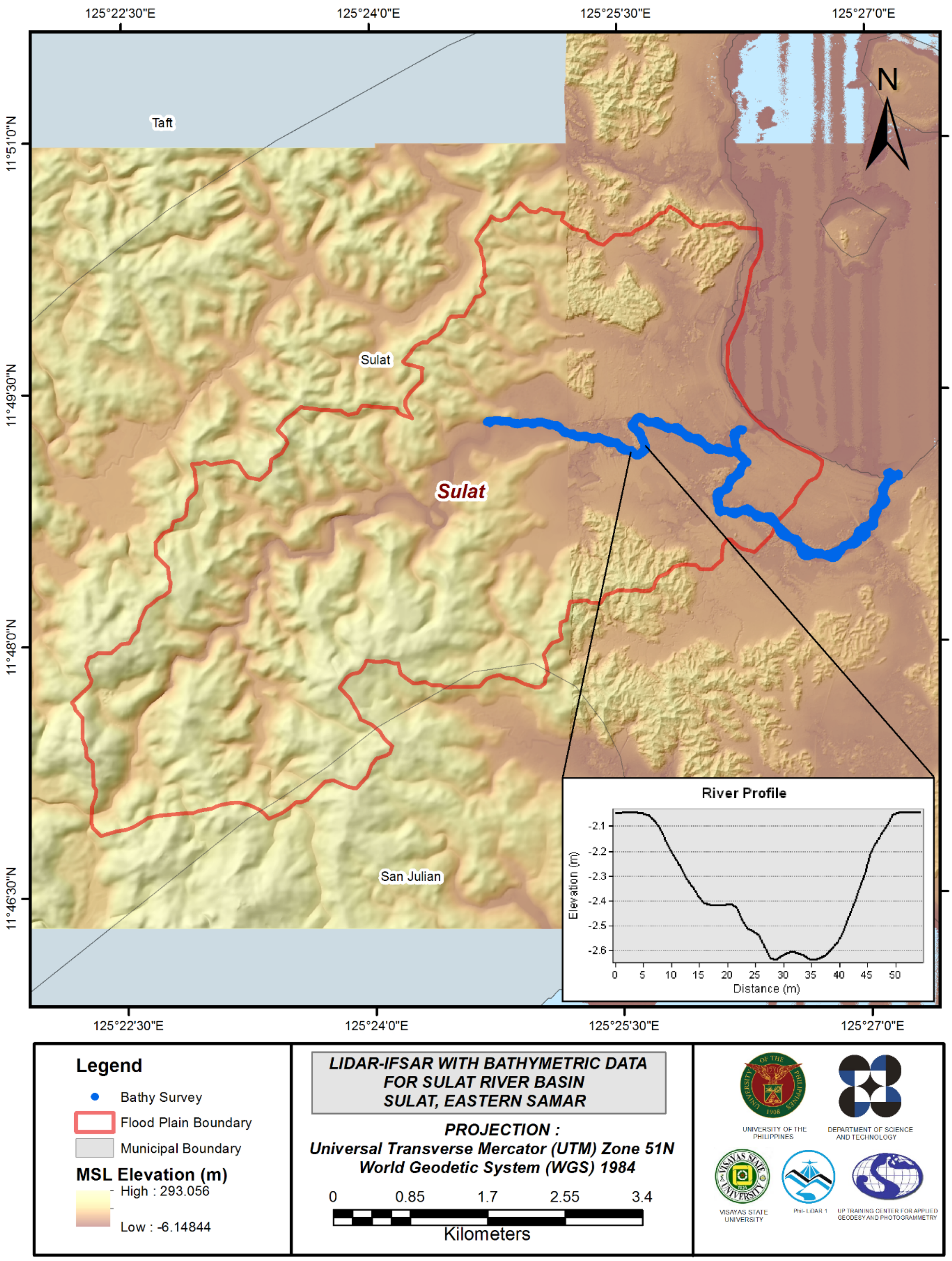

Figure 25. Map of Sulat floodplain with bathymetric survey points in blue.

3.12 Feature Extraction

The features salient in flood hazard exposure analysis include buildings, road networks, bridges, and water bodies within the floodplain area with a 200-meter buffer zone. Mosaicked LiDAR DEMs with a 1-m resolution were used to delineate footprints of building features, which comprised of residential buildings, government offices, medical facilities, religious institutions, and commercial establishments, among others. Road networks comprise of main thoroughfares such as highways and municipal and barangay roads essential for the routing of disaster response efforts. These features are represented by network of road centerlines.

3.12.1 Quality Checking (QC) of Digitized Features' Boundary

Sulat floodplain, including its 200-m buffer, has a total area of 33.79 sq km. For this area, a total of 1.0 sq. km., corresponding to a total of 128 building features, were considered for QC. Figure 26 shows the QC block for the Sulat floodplain.

Figure 26. Block (in blue) of Sulat building features that was subjected to QC.

Quality checking of Sulat building features resulted in the ratings shown in Table 15.

Table 15. Details of the quality checking ratings for the building features extracted for the Sulat River Basin

Floodplain	Completeness	Correctness	Quality	Remarks
Sulat	100.00	100.00	99.92	PASSED

3.12.2 Height Extraction

Height extraction was done for 477 building features in Sulat floodplain. Of these building features, 4 were filtered out after height extraction, resulting to 473 buildings with height attributes. The lowest building height is at 2.00 meters, while the highest building is at 7.14 meters.

3.12.3 Feature Attribution

The digitized features were marked and coded in the field using handheld GPS receivers. The attributes of non-residential buildings were first identified; all other buildings were then coded as residential. A DSM was generated using the LiDAR DEMs to extract the heights of the buildings. A minimum height of 2 meters was used to filter out the terrain features that were digitized as buildings. Buildings that were not yet constructed during the time of LiDAR acquisition were noted as new buildings in the attribute table.

Table 16 summarizes the number of building features per type, while Table 17 shows the total length of each road type. Table 18, on the other hand, shows the number of water features extracted per type.

Table 16. Building features extracted for Sulat Floodplain.

Facility Type	No. of Features
Residential	449
School	15
Market	0
Agricultural/Agro-Industrial Facilities	0
Medical Institutions	1
Barangay Hall	1
Military Institution	0
Sports Center/Gymnasium/Covered Court	0
Telecommunication Facilities	0
Transport Terminal	0
Warehouse	0
Power Plant/Substation	0
NGO/CSO Offices	0
Police Station	0
Water Supply/Sewerage	0
Religious Institutions	3
Bank	0
Factory	0
Gas Station	1
Fire Station	0
Other Government Offices	1
Other Commercial Establishments	2
Total	473

Table 17. Total length of extracted roads for Sulat Floodplain.

Floodplain	Road Network Length (km)					Total
	Barangay Road	City/ Municipal Road	Provincial Road	National Road	Others	
Sulat	7.36	0	0	3.93	0.00	**11.29**

Table 18. Number of extracted water bodies for Sulat Floodplain.

Floodplain	Water Body Type					Total
	Rivers/ Streams	Lakes/Ponds	Sea	Dam	Fish Pen	
Sulat	8	0	0	0	0	**8**

A total of 6 bridges and culverts over small channels that are part of the river network were also extracted for the floodplain.

3.12.4 Final Quality Checking of Extracted Features

All extracted ground features were given the complete required attributes. Respectively, all these output features comprise the flood hazard exposure database for the floodplain. The final quality checking completes the feature extraction phase of the project.

Figure 27 shows the completed Digital Surface Model (DSM) of the Sulat floodplain overlaid with its ground features.

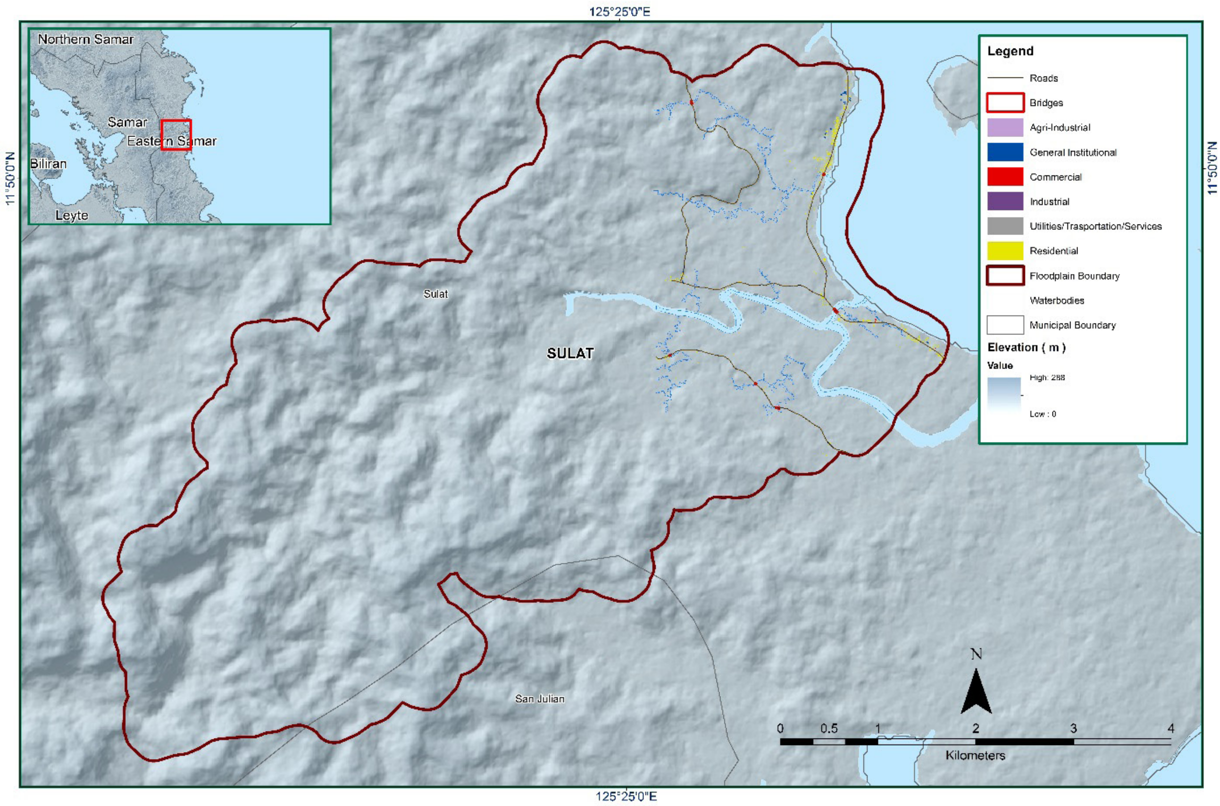

Figure 27. Extracted features of the Sulat Floodplain.

CHAPTER 4: LIDAR VALIDATION SURVEY AND MEASUREMENTS OF THE SULAT RIVER BASIN

Engr. Louie P. Balicanta, Engr. Joemarie S. Caballero, Ms. Patrizcia Mae. P. dela Cruz, Engr. Kristine Ailene B. Borromeo, Mr. Michael Anthony C. Labrador, Mr. Erlan Patrick T. Mendoza, Engr. Romalyn Francis P. Boado, For. Maridel P. Miras, For. Rodel C. Alberto, Engr. Caren Joy S. Ordoña

The methods applied in this chapter were based on the DREAM methods manual (Ang, et. al., 2014) and further enhanced and updated in Paringit, et. al. (2017).

4.1 Summary of Activities

The Data Validation and Bathymetry Component (DVBC) conducted a field survey in Sulat River on December 5 to 16, 2016 with the following scope: reconnaissance; control survey; cross-section and as-built survey at Sulat Bridge in Brgy. Maramara, Sulat, Eastern Samar; validation points acquisition of about 43 km covering the municipalities of Sulat, San Julian and Borongan City, Eastern Samar; and bathymetric survey from its upstream in Brgy. San Juan to the mouth of the river located in Brgy. Tabi, Sulat with an approximate length of 6.709 km using Ohmex™ single beam echo sounder and Trimble® SPS 882 GNSS PPK survey technique. The entire survey extent is illustrated in Figure 28.

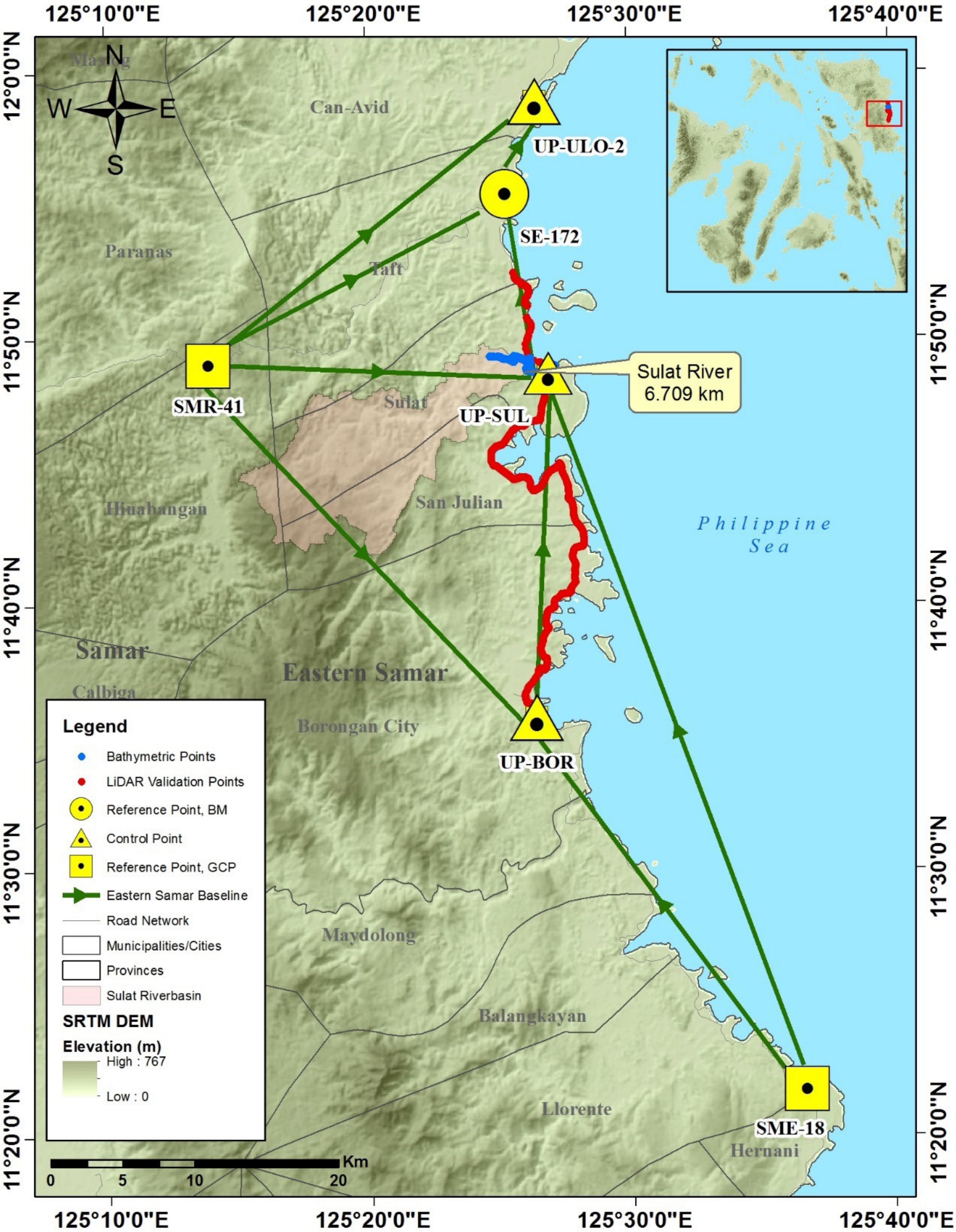

Figure 28. Sulat River Survey Extent

4.2 Control Survey

The GNSS network used for Sulat River survey is composed of four (4) loops established on December 10, 2016, occupying the following reference points: SME-18, a 2nd order NAMRIA GCP in Brgy. Cancildes, Municipality of Hernani, Eastern Samar; SMR-41, a 2nd order NAMRIA GCP in Brgy. Fatima, Municipality of Hinabangan, Samar; and, SE-172, a 1st order BM in Brgy. Nato, Municipality of Taft, Eastern Samar.

Three (3) control points were established in the area: UP-BOR located at the approach of Can-Obing Bridge in Brgy. Can-Abong, Borongan City, Eastern Samar; UP-SUL located at the approach of Sulat Bridge in Brgy. Maramara, Municipality of Sulat, Eastern Samar; and UP-ULO-2 located at the approach of Can-Avid Bridge in Brgy. Canteros, Municipality of Can-Avid, Eastern Samar.

Table 19 depicts the summary of reference and control points utilized, with their corresponding locations, while Figure 29 shows the GNSS network established in the Sulat River Survey.

Table 19. List of reference and control points used during the survey in Sulat River (Source: NAMRIA, UP-TCAGP).

Control Point	Order of Accuracy	Geographic Coordinates (WGS UTM Zone 52N)				
		Latitude	Longitude	Ellipsoid Height (m)	Elevation (MSL) (m)	Date of Establish-ment
Control Survey on December 10, 2016						
SME-18	2nd Order, GCP	11°21'43.08128"	125°36'37.41861"	78.216	17.659	12-10-16
SMR-41	2nd Order, GCP	11°49'03.09527"	125°13'56.04672"	232.562	-	12-10-16
SE-172	1st Order, BM	-	-	61.761	3.155	12-6-16
UP-BOR	UP established	-	-	67.048	-	12-6-16
UP-SUL	UP established	-	-	64.565	-	12-6-16
UP-ULO-2	UP established	-	-	63.77	-	12-9-16

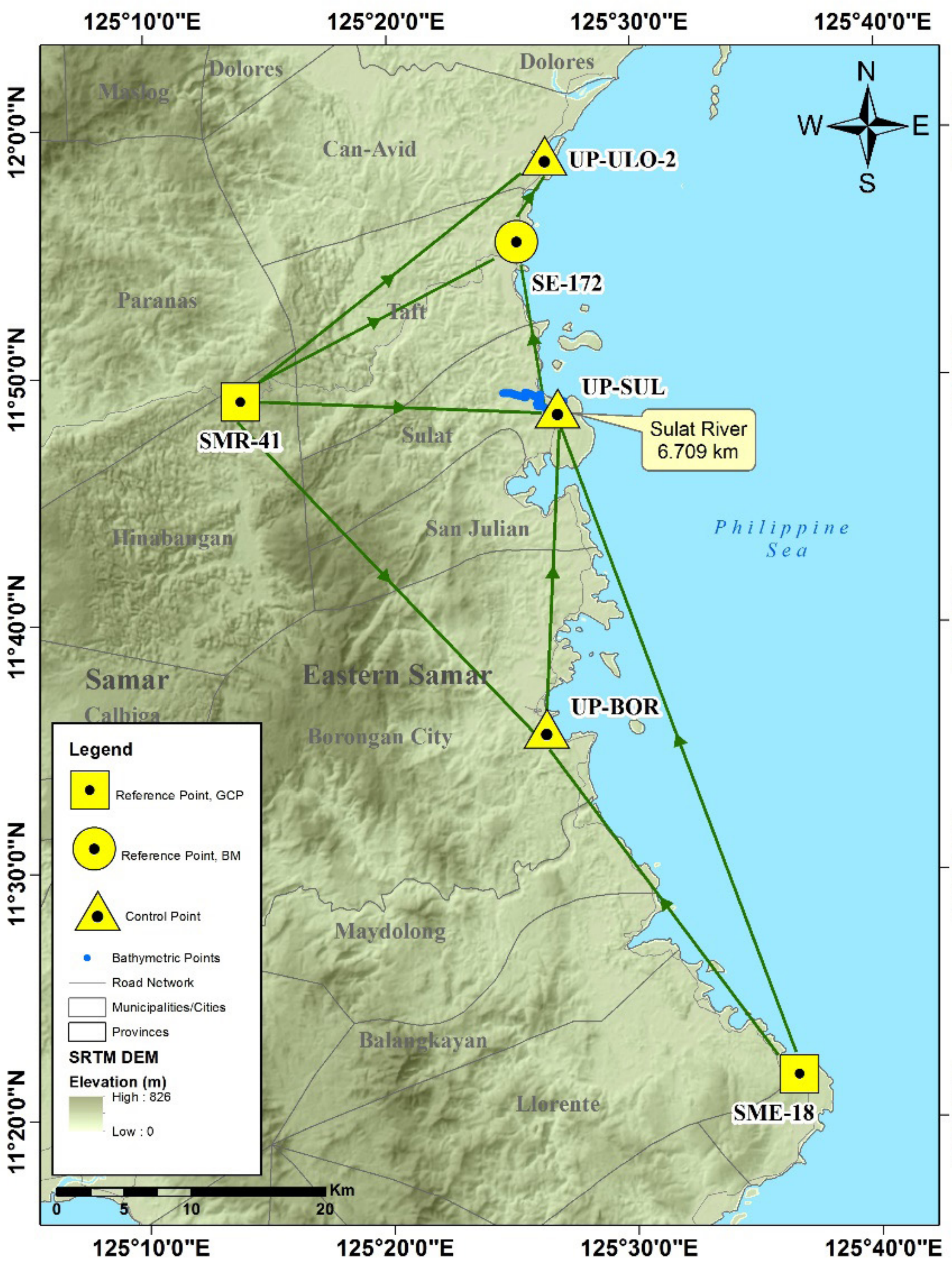

Figure 29. Sulat River Basin Control Survey Extent.

Figure 30 to Figure 35 depict the setup of the GNSS on recovered reference points and established control points in the Sulat River.

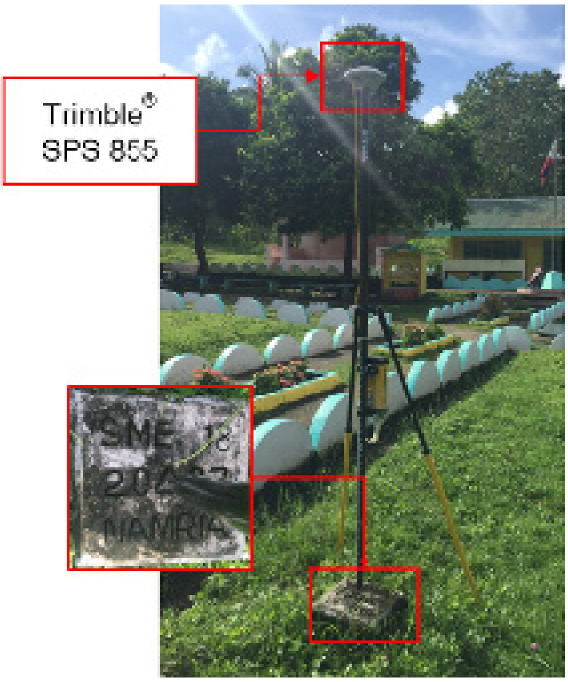

Figure 30. GNSS base set up, Trimble® SPS 852, SME-18, located within the grounds of San Jose Elementary School in Brgy. Canciledes, Municipality of Hernani, Eastern Samar

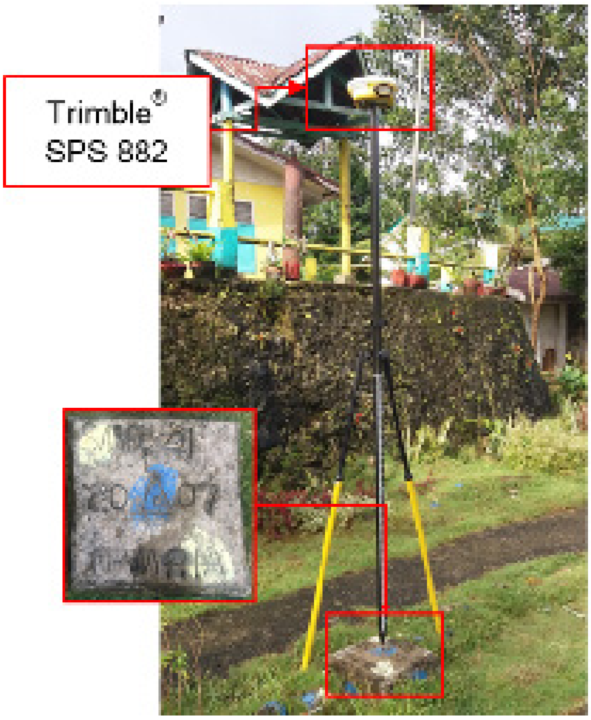

Figure 31. GNSS receiver set up, Trimble® SPS 882, at SMR-41, located in Brgy. Fatima, Municipality of Hinabangan, Samar.

Figure 32. GNSS receiver set up, Trimble® SPS 855 at SE-172, located in Brgy. Nato, Municipality of Taft, Eastern Samar

Figure 33. GNSS receiver set up, Trimble® SPS 855, at UP-BOR, located at the approach of Can-Obing Bridge in Brgy. Can-Abong, Borongan City, Eastern Samar

Figure 34. GNSS receiver set up, Trimble® SPS 985, at UP-SUL, located at the approach of Sulat Bridge in Brgy. Maramara, Municipality of Sulat, Eastern Samar

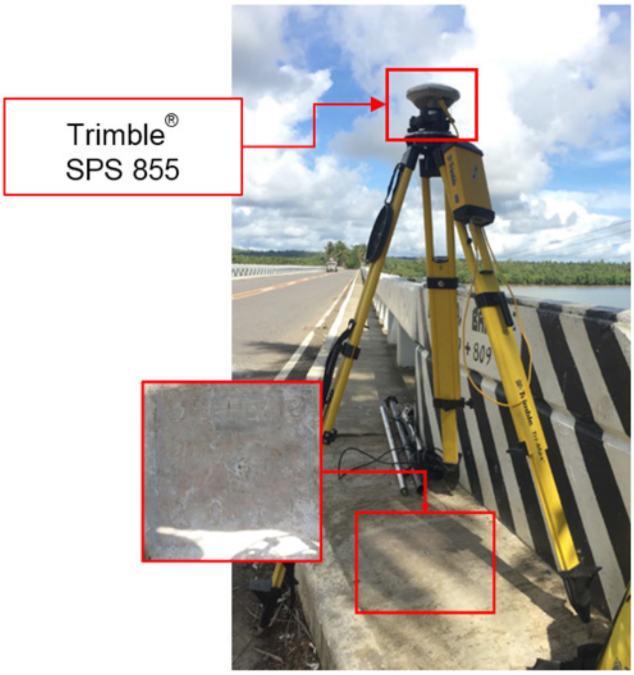

Figure 35. GNSS receiver setup, Trimble® SPS 855, at UP-ULO-2, located at the approach of Can-Avid Bridge in Brgy. Canteros, Municipality of Can-Avid, Eastern Samar

4.3 Baseline Processing

The GNSS Baselines were processed simultaneously in TBC by observing that all baselines have fixed solutions with horizontal and vertical precisions within +/- 20 cm and +/- 10 cm requirement respectively. In cases where one or more baselines did not meet all of these criteria, masking was performed. Masking is the removal or covering of portions of the baseline data using the same processing software. The data is then repeatedly processed until all baseline requirements are met. If the reiteration yields out of the required accuracy, a resurvey is initiated. Table 22 presents the baseline processing results of control points in the Sulat River Basin, as generated by the TBC software.

Table 20. The Baseline processing report for the Sulat River GNSS static observation survey.

Observation	Date of Observation	Solution Type	H. Prec. (Meter)	V. Prec. (Meter)	Geodetic Az.	Ellipsoid Dist. (Meter)	Δ Height (m)
SMR-41--- SE-172 (B1)	12-10-16	Fixed	0.003	0.019	60°19'56"	23782.994	-170.787
SMR-41 --- UP-ULO-2 (B2)	12-10-16	Fixed	0.004	0.027	51°26'56"	29152.677	-168.797
SE-172 --- UP-ULO-2 (B3)	12-10-16	Fixed	0.003	0.014	18°29'10"	6742.890	2.008
SMR-41 --- SE-172 (B6)	12-10-16	Fixed	0.003	0.017	60°19'55"	23782.982	-170.797
SMR-41 --- UP-SUL (B7)	12-10-16	Fixed	0.003	0.025	91°37'24"	23648.007	-168.014
SME-18 --- UP-SUL (B8)	12-10-16	Fixed	0.005	0.019	340°32'04"	52735.660	-13.625
UP-SUL --- SE-172 (B9)	12-10-16	Fixed	0.003	0.018	346°36'16"	12792.116	-2.807
UP-BOR --- UP-SUL (B10)	12-10-16	Fixed	0.003	0.014	2°25'05"	23870.045	-2.491
SMR-41 --- UP-BOR (B11)	12-10-16	Fixed	0.003	0.018	137°16'15"	33379.379	-165.537
SME-18 --- UP-BOR (B12)	12-10-16	Fixed	0.003	0.012	324°17'43"	31862.093	-11.163

As shown in Table 20, a total of ten (10) baselines were processed with the coordinates and the elevation value of reference points SME-18, SMR-41, and SE-172 held fixed; it is apparent that all baselines passed the required accuracy.

4.4 Network Adjustment

After the baseline processing procedure, the network adjustment is performed using the TBC software. Looking at the Adjusted Grid Coordinates table of the TBC-generated Network Adjustment Report, it is observed that the square root of the sum of the squares of x and y must be less than 20 cm and z less than 10 cm for each control point; or in equation form:

$$\sqrt{((x_e)^2 + (y_e)^2)} < 20\ cm \quad \text{and } z_e < 10\ cm$$

Where:

x_e is the Easting Error,
y_e is the Northing Error, and
z_e is the Elevation Error

For complete details, see the Network Adjustment Report shown in Table 21 to Table 24.

The three (3) control points, UP-BOR, UP-SUL, and UP-ULO-2 were occupied and observed simultaneously to form a GNSS loop. The coordinate values of SME-18 and SMR-41; elevation value of SME-18 and SE-172; and fixed values of SME-18, SMR-41, and SE-172 were held fixed during the processing of the control points as presented in Table 21. Through these reference points, the coordinates and elevation of the unknown control points will be computed.

Table 21. Constraints applied to the adjustment of the control points.

Point ID	Type	North (Meter)	East (Meter)	Height (Meter)	Elevation (Meter)
SME-18	Grid	Fixed	Fixed		Fixed
SMR-41	Global	Fixed	Fixed		
SE-172	Grid				Fixed
Fixed = 0.000001(Meter)					

Likewise, the list of adjusted grid coordinates, i.e. Northing, Easting, Elevation and computed standard errors of the control points in the network is indicated in Table 22.

Table 22. Adjusted grid coordinates for the control points used in the Sulat River flood plain survey.

Point ID	Easting (Meter)	Easting Error (Meter)	Northing (Meter)	Northing Error (Meter)	Elevation (Meter)	Elevation Error (Meter)	Constraint
SME-18	784907.431	?	1257282.043	?	17.659	?	ENe
SMR-41	743218.063	?	1307346.858	?	171.203	0.041	LL
SE-172	763795.614	0.007	1319288.604	0.006	3.155	?	e
UP-BOR	766068.889	0.006	1282998.400	0.005	5.989	0.039	
UP-SUL	766869.986	0.007	1306865.645	0.006	5.374	0.042	
UP-ULO-2	765878.376	0.010	1325704.856	0.009	5.912	0.05	

The results of the computation for accuracy are as follows

a. SME-18

horizontal accuracy = Fixed
vertical accuracy = Fixed

b. SMR-41

horizontal accuracy = Fixed
vertical accuracy = 4.1 < 10 cm

c. SE-172

horizontal accuracy = $\sqrt{((0.7)^2 + (0.6)^2}$
= $\sqrt{(0.49 + 0.36)}$
= 1.77 < 20 cm
vertical accuracy = Fixed

d. UP-BOR

horizontal accuracy = $\sqrt{((0.6)^2 + (0.5)^2}$
= $\sqrt{(0.36 + 0.25)}$
= 0.78 < 20 cm
vertical accuracy = 3.9 < 10 cm

e. UP-SUL

horizontal accuracy = $\sqrt{((0.7)^2 + (0.6)^2}$
= $\sqrt{(0.49 + 0.36)}$
= 0.92 < 20 cm
vertical accuracy = 4.2 < 10 cm

f. UP-ULO-2

horizontal accuracy = $\sqrt{((1)^2 + (0.9)^2}$
= $\sqrt{(1.81 + 1.44)}$
= 1.35 < 20 cm
vertical accuracy = 5.3 < 10 cm

Following the given formula, the horizontal and vertical accuracy result of the two (2) occupied control points are within the required precision.

Table 23. Adjusted geodetic coordinates for control points used in the Sulat River Flood Plain validation.

Point ID	Latitude	Longitude	Height (Meter)	Height Error (Meter)	Constraint
SME-18	N11°21'43.08128"	E125°36'37.41861"	78.216	?	ENe
SMR-41	N11°49'03.09527"	E125°13'56.04672"	232.562	0.041	LL
SE-172	N11°55'25.95794"	E125°25'18.96211"	61.761	?	e
UP-BOR	N11°35'44.89710"	E125°26'23.64085"	67.048	0.039	
UP-SUL	N11°48'41.00280"	E125°26'56.90219"	64.565	0.042	
UP-ULO-2	N11°58'54.06226"	E125°26'29.62952"	63.770	0.053	

The corresponding geodetic coordinates of the observed points are within the required accuracy as shown in Table 23. Based on the results of the computation, the accuracy conditions are satisfied; hence, the required accuracy for the program was met. The computed coordinates of the reference and control points utilized in the Sulat River GNSS Static Survey are seen in Table 24.

Table 24. The reference and control points utilized in the Sulat River Static Survey, with their corresponding locations (Source: NAMRIA, UP-TCAGP)

Control Point	Order of Accuracy	Geographic Coordinates (WGS 84)			UTM ZONE 51 N		
		Latitude	Longitude	Ellipsoidal Height (m)	Northing (m)	Easting (m)	BM Ortho (m)
SME-18	2nd Order, GCP	11°21'43.08128"	125°36'37.41861"	78.216	1257282.043	784907.431	17.659
SMR-41	2nd Order, GCP	11°49'03.09527"	125°13'56.04672"	232.562	1307346.858	743218.063	171.203
SE-172	1st Order, BM	11°55'25.95794"	125°25'18.96211"	61.761	1319288.604	763795.614	3.155
UP-BOR	UP established	11°35'44.89710"	125°26'23.64085"	67.048	1282998.400	766068.889	5.989
UP-SUL	UP established	11°48'41.00280"	125°26'56.90219"	64.565	1306865.645	766869.986	5.374
UP-ULO-2	UP established	11°58'54.06226"	125°26'29.62952"	63.77	1325704.856	765878.376	5.912

4.5 Cross-section and Bridge As-Built survey and Water Level Marking

The bridge cross-section and as-built surveys were conducted on December 8, 2016 at the downstream side of Sulat Bridge in Brgy. Maramara, Municipality of Sulat, Eastern Samar. GNSS receiver Trimble® SPS 985 in PPK survey technique was utilized for this survey (Figure 36 and Figure 37).

Figure 36. Sulat Bridge facing upstream.

Figure 37. As-built survey conducted at Sulat Bridge.

The length of the cross-sectional line surveyed at Sulat Bridge is about 281.712 (Figure 36) with three hundred sixty three (363) cross-sectional points acquired using the control point UP-SUL as the GNSS base station. The location map, cross-section diagram and the accomplished bridge data form are shown in Figure 38, Figure 39 and Figure 40.

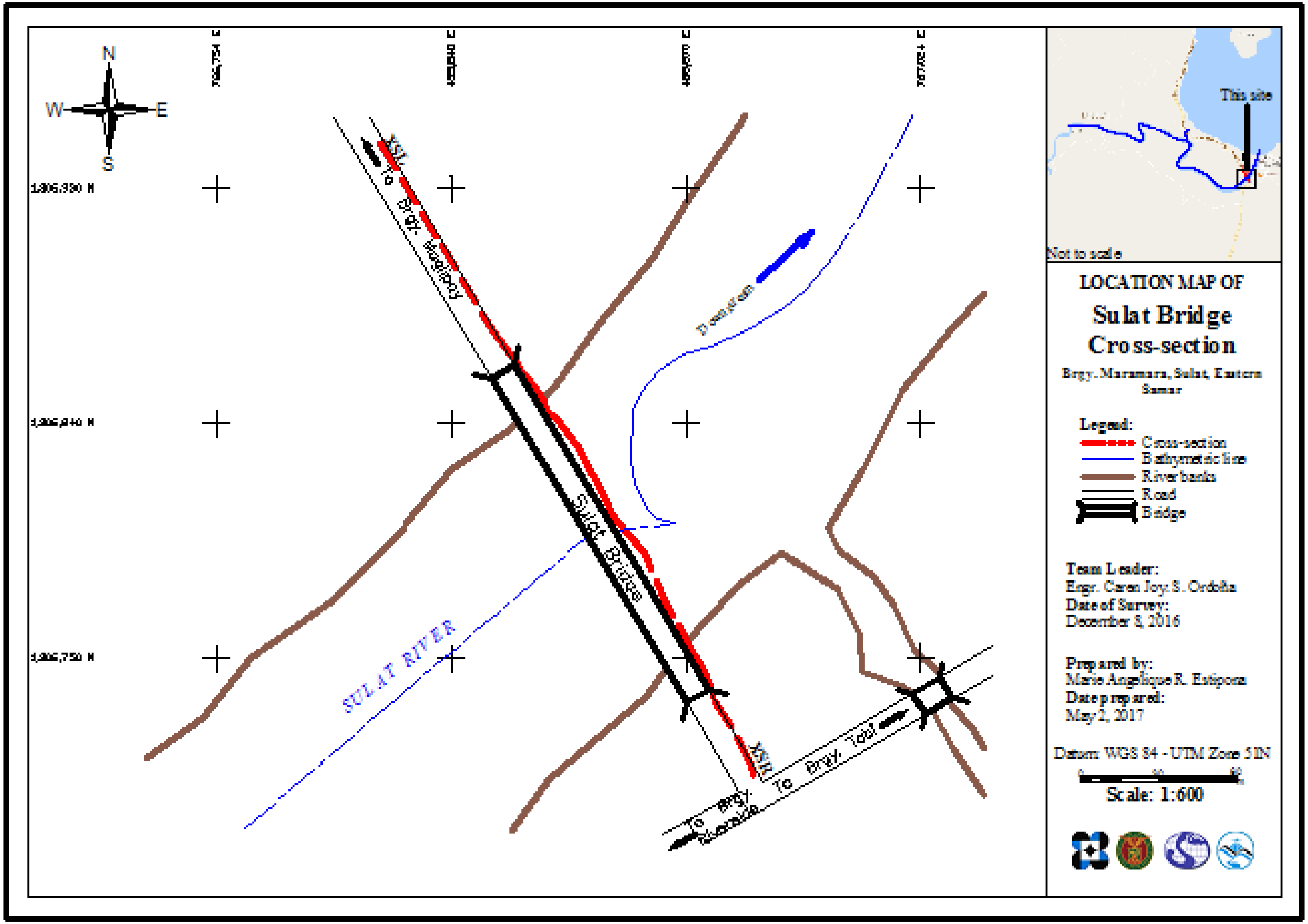

Figure 38. Location map of the Sulat Bridge Cross Section

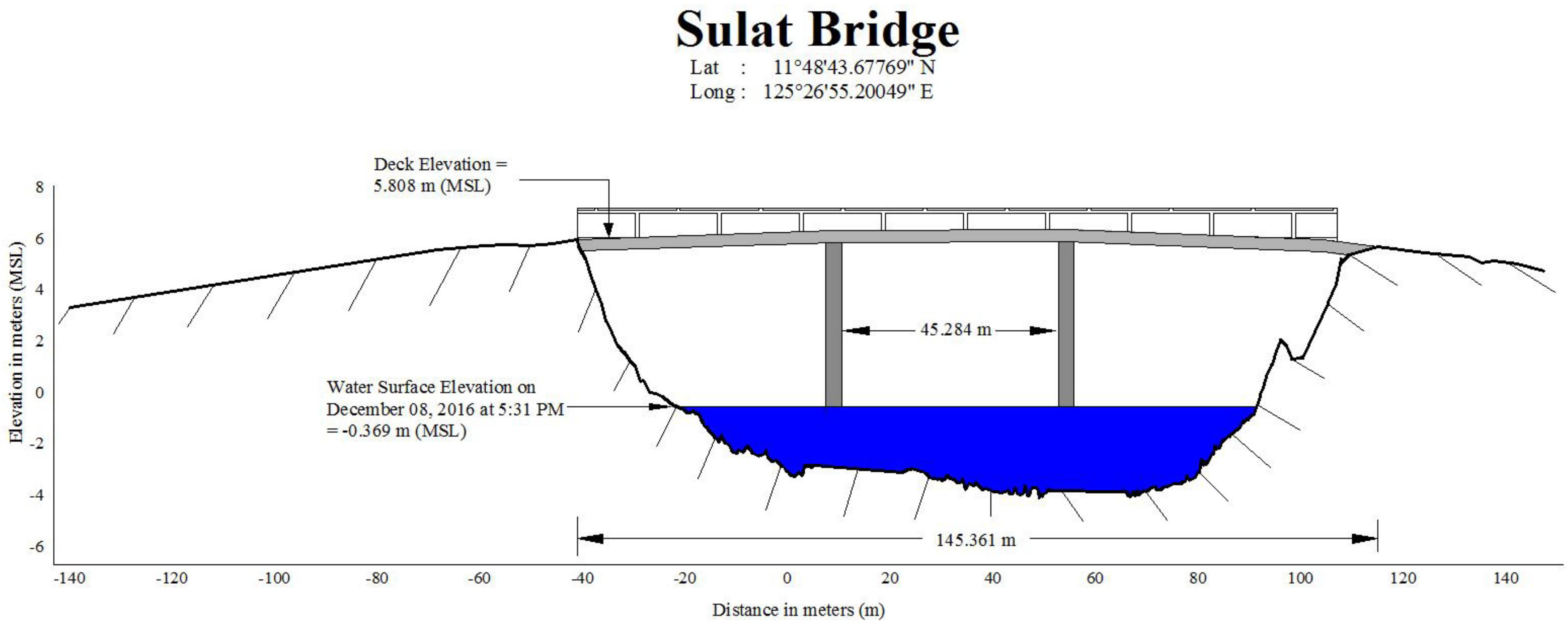

Figure 39. The Sulat Bridge cross-section diagram.

Bridge Data Form

Bridge Name: Sulat Bridge	Date: December 08, 2016
River Name: Sulat River	Time: 05:31 PM
Location (Brgy, City,Region): Brgy. Maramara, Sulat, Eastern Samar	
Survey Team: Caren Joy Ordoña, Marion Dimain, John Christopher Santos	
Flow condition: average	Weather Condition: fair
Latitude: 11°48'43.67769"N	Longitude: 125°26'55.20049"E

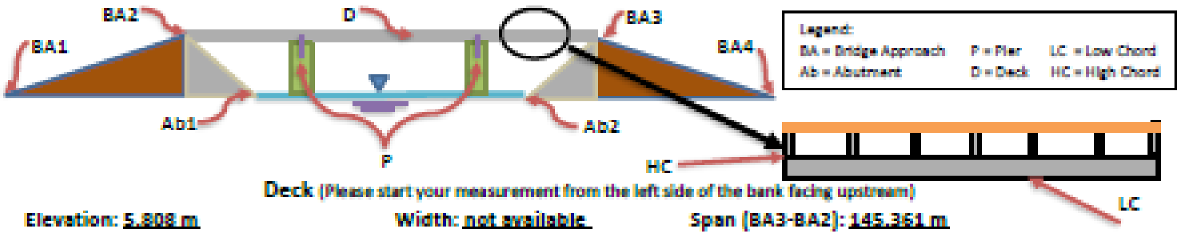

Deck (Please start your measurement from the left side of the bank facing upstream)

Elevation: 5.808 m Width: not available Span (BA3-BA2): 145.361 m

	Station	High Chord Elevation	Low Chord Elevation
1	Not available	Not available	Not available

Bridge Approach (Please start your measurement from the left side of the bank facing upstream)

	Station(Distance from BA1)	Elevation		Station(Distance from BA1)	Elevation
BA1	0	3.258 m	BA3	244.389 m	5.906 m
BA2	99.028 m	5.930 m	BA4	275.068 m	5.012 m

Abutment: Is the abutment sloping? ; If yes, fill in the following information:

	Station (Distance from BA1)	Elevation
Ab1	Not available	Not available
Ab2	Not available	Not available

Pier (Please start your measurement from the left side of the bank facing upstream)

Shape: round Number of Piers: 2 Height of column footing: Not available

	Station (Distance from BA1)	Elevation	Pier Diameter
Pier 1	148.958 m	6.261 m	
Pier 2	194.243 m	6.316 m	

NOTE: Use the center of the pier as reference to its station

DREAM
Disaster Risk and Exposure Assessment for Mitigation

Figure 40. The Sulat Bridge as-built survey data.

The water surface elevation of Sulat River was determined by a survey grade GNSS receiver Trimble® SPS 882 in PPK survey technique on December 8, 2016 at 5:31 PM at Sulat Bridge with a value of -0.369 m in MSL as shown in Figure 39. This was translated into marking on the bridge's deck as shown in Figure 41. It now serves as the reference for flow data gathering and depth gauge deployment of the Visayas State University, the partner HEI responsible for the monitoring of the Sulat River.

Figure 41. Water-level markings on Sulat Bridge.

4.6 Validation Points Acquisition Survey

The validation points acquisition survey was conducted on December 7, 2016 using a survey GNSS rover receiver Trimble® SPS 882 mounted on a range pole, which was attached in front of the vehicle as shown in Figure 42. It was secured with a nylon rope to ensure that it was horizontally and vertically balanced. The antenna height was 2.305 m and measured from the ground up to the bottom of notch of the GNSS Rover receiver. The PPK technique utilized for the conduct of the survey was set to continuous topo mode with UP-SUL occupied as the GNSS base station in the conduct of the survey.

Figure 42. GNSS Receiver Trimble® SPS 882 installed on a vehicle for Ground Validation Survey.

The survey started from Barangay Can-Abong, Borongan City going north along national highway covering thirty-four (34) barangays in in Borongan City, San Julian and Taft, ended in Brgy. Mantang, Municipality of Taft, Eastern Samar. A total of 8,323 points were gathered with approximate length of 43 km using UP-SUL as GNSS base station for the entire extent validation points acquisition survey as illustrated in the map in Figure 43.

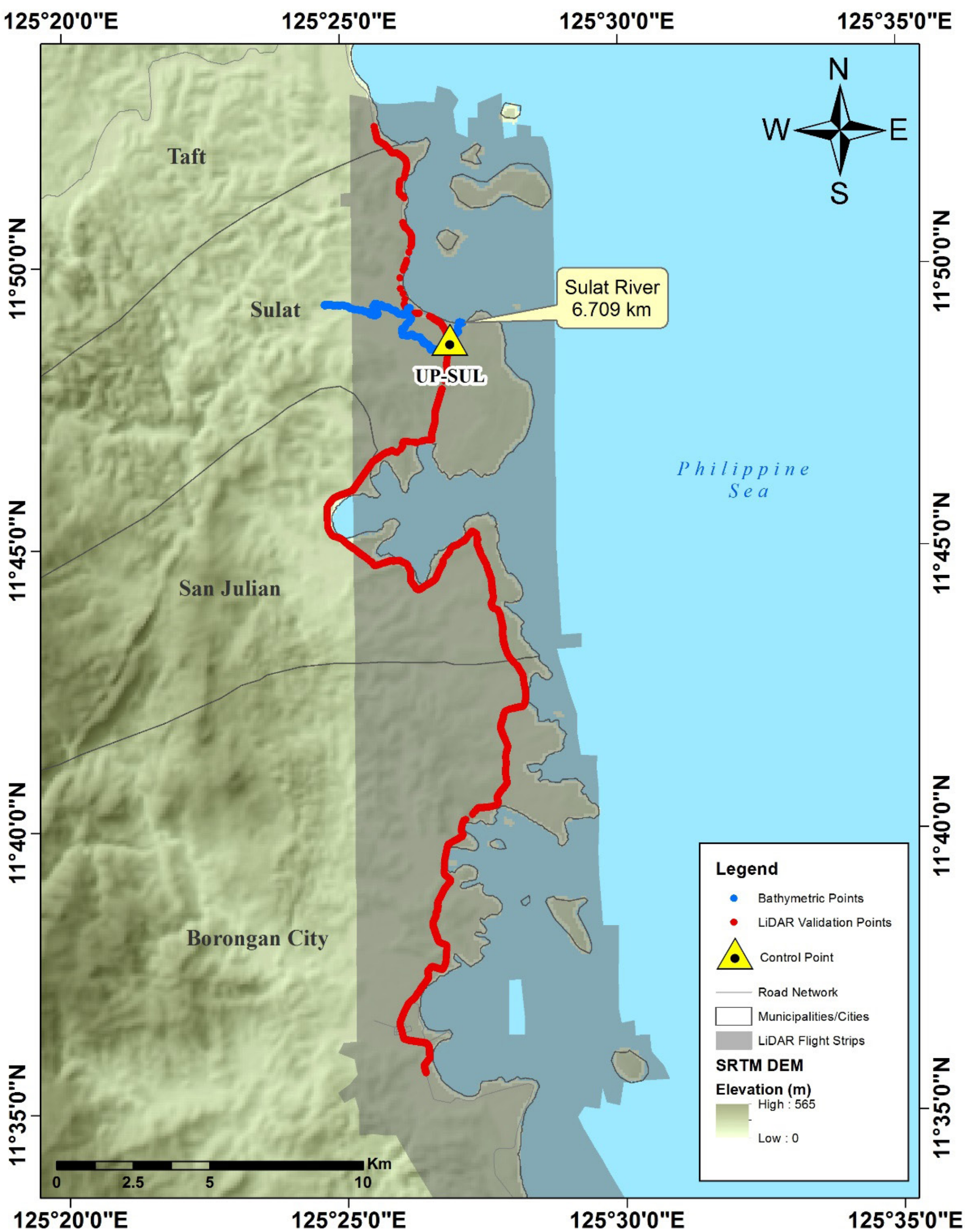

Figure 43. The extent of the LiDAR ground validation survey (in red) for Sulat River Basin.

4.7 River Bathymetric Survey

A bathymetric survey was performed on December 7, 2016 using an Ohmex ™ single beam echo sounder and Trimble® SPS 882 in GNSS PPK survey technique in continuous topo mode as shown in Figure 44.

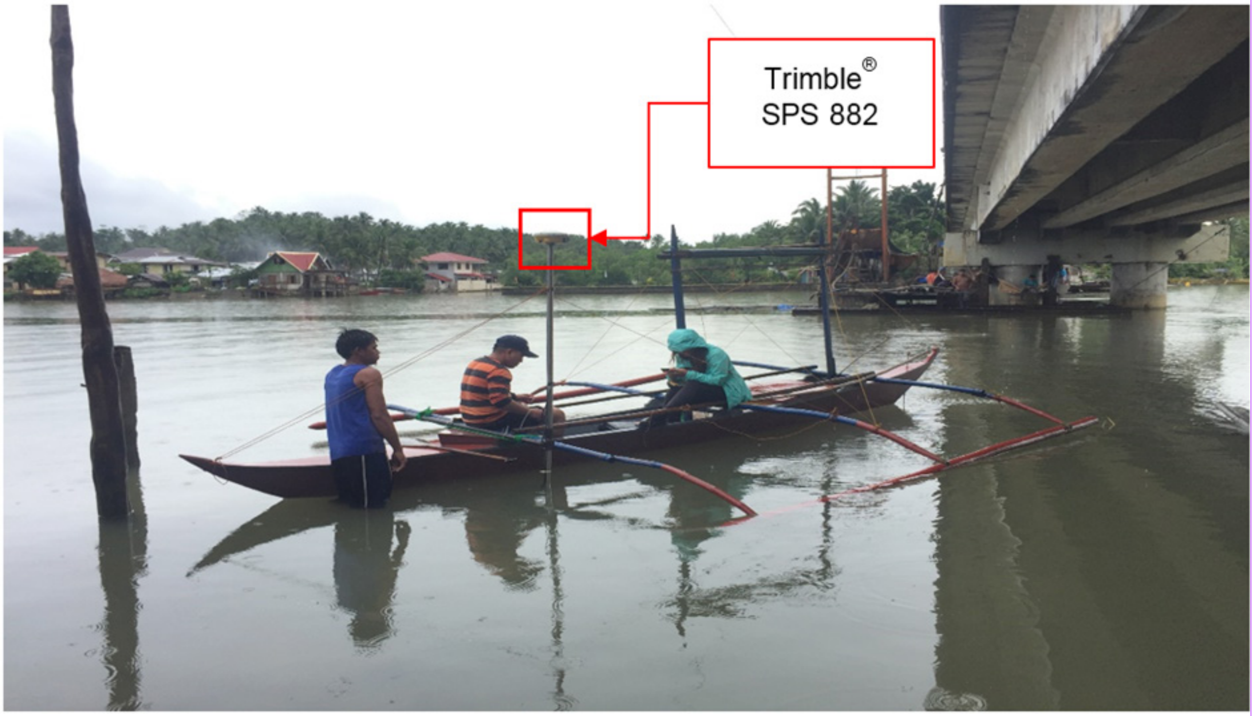

Figure 44. Set up of the bathymetric survey at Sulat River using Trimble® SPS 882 in GNSS PPK survey technique.

The survey started in Brgy. San Juan, Municipality of Sulat with coordinates 11°49’19.10658”N, 125°24’41.59389”E, traversed down the river by boat and ended at the mouth of the river in Brgy. Tabi, Municipality of Sulat, Eastern Samar with coordinates 11°49’00.15238”N, 125°27’07.65940”E. The control points UP-SUL was used as GNSS base stations all throughout the entire survey.

Overall, the bathymetric survey for Sulat River gathered a total of 6,721 points of the river traversing Brgy. San Juan, Municipality of Sulat Eastern Samar. The extent of the bathymetric survey for the Sulat River is shown in Figure 45. To further illustrate this, a CAD drawing of the riverbed profile of the Sulat River was produced. As seen in Figure 46, the highest and lowest elevation has a 5.739-m difference. The highest elevation observed was -0.510 m below MSL located at the downstream part of the river; while the lowest was -6.249 m below MSL located in the middle portion of the river.

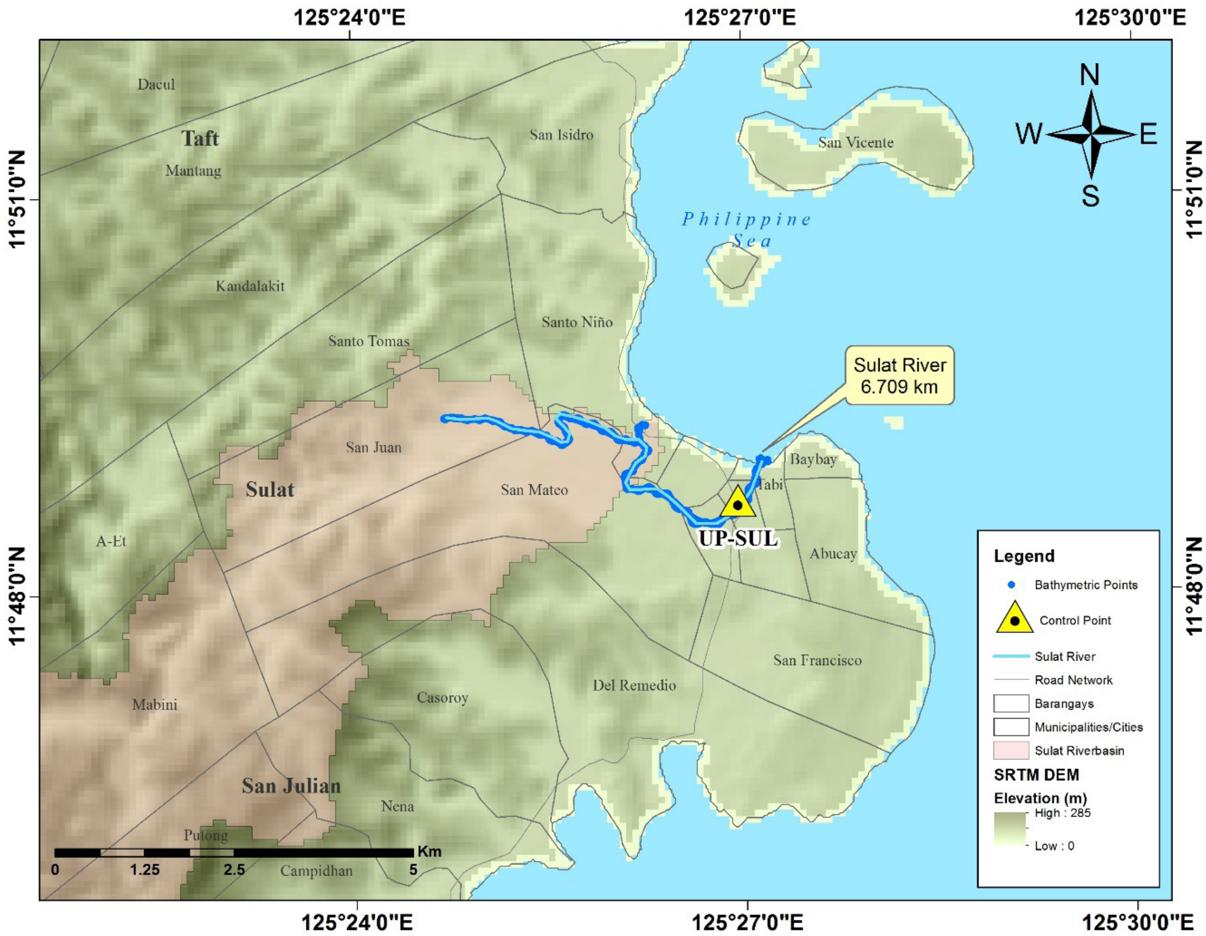

Figure 45. The extent of the Sulat River Bathymetry Survey.

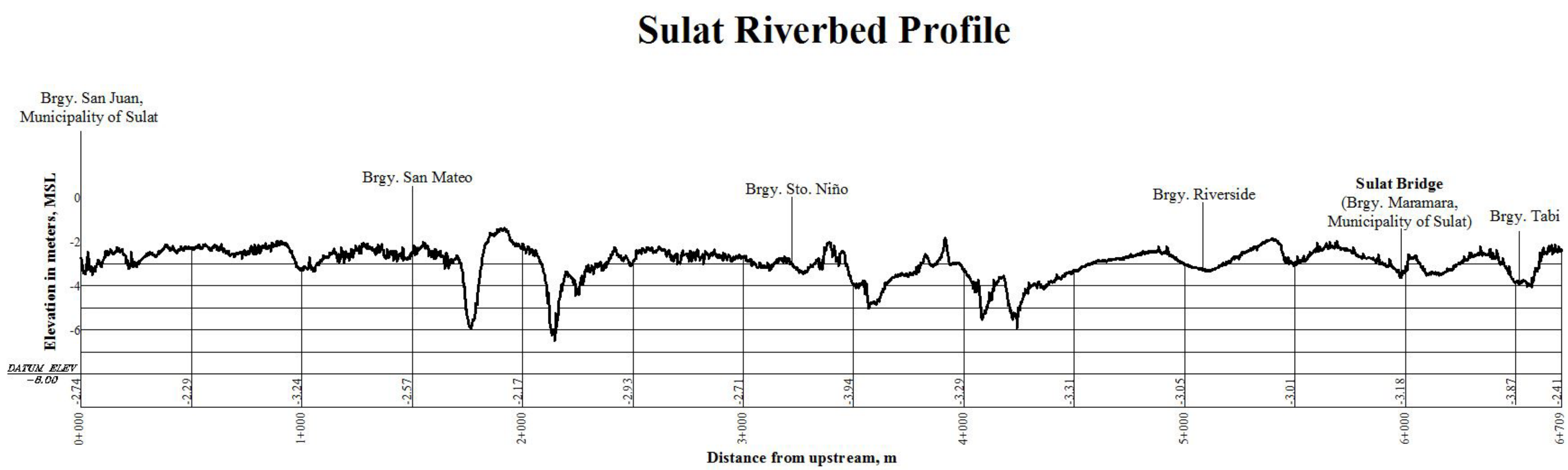

Figure 46. The Sulat Riverbed Profile.

CHAPTER 5: FLOOD MODELING AND MAPPING

Dr. Alfredo Mahar Lagmay, Christopher Uichanco, Sylvia Sueno, Marc Moises, Hale Ines, Miguel del Rosario, and Kenneth Punay, Neil Tingin

The methods applied in this chapter were based on the DREAM methods manual (Ang, et. al., 2014) and further enhanced and updated in Paringit, et. al. (2017).

5.1 Data Used for Hydrologic Modeling

5.1.1 Hydrometry and Rating Curves

All components and data, such as rainfall, water level, and flow in a certain period of time, which may affect the hydrologic cycle of the Sulat River Basin were monitored, collected, and analyzed.

5.1.2 Precipitation

Precipitation data was taken from a pre-installed automatic rain gauge (ARG). The location of the Aet ARG is illustrated in Figure 47.

The total precipitation for this event in the installed rain gauge was 80.5 mm. It has a peak rainfall of 14.5 mm. on January 10, 2017 at 7:45 AM. The lag time between the peak rainfall and discharge is 7 hours and 45 minutes.

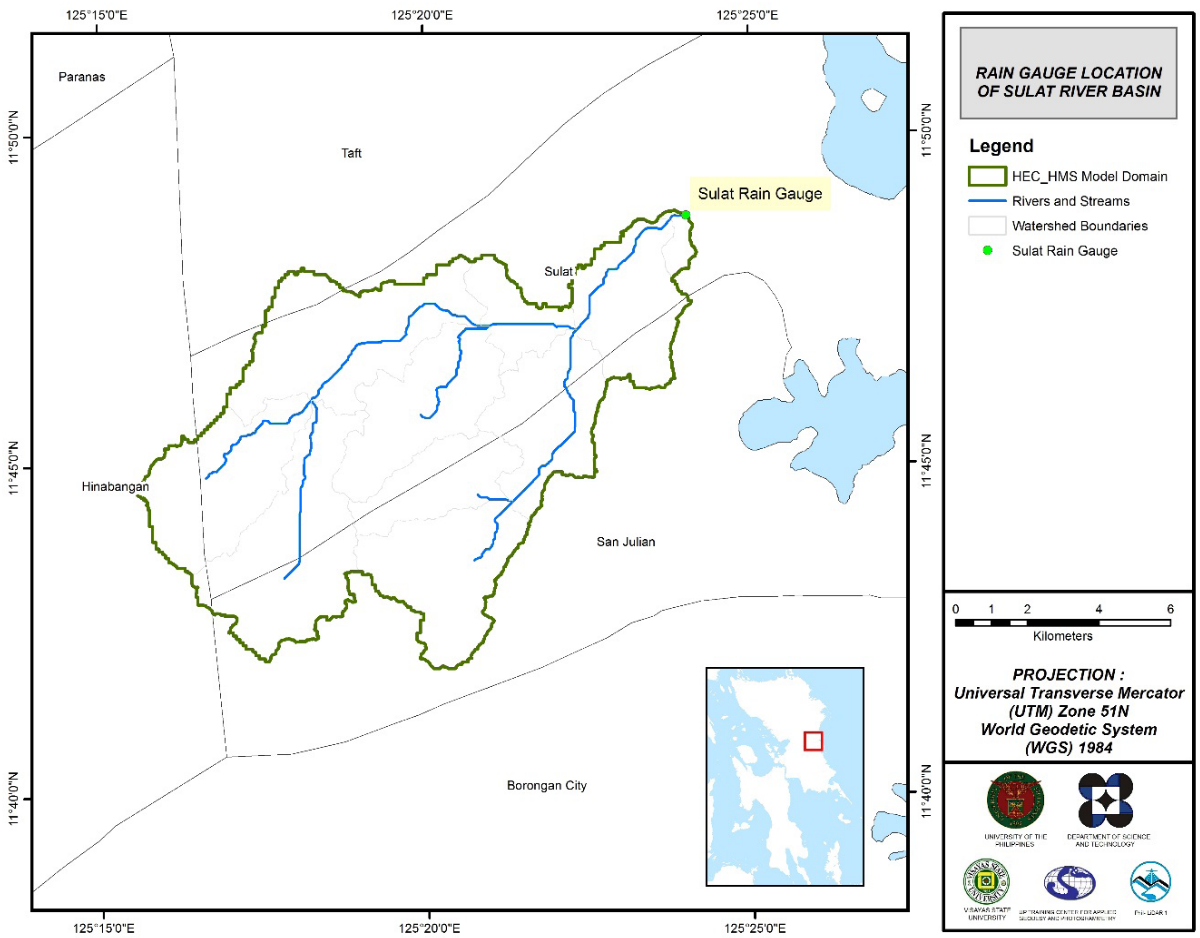

Figure 47. Location Map of the Sulat HEC-HMS model used for calibration.

5.1.3 Rating Curves and River Outflow

A rating curve was developed at Sulat Bridge, Sulat, Eastern Samar (11° 48'.39.09"N, 125°26'57.96E) to establish the relationship between the observed water levels (H) at Sulat Bridge and outflow (Q) of the watershed at this location.

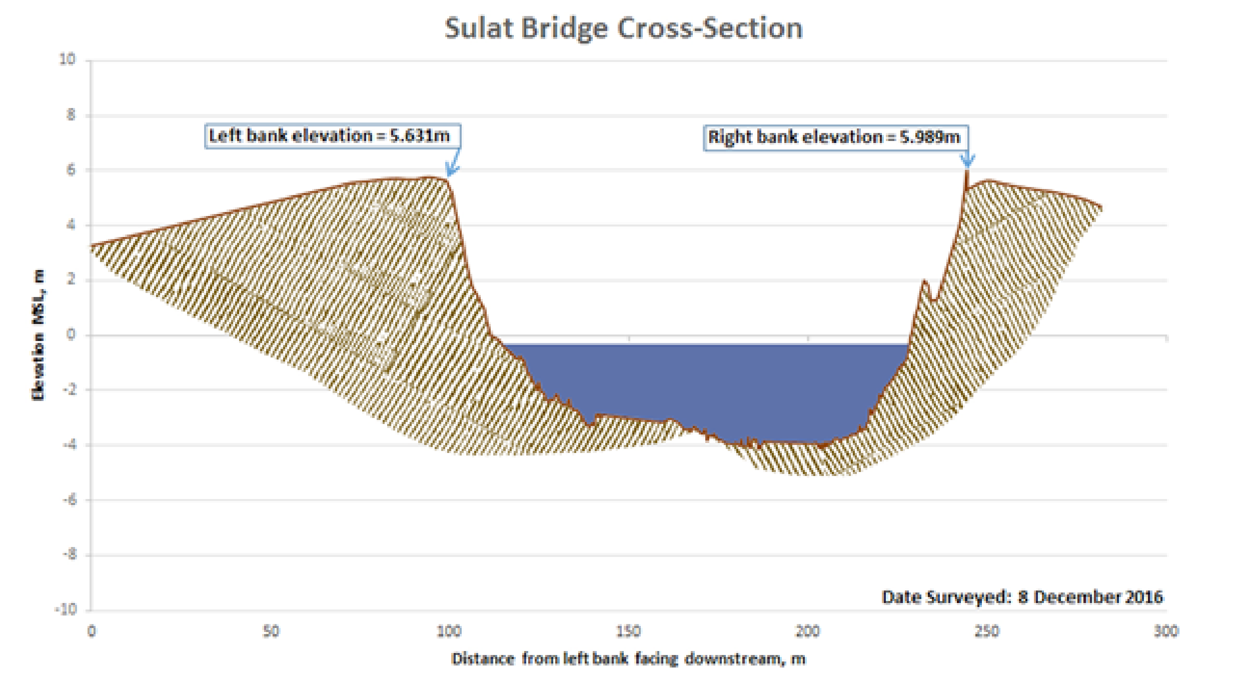

Figure 48. Cross-Section Plot of Sulat Bridge.

For Sulat Bridge, the rating curve is expressed as $Q = 60.103^{6.997h}$ as shown in Figure 49.

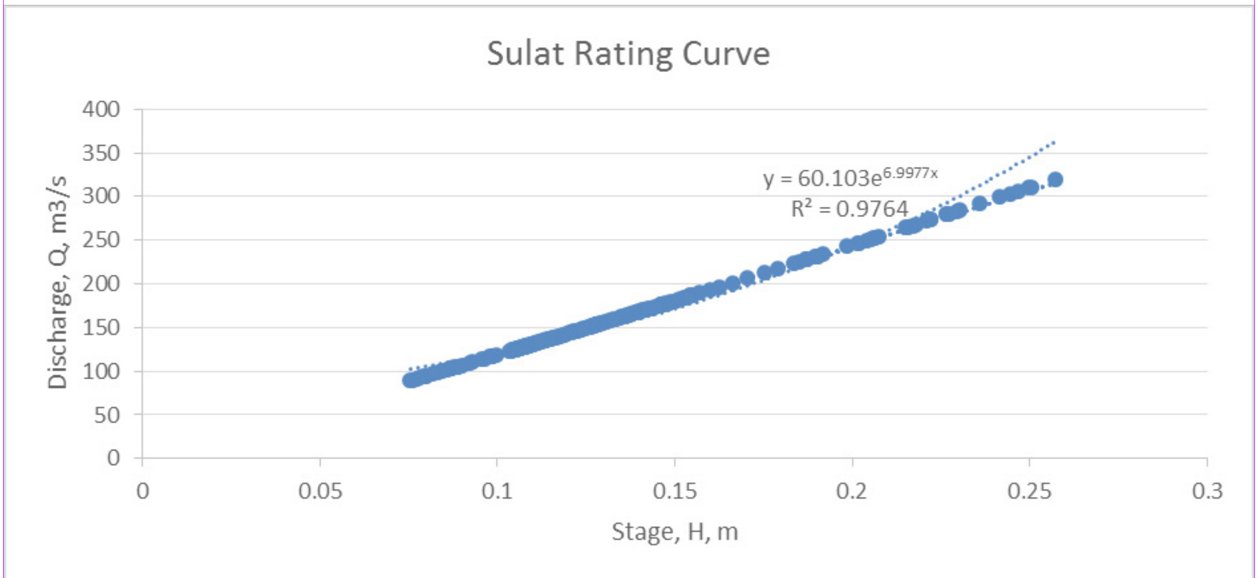

Figure 49. The rating curve at Sulat Bridge, Sulat, Samar.

This rating curve equation was used to compute the river outflow at Sulat Bridge for the calibration of the HEC-HMS model for Sulat shown in Figure 50. The total rainfall for this event in Aet rain gauge is 80.5 mm and peaked to 14.5mm at 7:45 AM of January 10, 2017.

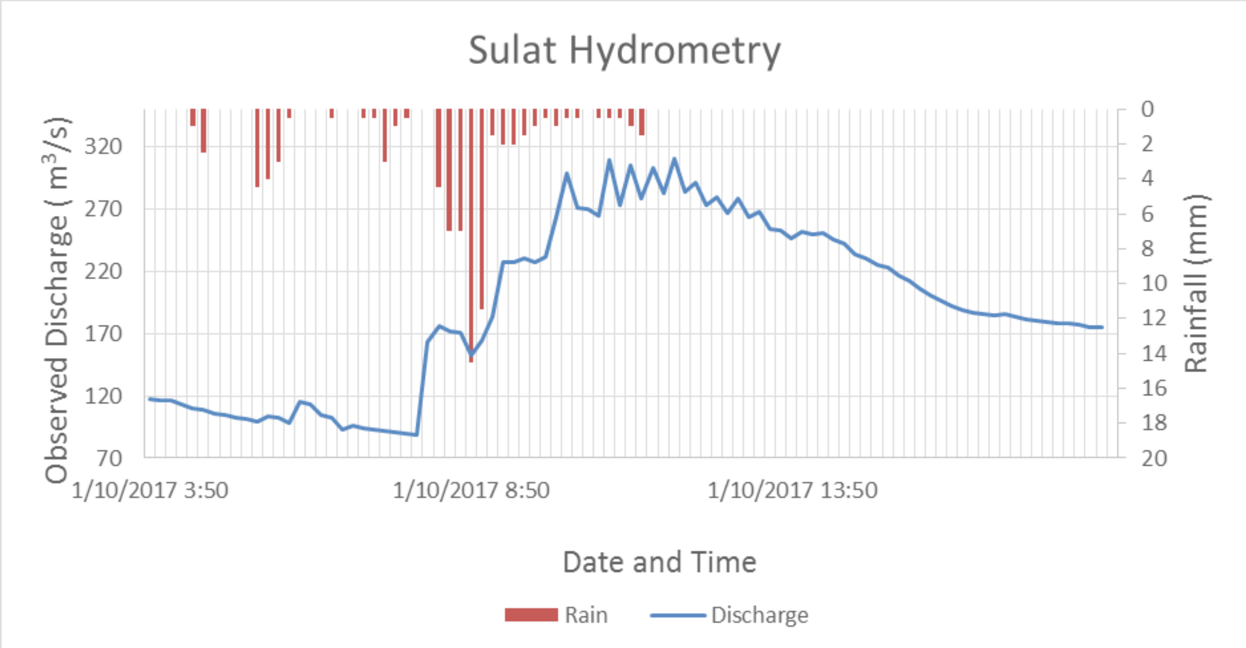

Figure 50. Rainfall and outflow data at Sulat Bridge, which was used for modeling.

5.2 RIDF Station

PAGASA computed the Rainfall Intensity Duration Frequency (RIDF) values for the Borongan Rain Gauge (Table 25). The RIDF rainfall amount for 24 hours was converted into a synthetic storm by interpolating and re-arranging the values in such a way that certain peak values will be attained at a certain time (Figure 51). This station was selected based on its proximity to the Sulat watershed. The extreme values for this watershed were computed based on a 36-year record.

Table 25. RIDF values for the Sulat River Basin based on average RIDF data of Borongan station, as computed by PAGASA.

COMPUTED EXTREME VALUES (in mm) OF PRECIPITATION									
T (yrs)	10 mins	20 mins	30 mins	1 hr	2 hrs	3 hrs	6 hrs	12 hrs	24 hrs
2	22.5	35.3	44.5	60.6	83.7	100.8	133.7	170.7	201.4
5	31.5	49.1	61	82.3	116.1	140.8	186.5	241	283.8
10	37.4	58.2	71.9	96.6	137.6	167.2	221.4	287.6	338.4
15	40.7	63.3	104.7	104.7	149.8	182.1	241.2	313.9	369.2
20	43	66.9	110.4	110.4	158.3	192.6	255	332.3	390.8
25	44.8	69.7	114.8	114.8	164.8	200.6	265.6	346.4	407.4
50	50.4	78.2	128.3	128.3	185	225.4	298.4	390.1	458.6
100	55.9	86.7	141.6	141.6	205	205	330.9	433.4	509.4

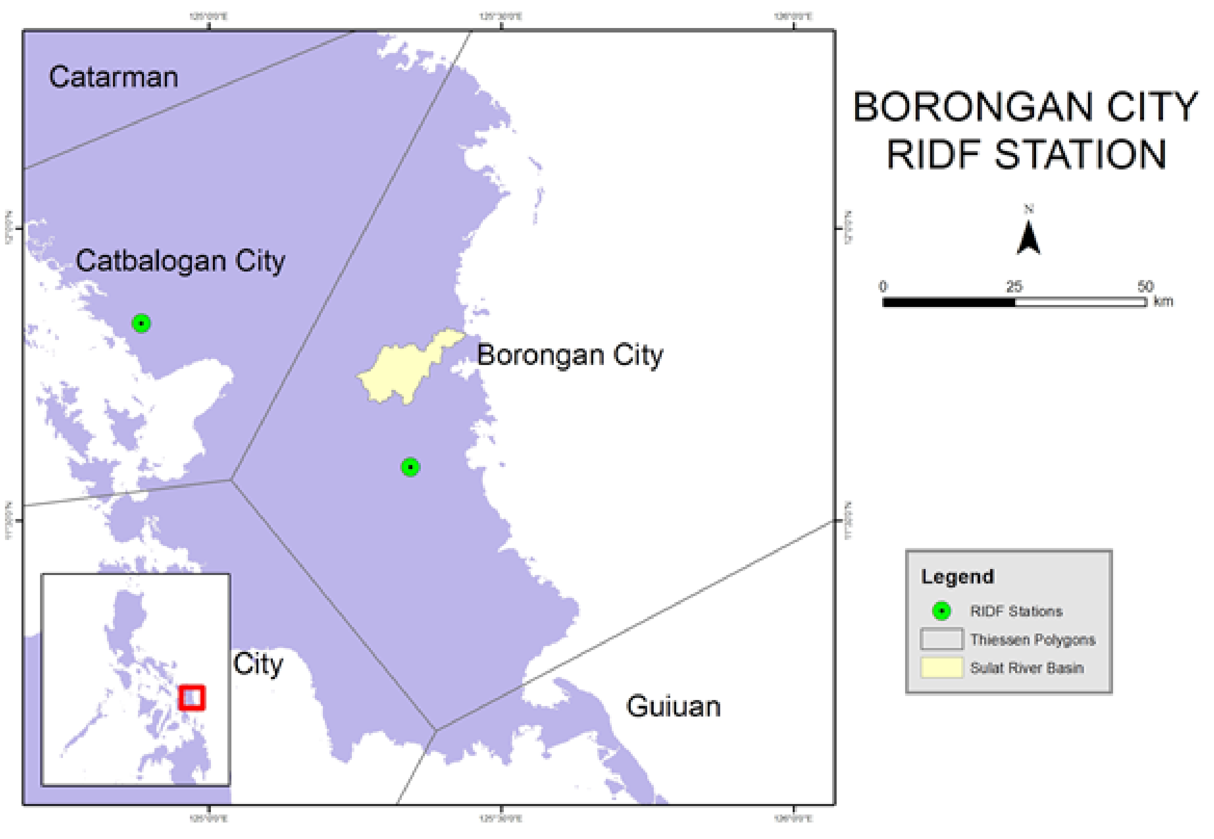

Figure 51. The location of the Borongan RIDF station relative to the Sulat River Basin.

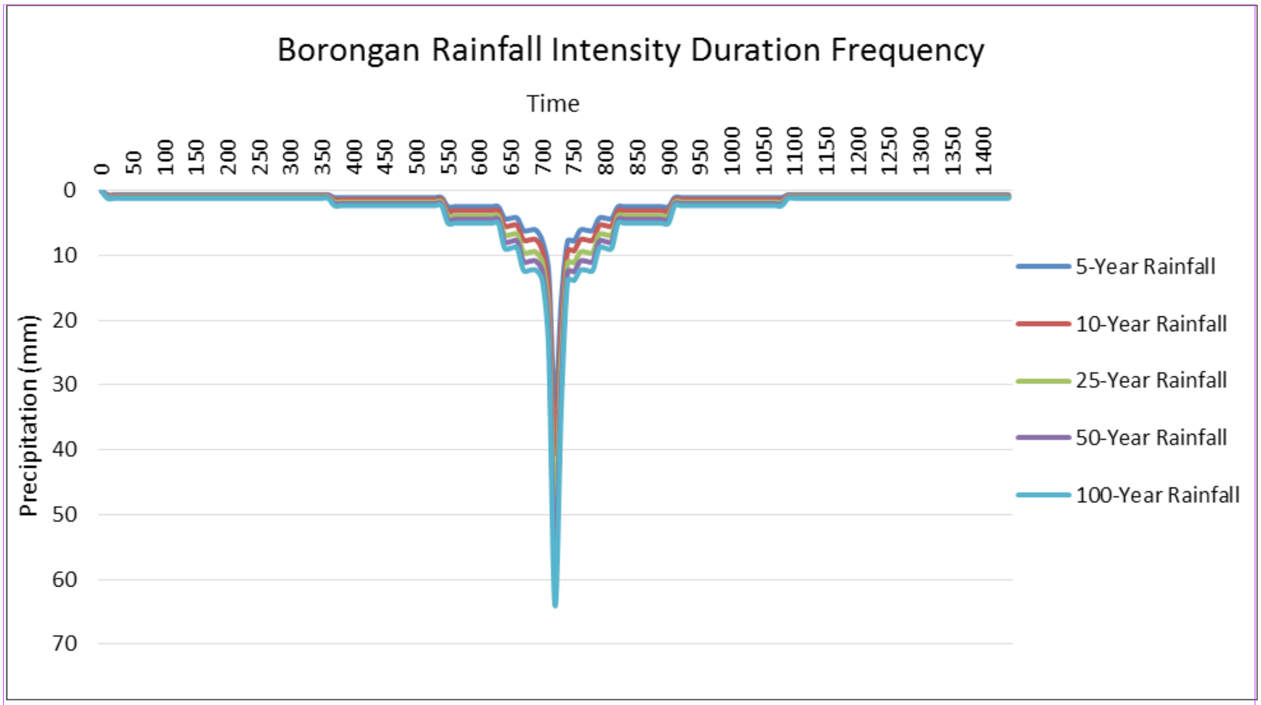

Figure 52. The synthetic storm generated for a 24-hour period rainfall for various return periods.

5.3 HMS Model

These soil dataset was taken on 2004 from the Bureau of Soils and Water Management (BSWM). It is under the Department of Agriculture (DA). The land cover dataset is from the National Mapping and Resource information Authority (NAMRIA). The soil and land cover of the Sulat River Basin are shown in Figure 53 and Figure 54, respectively.

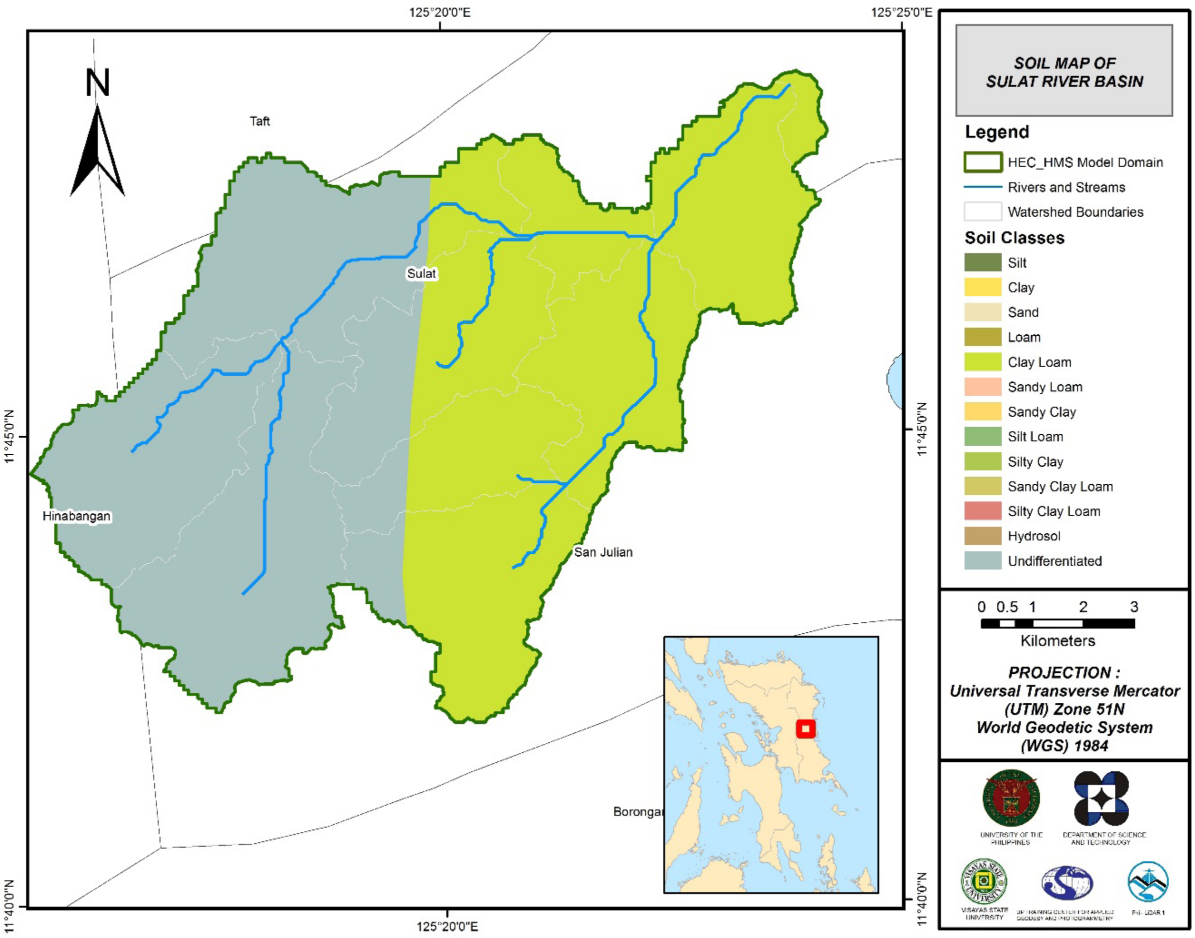

Figure 53. Soil Map of Sulat River Basin.

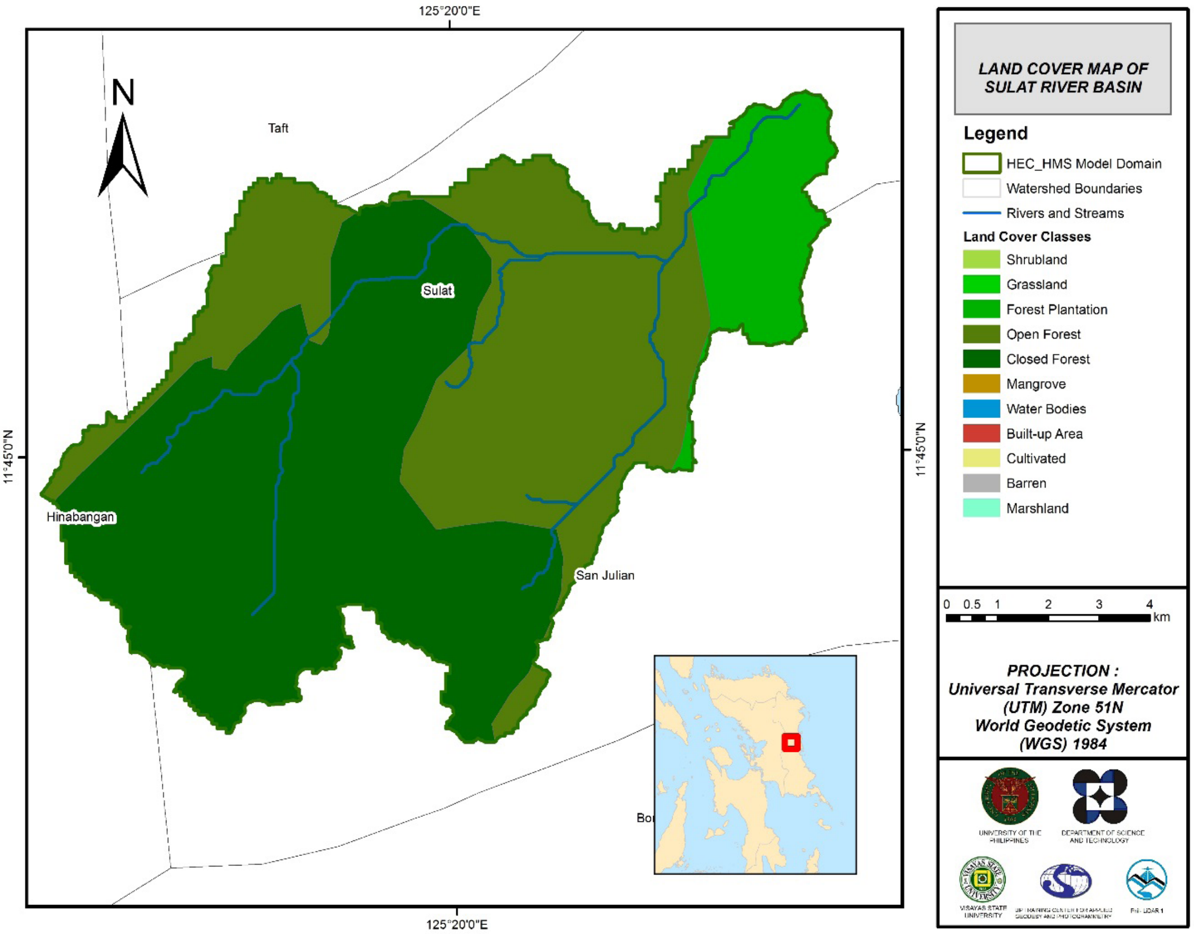

Figure 54. Land Cover Map of Sulat River Basin.

For Sulat, two soil classes were identified. These are clay loam, and undifferentiated land. Moreover, three land cover classes were identified. These are forest plantation, open forest, and closed forest.

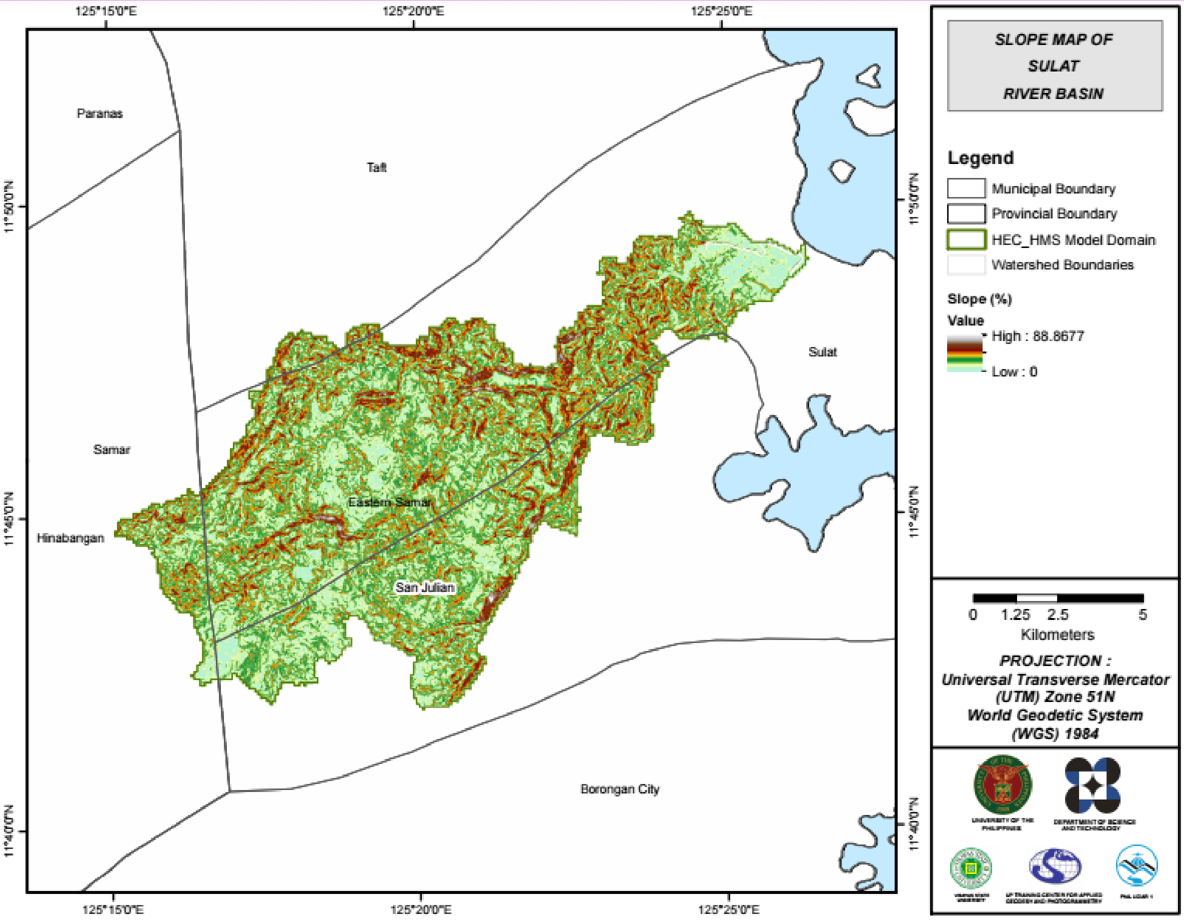

Figure 55. Slope Map of the Sulat River Basin.

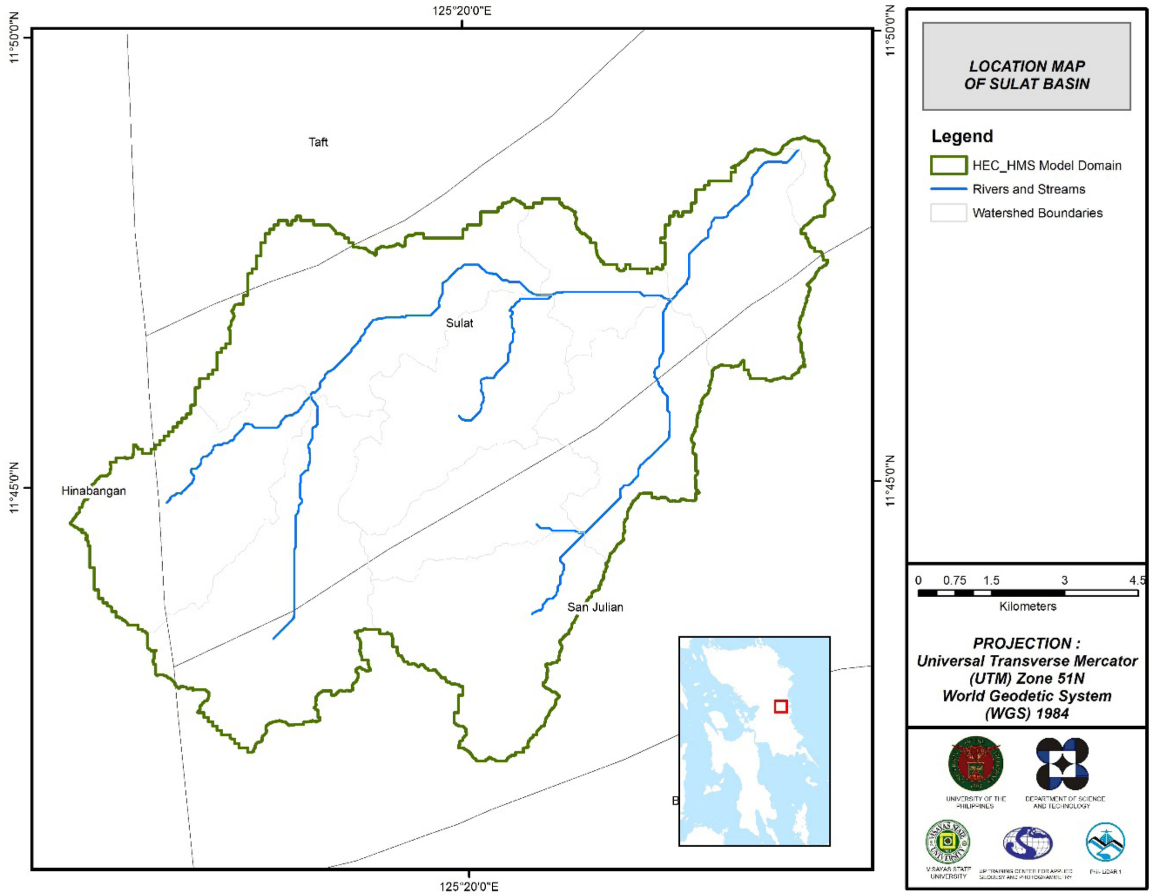

Figure 56. Stream Delineation Map of Sulat River Basin

Using the SAR-based DEM, the Sulat basin was delineated and further subdivided into subbasins. The model consists of 9 sub basins, 4 reaches, and 4 junctions as shown in Figure 57. The main outlet is Outlet 1 at Sulat Bridge.

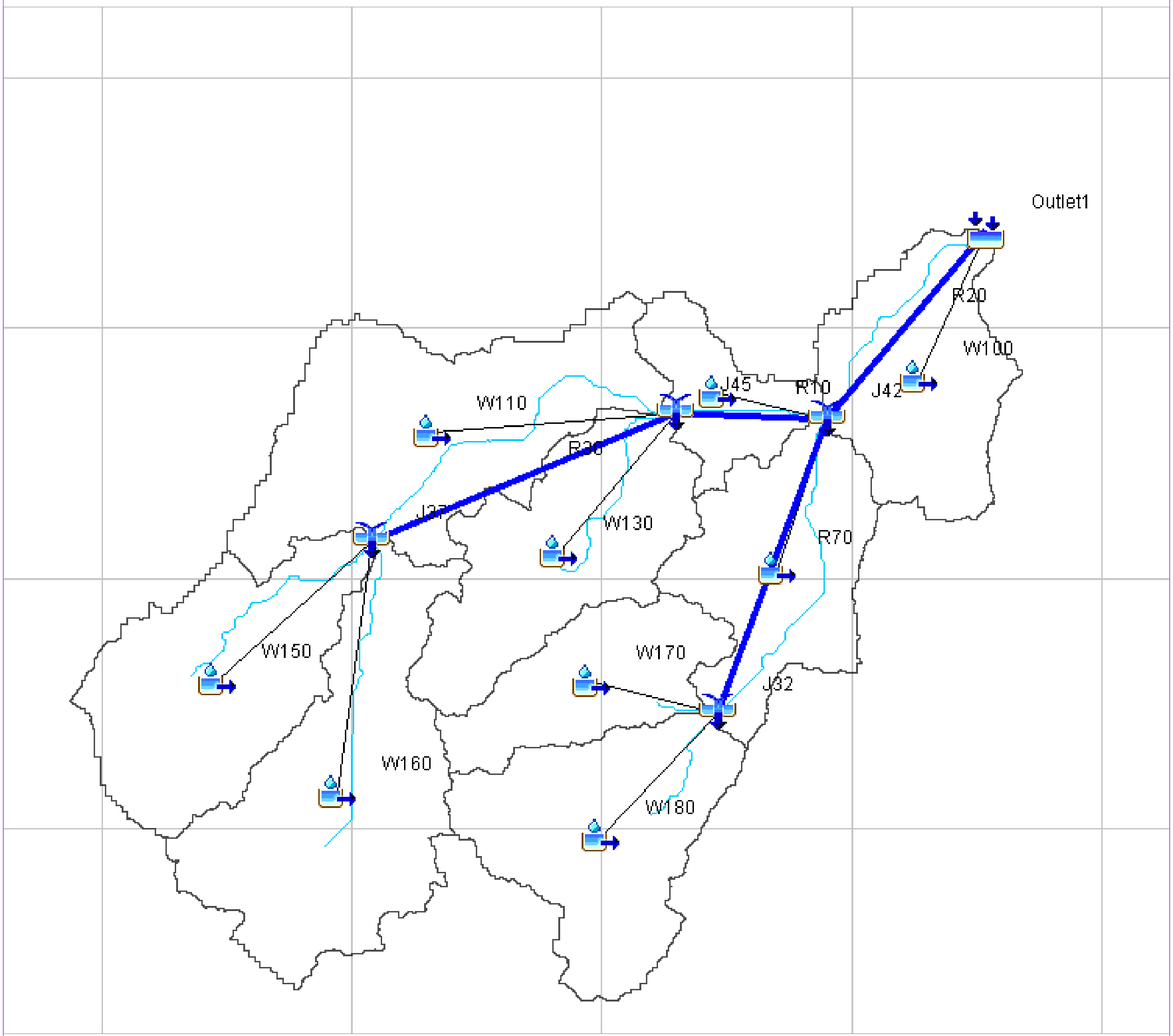

Figure 57. Sulat river basin model generated in HEC-HMS.

5.4 Cross-section Data

The riverbed cross-sections of the watershed were necessary in the HEC-RAS model setup. The cross-section data for the HEC-RAS model was derived from the LiDAR DEM data, which was defined using the Arc GeoRAS tool and was post-processed in ArcGIS (Figure 58).

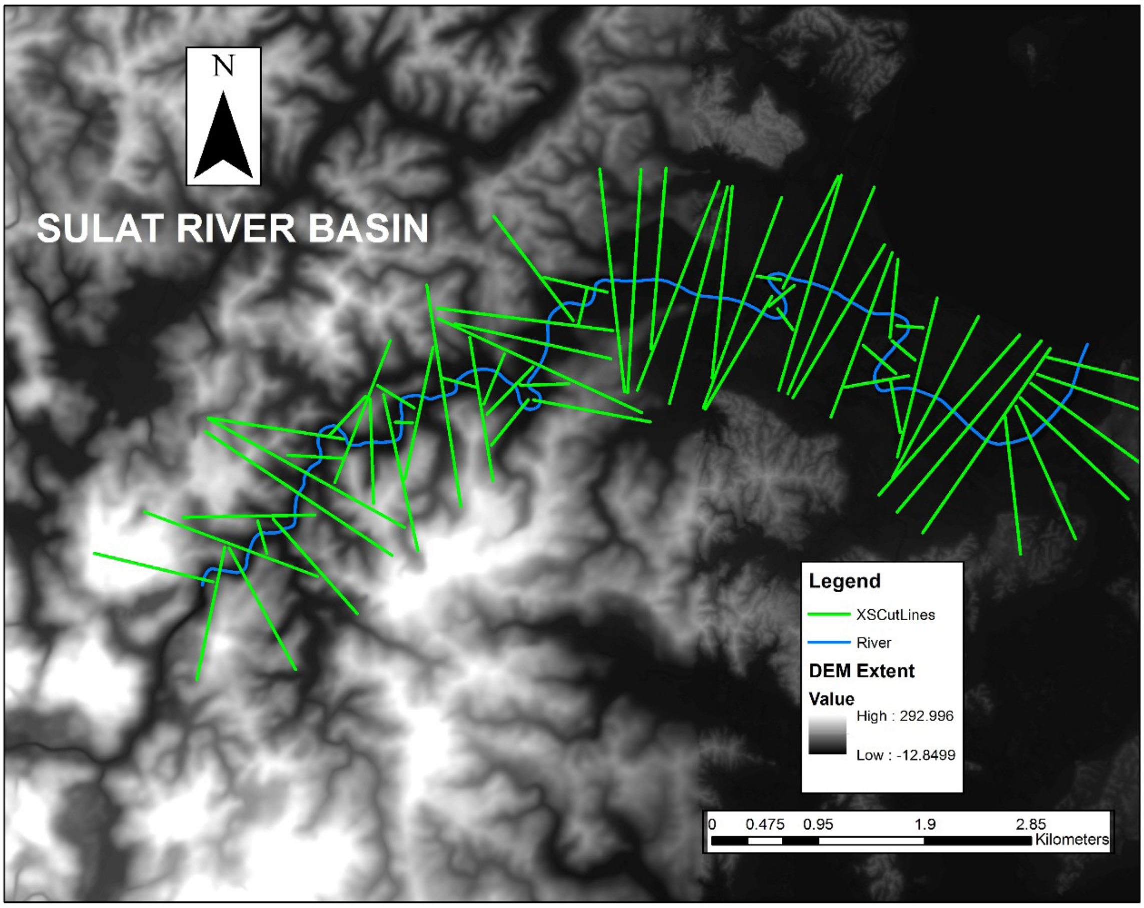

Figure 58. River cross-section of the Sulat River through the ArcMap HEC GeoRas tool.

5.5 Flo 2D Model

The automated modelling process allows for the creation of a model with boundaries that are almost exactly coincidental with that of the catchment area. As such, they have approximately the same land area and location. The entire area is divided into square grid elements, 10 meter by 10 meter in size. Each element is assigned a unique grid element number which serves as its identifier, then attributed with the parameters required for modelling such as x-and y-coordinate of centroid, names of adjacent grid elements, Manning coefficient of roughness, infiltration, and elevation value. The elements are arranged spatially to form the model, allowing the software to simulate the flow of water across the grid elements and in eight directions (north, south, east, west, northeast, northwest, southeast, southwest).

Based on the elevation and flow direction, it is seen that the water will generally flow from the northeast of the model to the west, following the main channel. As such, boundary elements in those particular regions of the model are assigned as inflow and outflow elements respectively.

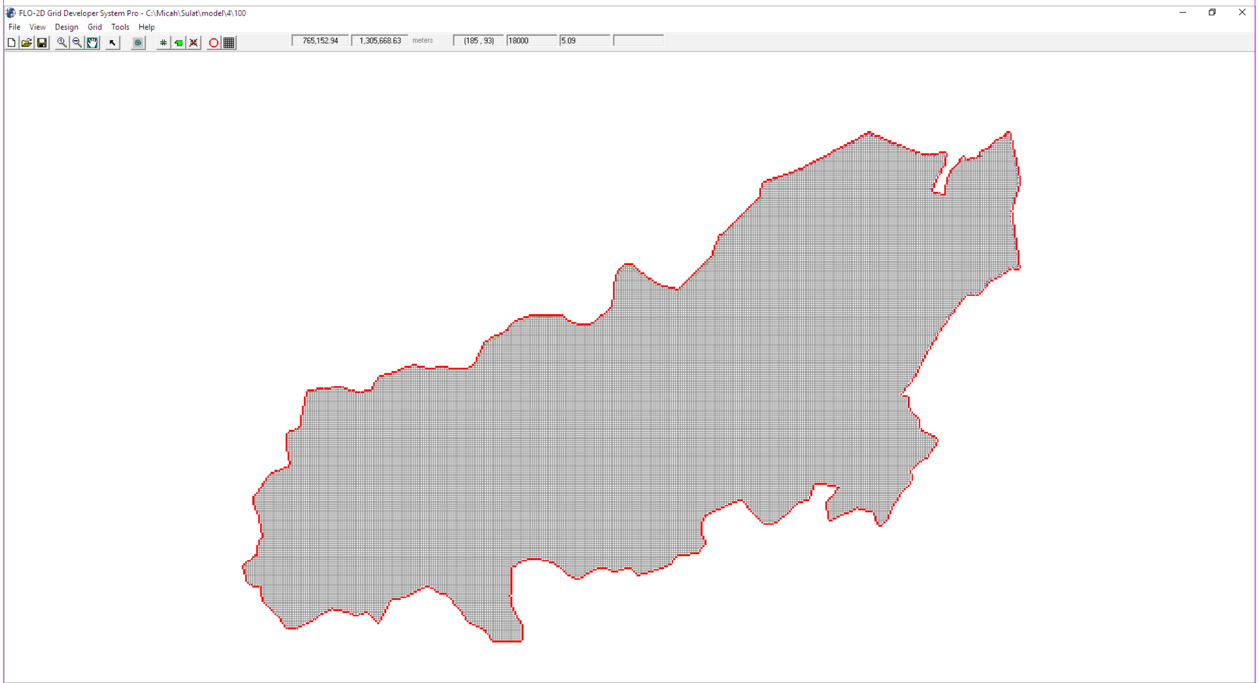

Figure 59. A screenshot of the river sub-catchment with the computational area to be modeled in FLO-2D Grid Developer System Pro (FLO-2D GDS Pro).

The simulation is then run through FLO-2D GDS Pro. This particular model had a computer run time of 53.15430 hours. After the simulation, FLO-2D Mapper Pro is used to transform the simulation results into spatial data that shows flood hazard levels, as well as the extent and inundation of the flood. Assigning the appropriate flood depth and velocity values for Low, Medium, and High creates the following food hazard map. Most of the default values given by FLO-2D Mapper Pro are used, except for those in the Low hazard level. For this particular level, the minimum h (Maximum depth) is set at 0.2 m while the minimum vh (Product of maximum velocity (v) times maximum depth (h)) is set at 0 m^2/s. The generated hazard maps for Sulat are in Figure 63, Figure 65, and Figure 67.

The creation of a flood hazard map from the model also automatically creates a flow depth map depicting the maximum amount of inundation for every grid element. The legend used by default in Flo-2D Mapper is not a good representation of the range of flood inundation values, so a different legend is used for the layout. In this particular model, the inundated parts cover a maximum land area of 20 409 100.00 m^2. The generated flood depth maps for Sulat are in Figure 64, Figure 66, and Figure 68.

There is a total of 142 591 389.45 m^3 of water entering the model. Of this amount, 8 999 786.63 m^3 is due to rainfall while 133 591 602.81 m^3 is inflow from other areas outside the model. 2 344 289.25 m^3 of this water is lost to infiltration and interception, while 1 180 884.23 m^3 is stored by the flood plain. The rest, amounting up to 139 066 229.25 m^3, is outflow.

5.6 Results of HMS Calibration

After calibrating the Sulat HEC-HMS river basin model, its accuracy was measured against the observed values. Figure 60 shows the comparison between the two discharge data.

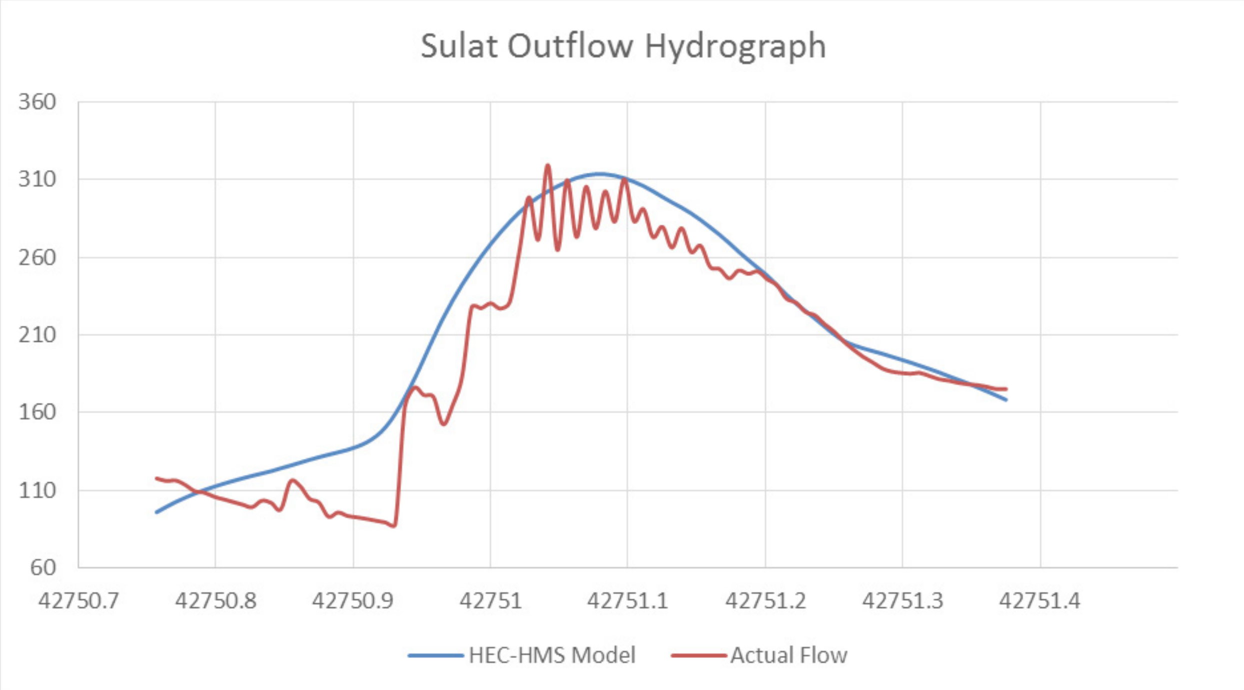

Figure 60. Outflow Hydrograph of Sulat produced by the HEC-HMS model compared with observed outflow.

Table 26 shows the adjusted ranges of values of the parameters used in calibrating the model.

Table 26. Range of calibrated values for the Sulat River Basin.

Hydrologic Element	Calculation Type	Method	Parameter	Range of Calibrated Values
Basin	Loss	SCS Curve Number	Initial Abstraction (mm)	0.001 – 0.01
			Curve Number	99
	Transform	Clark Unit Hydrograph	Time of Concentration (hr)	5 - 16
			Storage Coefficient (hr)	0.05 – 0.2
	Baseflow	Recession	Recession Constant	0.7
			Ratio to Peak	0.3
Reach	Routing	Muskingum-Cunge	Manning's Coefficient	0.04

Initial abstraction defines the amount of precipitation that must fall before surface runoff. The magnitude of the outflow hydrograph increases as initial abstraction decreases. The range of values from 0.001mm to 0.01mm means that there is very minimal amount of infiltration or rainfall interception by vegetation.

Curve number is the estimate of the precipitation excess of soil cover, land use, and antecedent moisture. The magnitude of the outflow hydrograph increases as curve number increases. The value of 99 for curve number is the highest value possible for watersheds.

Time of concentration and storage coefficient are the travel time and index of temporary storage of runoff in a watershed. The range of calibrated values from 0.05 hours to 16 hours determines the reaction time of the model with respect to the rainfall. The peak magnitude of the hydrograph also decreases when these parameters are increased.

Recession constant is the rate at which baseflow recedes between storm events and ratio to peak is the ratio of the baseflow discharge to the peak discharge. Recession constant of 0.7 indicates that the basin is unlikely to quickly go back to its original discharge and instead, will be higher. Ratio to peak of 0.3 indicates a steeper receding limb of the outflow hydrograph.

Manning's roughness coefficient of 0.04 corresponds to the common roughness in the Sulat watershed, which is determined to be cultivated with mature field crops (Brunner, 2010).

Table 27. Summary of the Efficiency Test of the Sulat HMS Model

Accuracy measure	Value
RMSE	11.9
r^2	0.9764
NSE	0.85
PBIAS	-8.82
RSR	0.38

The Root Mean Square Error (RMSE) method aggregates the individual differences of these two measurements. It was computed as 11.9 m^3/s.

The Pearson correlation coefficient (r^2) assesses the strength of the linear relationship between the observations and the model. This value being close to 1 corresponds to an almost perfect match of the observed discharge and the resulting discharge from the HEC HMS model. Here, it measured 0.9674.

The Nash-Sutcliffe (E) method was also used to assess the predictive power of the model. Here the optimal value is 1. The model attained an efficiency coefficient of 0.85.

A positive Percent Bias (PBIAS) indicates a model's propensity towards under-prediction. Negative values indicate bias towards over-prediction. Again, the optimal value is 0. In the model, the PBIAS is -8.82.

The Observation Standard Deviation Ratio, RSR, is an error index. A perfect model attains a value of 0 when the error in the units of the valuable a quantified. The model has an RSR value of 0.38.

5.7 Calculated Outflow hydrographs and Discharge Values for different Rainfall Return Periods

5.7.1 Hydrograph using the Rainfall Runoff Model

The summary graph (Figure 61) shows the Sulat outflow using the Borongan Rainfall Intensity-Duration-Frequency curves (RIDF) in 5 different return periods (5-year, 10-year, 25-year, 50-year, and 100-year rainfall time series) based on the Philippine Atmospheric Geophysical and Astronomical Services Administration (PAGASA) data. The simulation results reveal increasing outflow magnitude as the rainfall intensity increases for a range of durations and return periods.

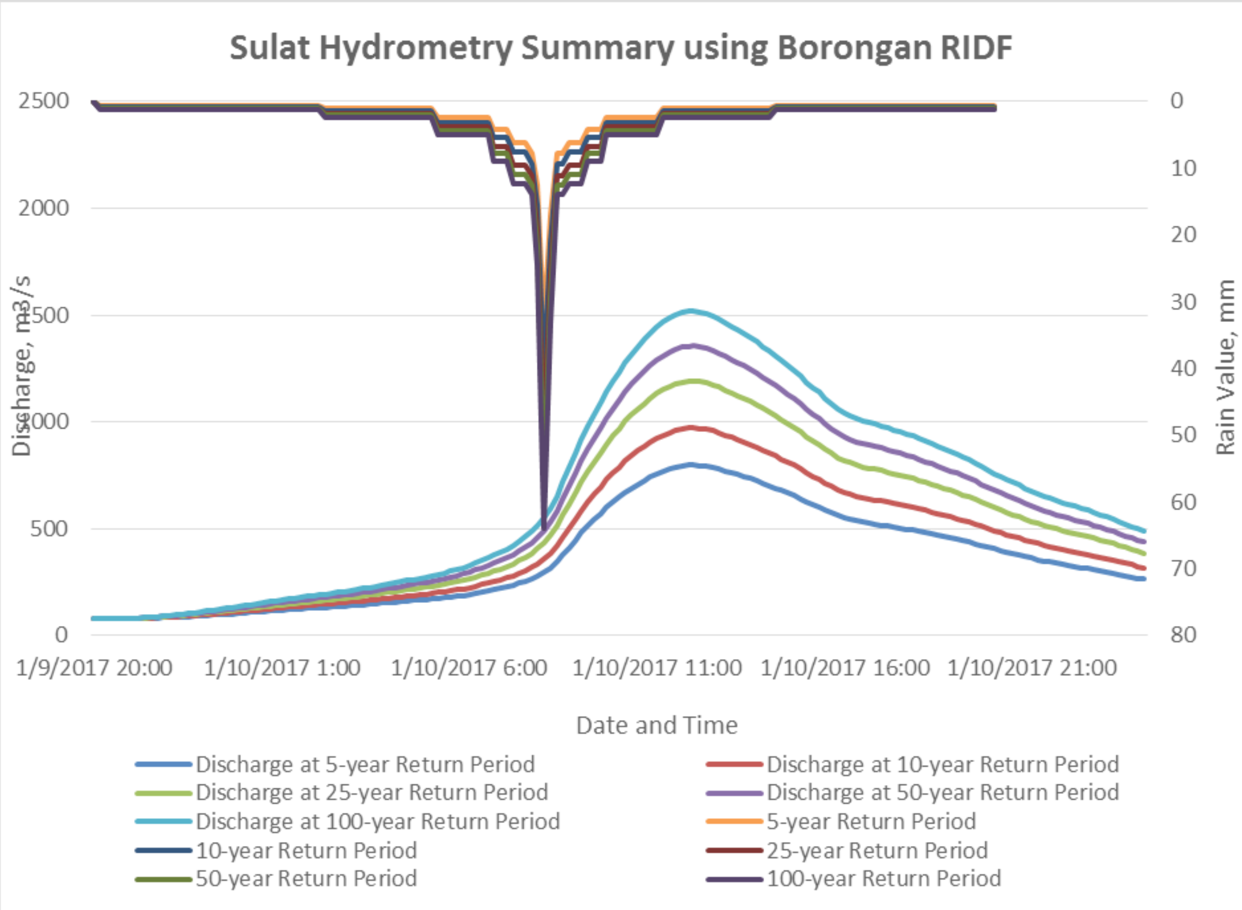

Figure 61. The Outflow hydrograph at the Sulat Station, generated using the Borongan RIDF simulated in HEC-HMS.

A summary of the total precipitation, peak rainfall, peak outflow and time to peak of the Sulat discharge using the Borongan Rainfall Intensity-Duration-Frequency curves (RIDF) in five different return periods is shown in Table 28.

Table 28. The peak values of the Sulat HEC-HMS Model outflow using the Borongan RIDF.

RIDF Period	Total Precipitation (mm)	Peak rainfall (mm)	Peak outflow (m^3/s)	Time to Peak
5-Year	278.6	33.2	797.9	4 hours
10-Year	344.7	40.6	972	4 hours
25-Year	428.2	50.1	1192	4 hours
50-Year	490.2	57.1	1355.6	4 hours
100-Year	551.7	64	1517.6	4 hours

5.8 River Analysis (RAS) Model Simulation

The HEC-RAS Flood Model produced a simulated water level at every cross-section for every time step for every flood simulation created. The resulting model will be used in determining the flooded areas within the model. The simulated model will be an integral part in determining real-time flood inundation extent of the river after it has been automated and uploaded on the DREAM website. Figure 62 shows a generated sample map of the Sulat River using the calibrated HMS base flow.

Figure 62. Sample output map of the Sulat RAS Model.

5.9 Flow Depth and Flood Hazard

The resulting hazard and flow depth maps have a 10m resolution. Figure 63 to Figure 68 shows the 5-, 25-, and 100-year rain return scenarios of the Sulat floodplain. The floodplain, with an area of 54.62 sq. km., covers three municipalites namely San Julian, Sulat, and Taft. Table 29 shows the percentage of area affected by flooding per municipality.

Table 29. Municipalities affected in Sulat floodplain.

City / Municipality	Total Area	Area Flooded	% Flooded
San Julian	127.43	1.79	1%
Sulat	150.05	50.14	33%
Taft	230.27	2.68	1%

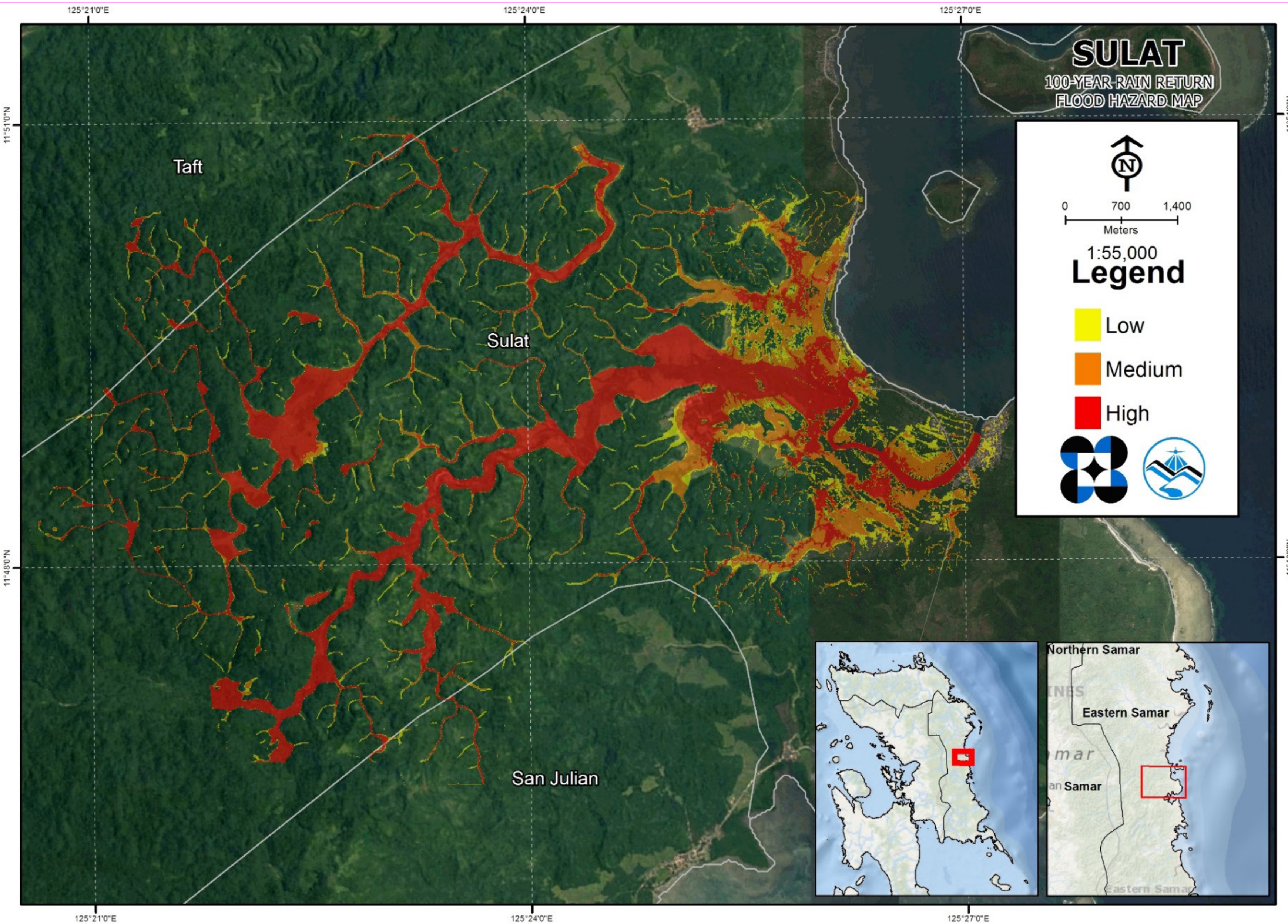

Figure 63. A 100-year Flood Hazard Map for Sulat Floodplain overlaid on Google Earth imagery.

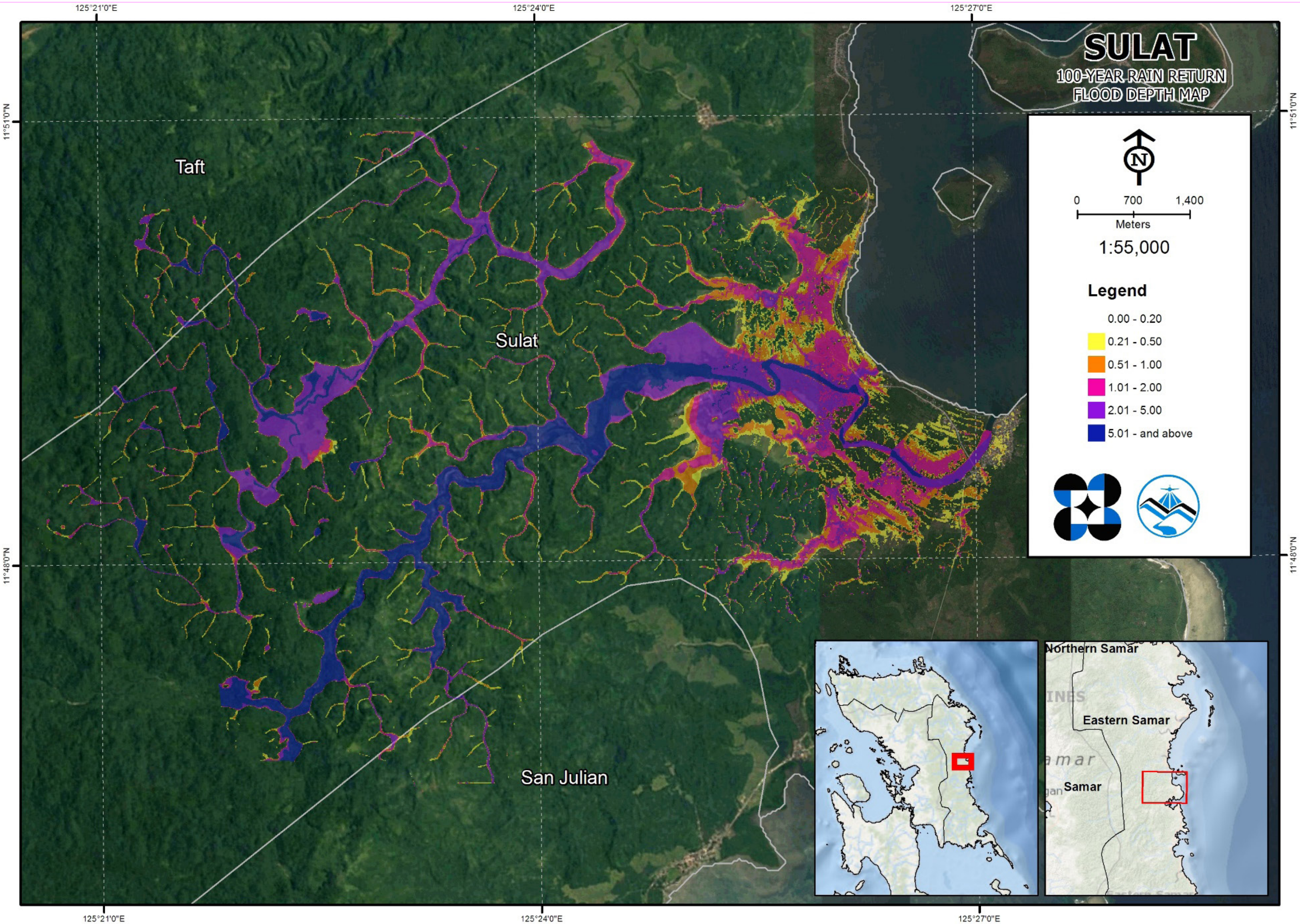

Figure 64. A 100-year Flow Depth Map for Sulat Floodplain overlaid on Google Earth imagery.

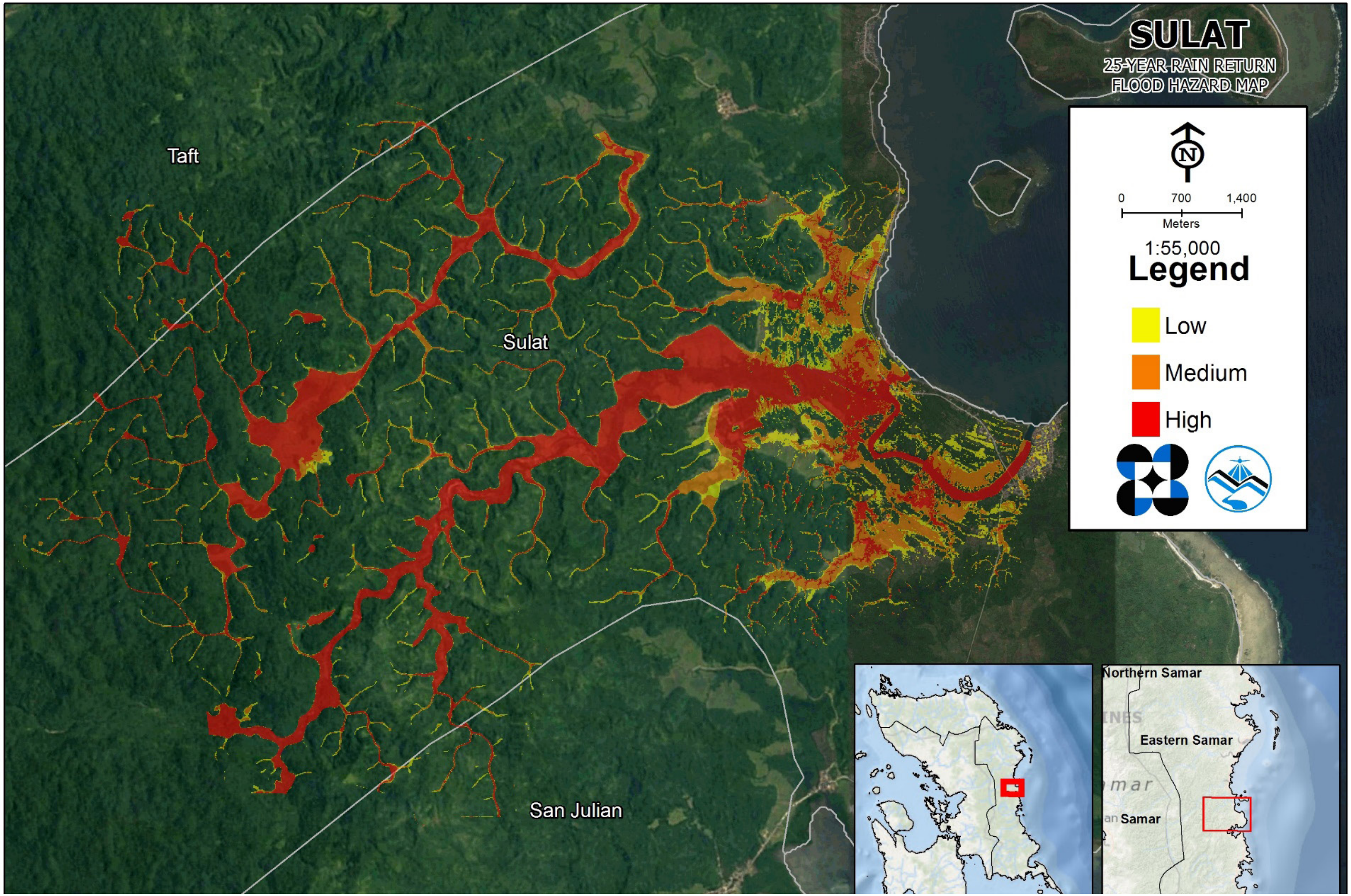

Figure 65. A 25-year Flood Hazard Map for Sulat Floodplain overlaid on Google Earth imagery.

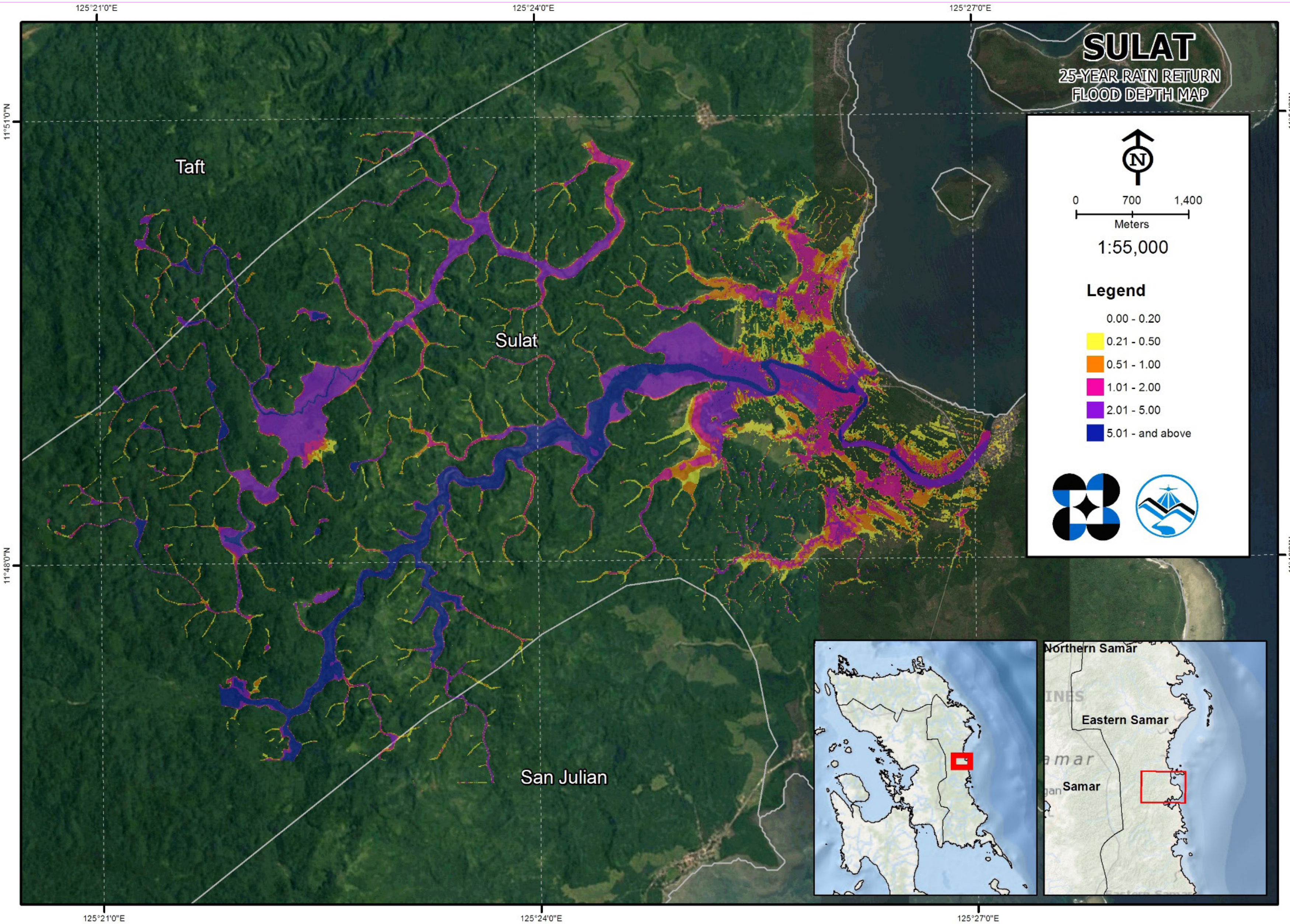

Figure 66. A 25-year Flow Depth Map for Sulat Floodplain overlaid on Google Earth imagery.

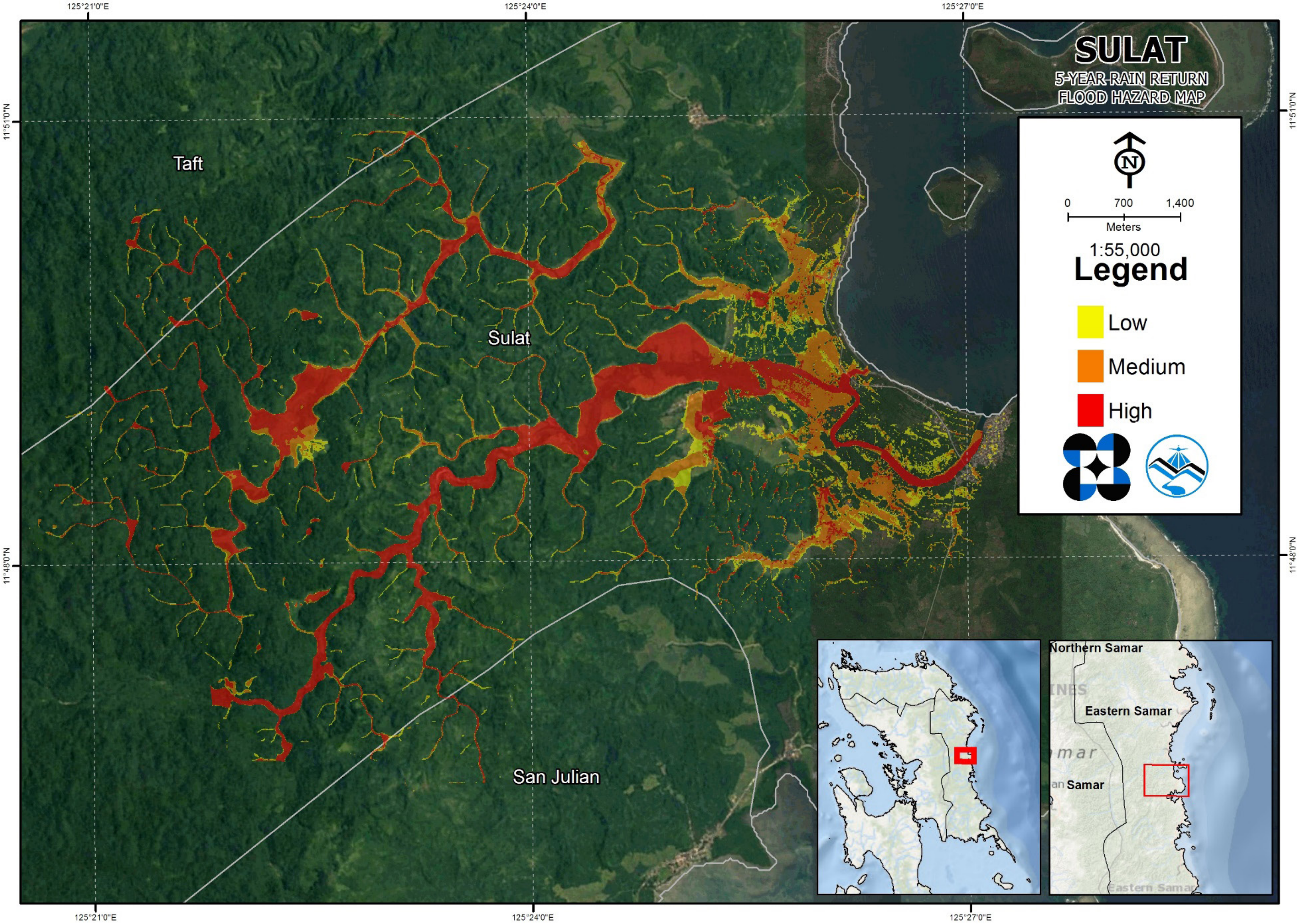

Figure 67. A 5-year Flood Hazard Map for Sulat Floodplain overlaid on Google Earth imagery.

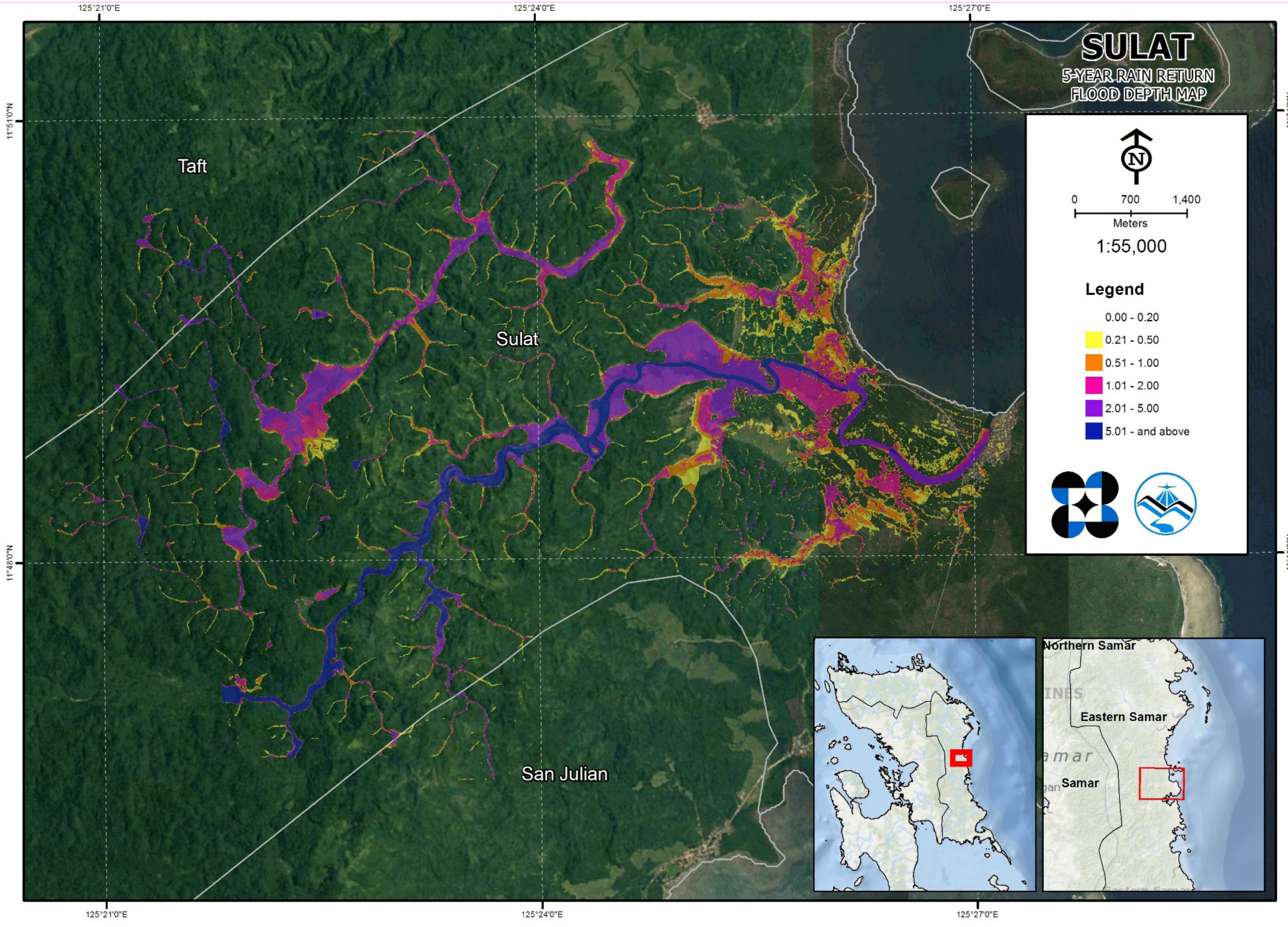

Figure 68. A 5-year Flood Depth Map for Sulat Floodplain overlaid on Google Earth imagery.

5.10 Inventory of Areas Exposed to Flooding

Listed below are the affected barangays in the Sulat River Basin, grouped accordingly by municipality. For the said basin, three municipalities are expected to experience flooding when subjected to 5-yr rainfall return period.

For the 5-year return period, 1.37% of the municipality of San Julian with an area of 127.43 sq. km. will experience flood levels of less 0.20 meters. 0.022% of the area will experience flood levels of 0.21 to 0.50 meters while 0.011%, 0.014% and 0.014% of the area will experience flood depths of 0.51 to 1 meter, 1.01 to 2 meters, and more than 2 meters, respectively. Listed in Table 30 are the affected areas in San Julian in square kilometers by flood depth per barangay. ANNEX 12 and ANNEX 13 show the educational and health institutions exposed to flooding.

Table 30. Affected Areas in San Julian, Eastern Samar during 5-Year Rainfall Return Period.

Affected area (sq. km.) by flood depth (in m.)	Areas of affected Barangays in San Julian (in sq.km.)		
	Casoroy	Nena	Putong
0.03-0.20	0.26	0.98	0.5
0.21-0.50	0.0022	0.015	0.011
0.51-1.00	0	0.0071	0.0071
1.01-2.00	0.0001	0.014	0.0044
2.01-5.00	0	0.017	0.0012
> 5.00	0	0	0

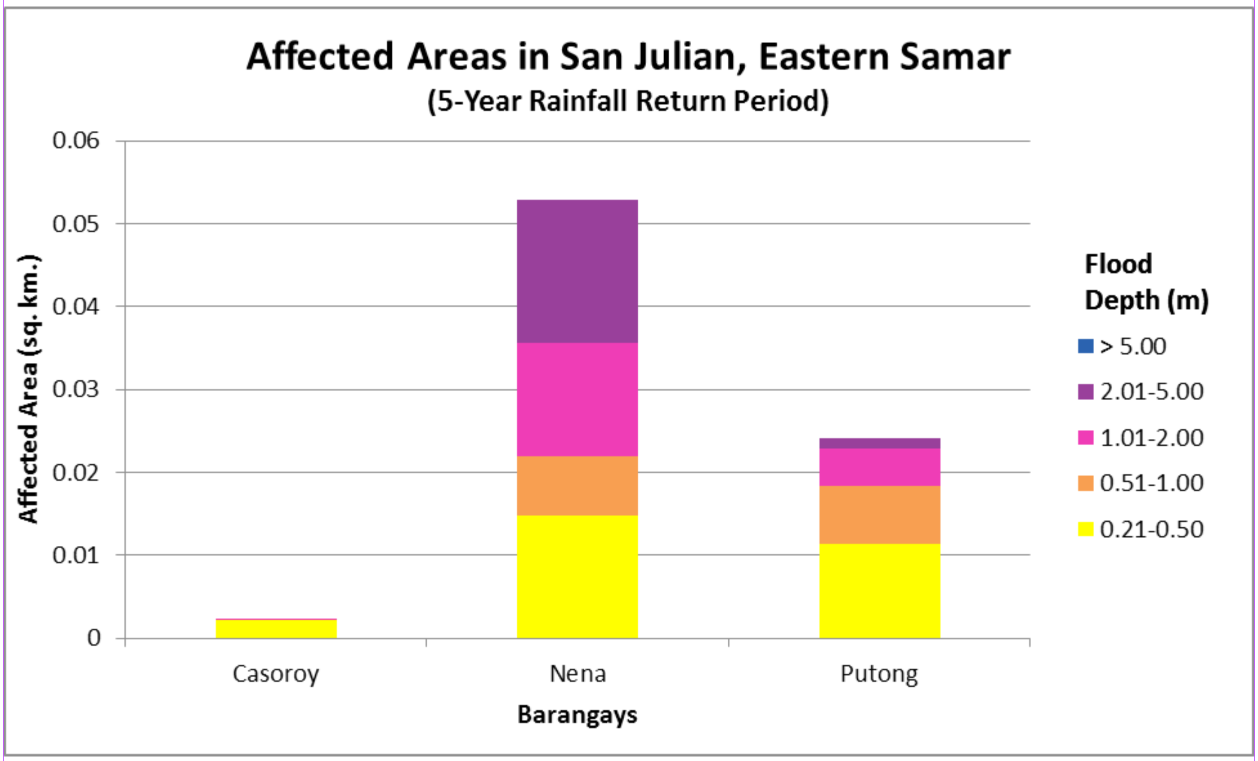

Figure 69. Affected Areas in San Julian, Eastern Samar during 5-Year Rainfall Return Period.

For the municipality of Sulat, with an area of 150.05 sq. km., 27.46% will experience flood levels of less 0.20 meters. 1.08% of the area will experience flood levels of 0.21 to 0.50 meters while 1.11%, 1.43%, 1.65% and 0.8% of the area will experience flood depths of 0.51 to 1 meter, 1.01 to 2 meters, 2.01 to 5 meters, and more than 5 meters respectively. Listed in Table 31 are the affected areas in Sulat in square kilometers by flood depth per barangay.

Table 31. Affected Areas in Sulat, Eastern Samar during 5-Year Rainfall Return Period.

Affected Area (sq. km.) by flood depth (in m.)	Areas of affected Barangays in Sulat (in sq.km.)								
	A-Et	Del Remedio	Kandalakit	Mabini	Maglipay	San Juan	San Mateo	Santo Niño	Santo Tomas
0.03-0.20	4.54	2.99	9.36	5.7	0.09	5.24	4.95	2.73	5.62
0.21-0.50	0.14	0.058	0.18	0.11	0.011	0.15	0.37	0.45	0.16
0.51-1.00	0.12	0.042	0.19	0.074	0.0041	0.22	0.33	0.51	0.18
1.01-2.00	0.34	0.04	0.25	0.087	0.0025	0.21	0.55	0.41	0.24
2.01-5.00	0.41	0.058	0.27	0.1	0.0015	0.94	0.35	0.12	0.24
> 5.00	0.029	0.059	0.033	0.33	0	0.5	0.24	0.0059	0

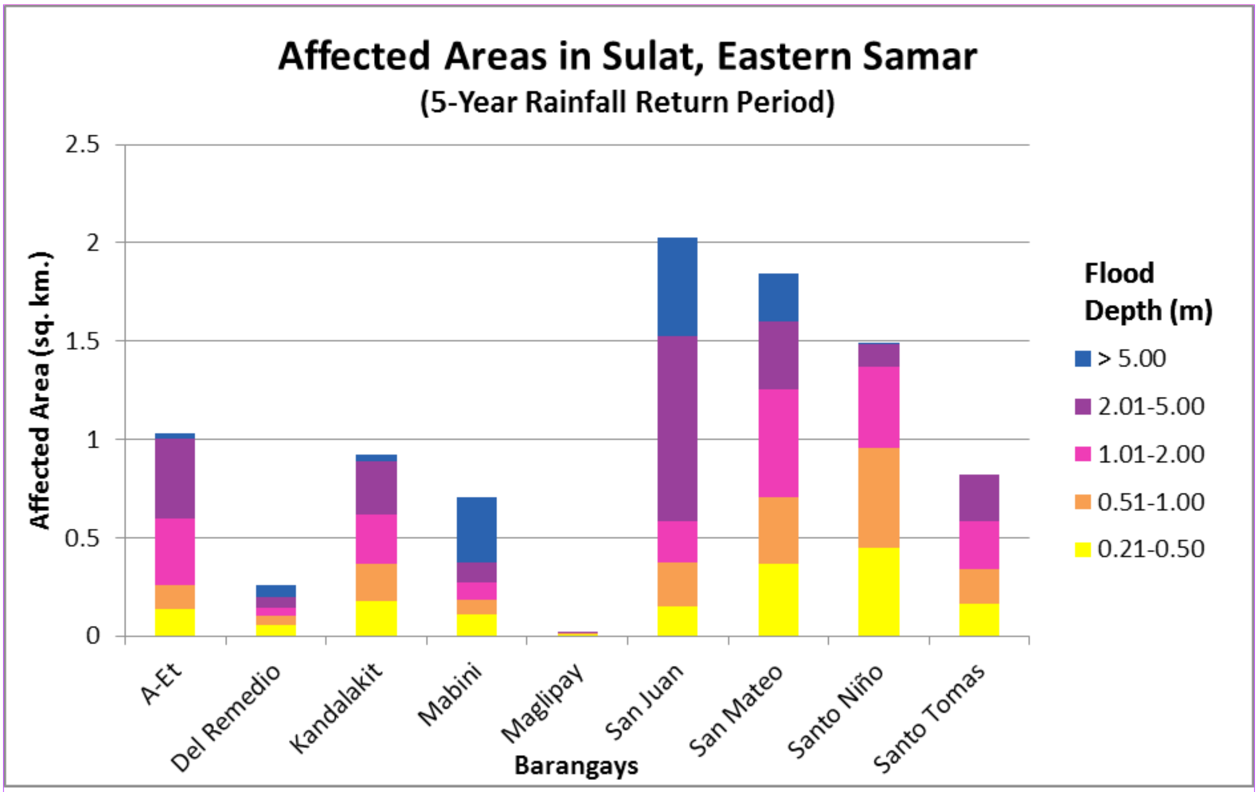

Figure 70. Affected Areas in Sulat, Eastern Samar during 5-Year Rainfall Return Period.

For the municipality of Taft, with an area of 230.27 sq. km., 1.09% will experience flood levels of less 0.20 meters. 0.025% of the area will experience flood levels of 0.21 to 0.50 meters while 0.018%, 0.02%, 0.024% and 0.005% of the area will experience flood depths of 0.51 to 1 meter, 1.01 to 2 meters, 2.01 to 5 meters and more than 5 meters respectively. Listed in Table 32 are the affected areas in square kilometres by flood depth per barangay.

Table 32. Affected Areas in Taft, Eastern Samar during 5-Year Rainfall Return Period.

Affected Area (sq. km.) by flood depth (in m.)	Areas of affected Barangays in Taft (in sq.km.)	
	Malinao	Mantang
0.03-0.20	1.19	1.33
0.21-0.50	0.029	0.029
0.51-1.00	0.021	0.021
1.01-2.00	0.022	0.023
2.01-5.00	0.029	0.026
> 5.00	0.00018	0.011

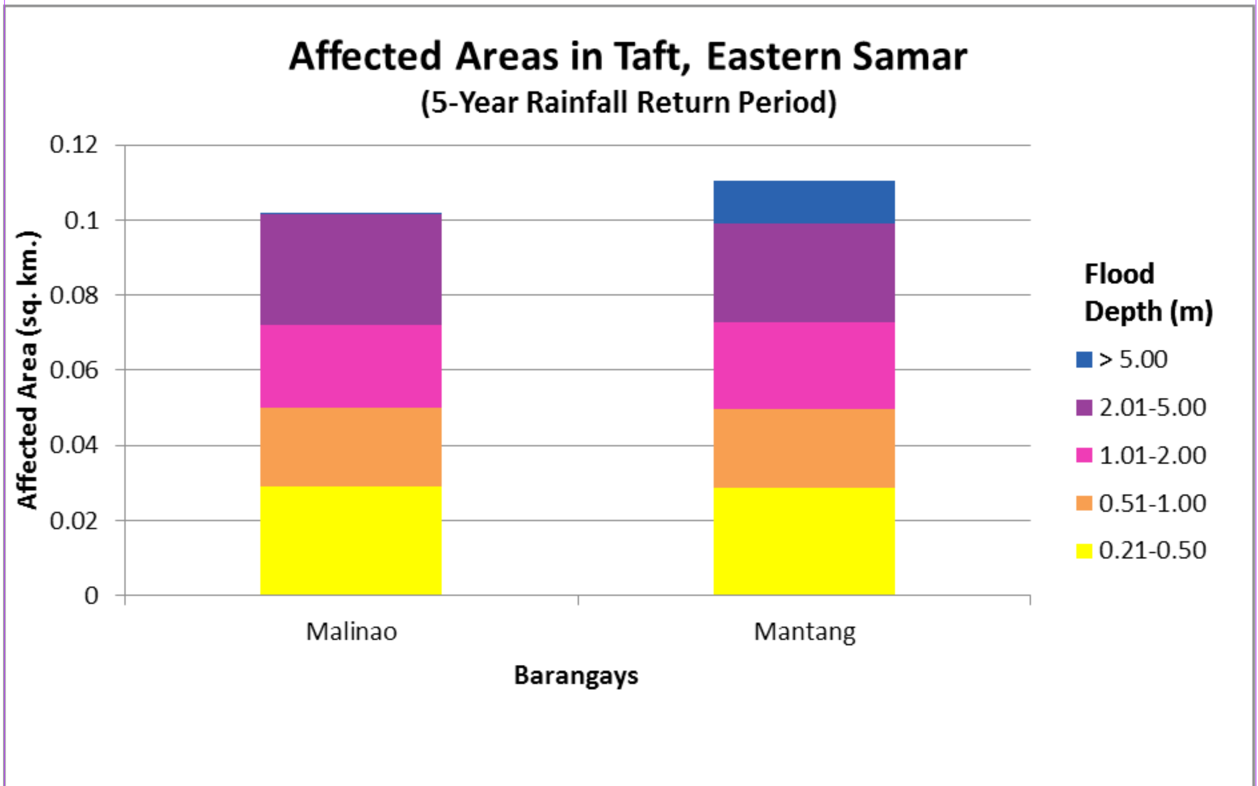

Figure 71. Affected Areas in Taft, Eastern Samar during 5-Year Rainfall Return Period.

For the 25-year return period, 1.35% of the municipality of San Julian with an area of 127.43 sq. km. will experience flood levels of less 0.20 meters. 0.029% of the area will experience flood levels of 0.21 to 0.50 meters while 0.013%, 0.014%, 0.019% and 0.0002% of the area will experience flood depths of 0.51 to 1 meter, 1.01 to 2 meters, 2.01 to 5 meters and more than 5 meters, respectively. Listed in Table 33 are the affected areas in San Julian in square kilometers by flood depth per barangay.

Table 33. Affected Areas in San Julian, Eastern Samar during 25-Year Rainfall Return Period.

Affected Area (sq. km.) by flood depth (in m.)	Areas of affected Barangays in San Julian (in sq.km.)		
	Casoroy	Nena	Putong
0.03-0.20	0.26	0.97	0.5
0.21-0.50	0.0042	0.021	0.012
0.51-1.00	0	0.0086	0.0085
1.01-2 .00	0.0001	0.012	0.0056
2.01-5.00	0	0.023	0.0024
> 5.00	0	0.0003	0

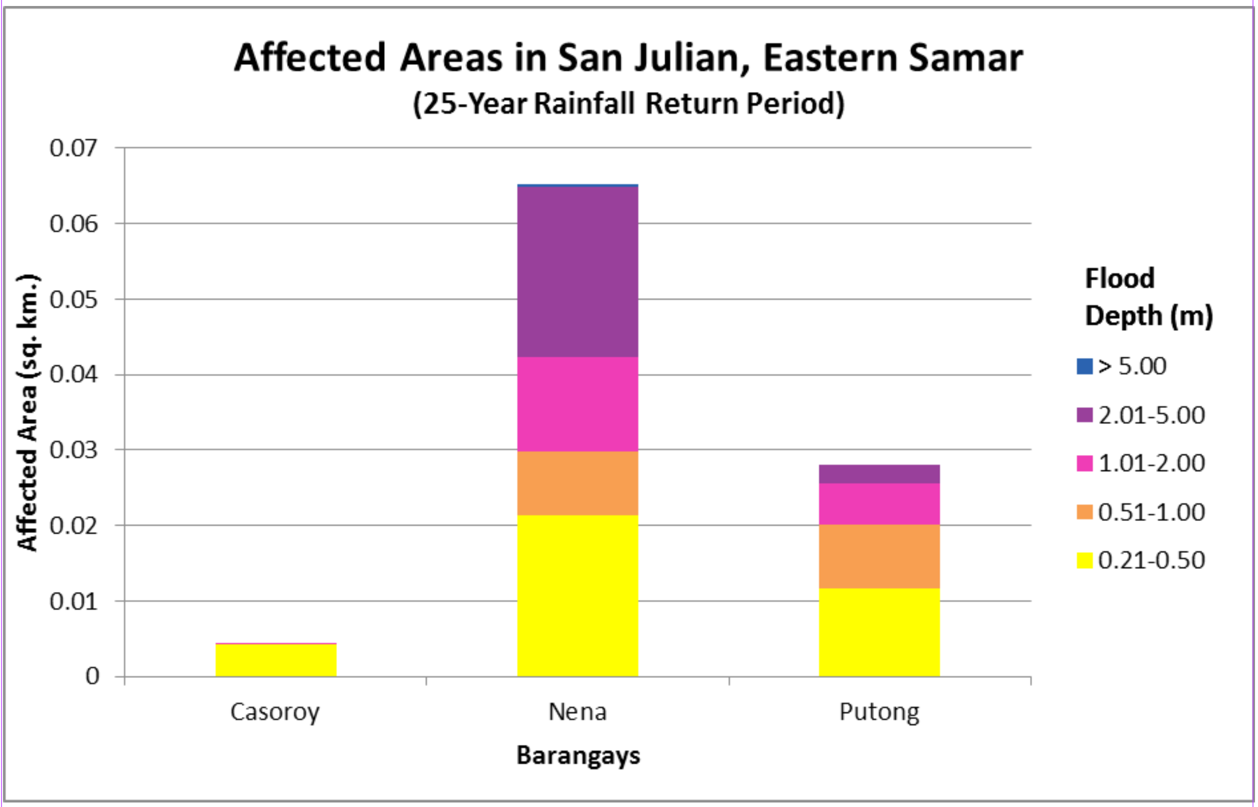

Figure 72. Affected Areas in San Julian, Eastern Samar during 25-Year Rainfall Return Period.

For the municipality of Sulat, with an area of 150.05 sq. km., 26.48% will experience flood levels of less 0.20 meters. 1.14% of the area will experience flood levels of 0.21 to 0.50 meters while 1.07%, 1.43%, 2.12% and 1.3% of the area will experience flood depths of 0.51 to 1 meter, 1.01 to 2 meters, 2.01 to 5 meters, and more than 5 meters respectively. Listed in Table 34 are the affected areas in Sulat in square kilometers by flood depth per barangay.

Table 34. Affected Areas in Sulat, Eastern Samar during 25-Year Rainfall Return Period.

Affected Area (sq. km.) by flood depth (in m.)	Areas of affected Barangays in Sulat (in sq.km.)								
	A-Et	Del Remedio	Kandalakit	Mabini	Maglipay	San Juan	San Mateo	Santo Niño	Santo Tomas
0.03-0.20	4.44	2.93	9.24	5.51	0.083	5.07	4.56	2.37	5.52
0.21-0.50	0.12	0.066	0.19	0.12	0.016	0.14	0.42	0.48	0.17
0.51-1.00	0.098	0.043	0.17	0.072	0.0049	0.19	0.38	0.49	0.16
1.01-2.00	0.13	0.04	0.23	0.071	0.002	0.21	0.55	0.7	0.21
2.01-5.00	0.7	0.05	0.37	0.16	0.0023	0.81	0.56	0.16	0.37
> 5.00	0.083	0.11	0.073	0.47	0	0.84	0.33	0.026	0.012

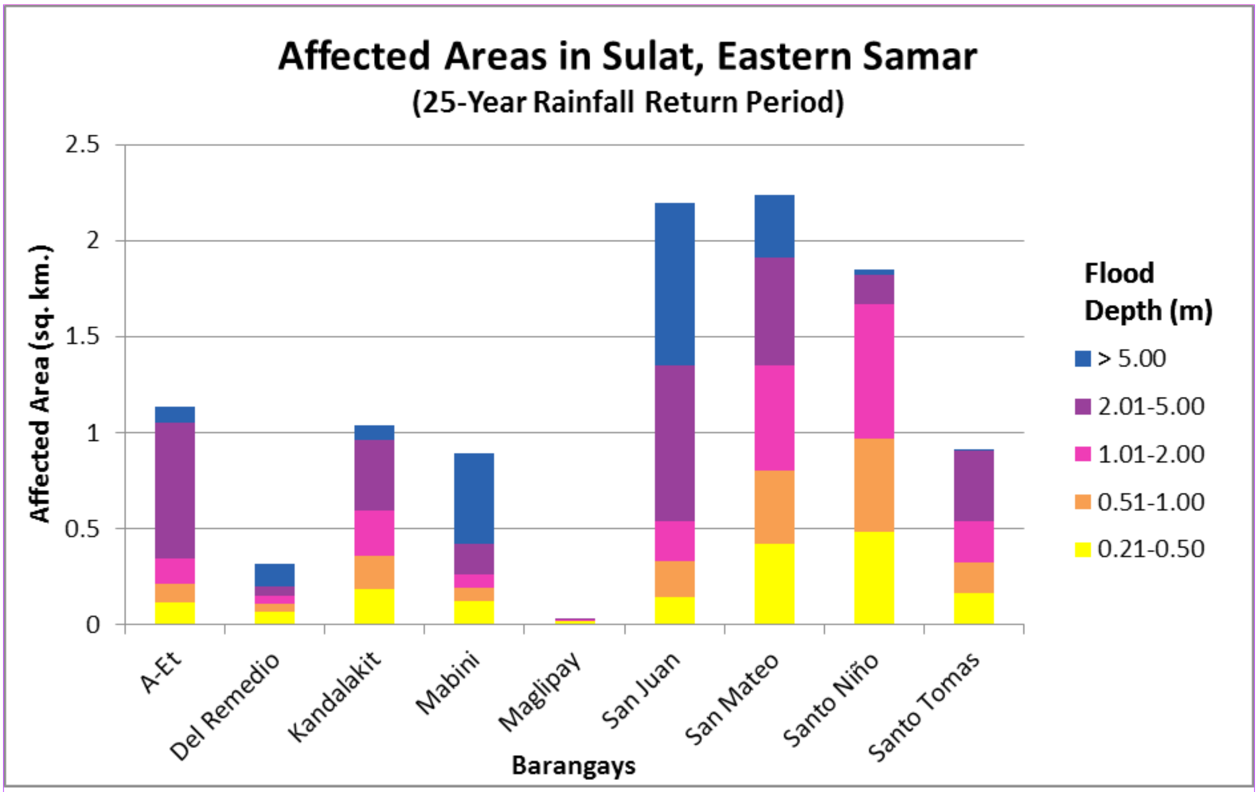

Figure 73. Affected Areas in Sulat, Eastern Samar during 25-Year Rainfall Return Period.

For the municipality of Taft, with an area of 230.27 sq. km., 1.08% will experience flood levels of less 0.20 meters. 0.027% of the area will experience flood levels of 0.21 to 0.50 meters while 0.02%, 0.02%, 0.03% and 0.011% of the area will experience flood depths of 0.51 to 1 meter, 1.01 to 2 meters, 2.01 to 5 meters and more than 5 meters respectively. Listed in Table 35 are the affected areas in square kilometres by flood depth per barangay.

Table 35. Affected Areas in Taft, Eastern Samar during 25-Year Rainfall Return Period.

Affected Area (sq. km.) by flood depth (in m.)	Areas of affected Barangays in Taft (in sq.km.)	
	Malinao	Mantang
0.03-0.20	1.18	1.31
0.21-0.50	0.032	0.03
0.51-1.00	0.023	0.024
1.01-2.00	0.021	0.026
2.01-5.00	0.04	0.026
> 5.00	0.0012	0.023

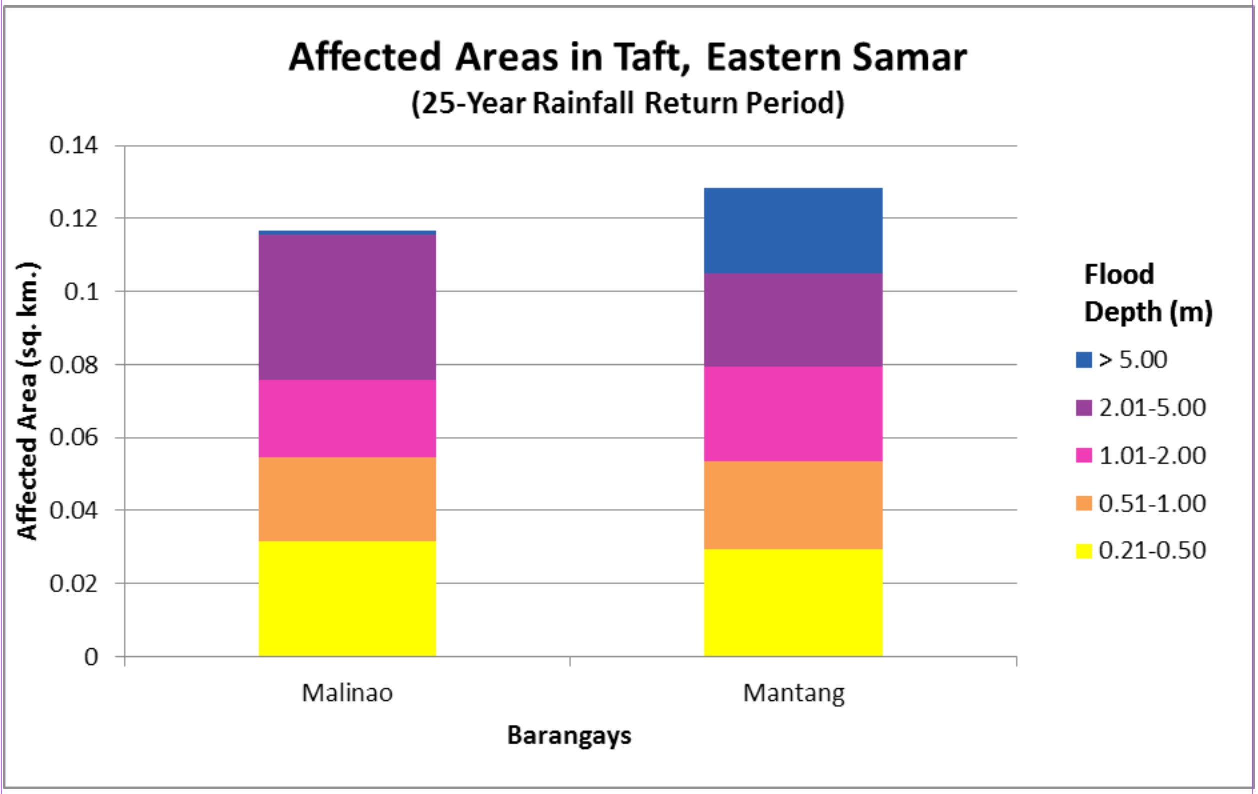

Figure 74. Affected Areas in Taft, Eastern Samar during 25-Year Rainfall Return Period.

For the 100-year return period, 1.34% of the municipality of San Julian with an area of 127.43 sq. km. will experience flood levels of less 0.20 meters. 0.034% of the area will experience flood levels of 0.21 to 0.50 meters while 0.015%, 0.013%, 0.023% and 0.0009% of the area will experience flood depths of 0.51 to 1 meter, 1.01 to 2 meters, 2.01 to 5 meters and more than 5 meters, respectively. Listed in Table 36 are the affected areas in San Julian in square kilometers by flood depth per barangay.

Table 36. Affected Areas in San Julian, Eastern Samar during 100-Year Rainfall Return Period.

Affected Area (sq. km.) by flood depth (in m.)	Areas of affected Barangays in San Julian (in sq.km.)		
	Casoroy	Nena	Putong
0.03-0.20	0.26	0.96	0.49
0.21-0.50	0.0054	0.024	0.014
0.51-1.00	0.00005	0.01	0.009
1.01-2 .00	0.0001	0.011	0.006
2.01-5.00	0	0.027	0.0032
> 5.00	0	0.0011	0

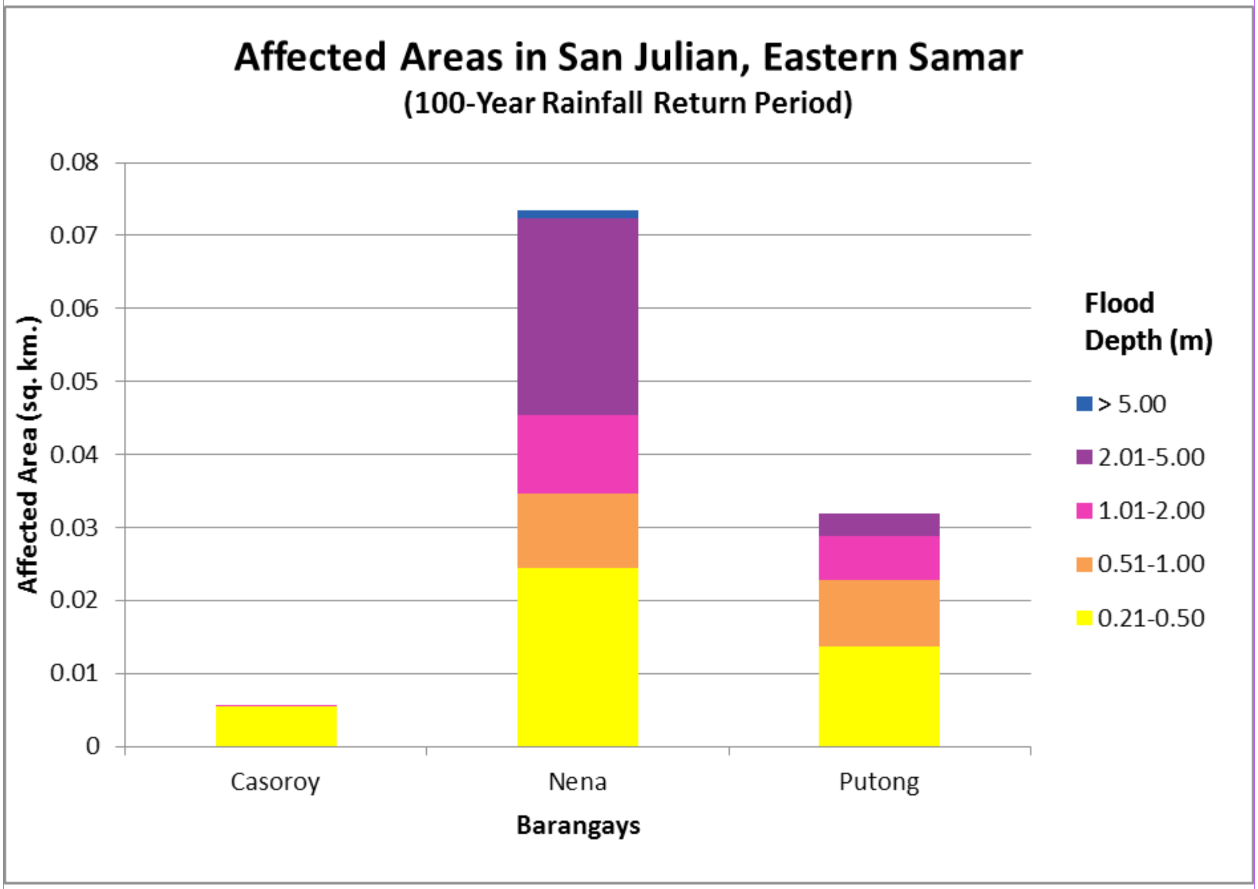

Figure 75. Affected Areas in San Julian, Eastern Samar during 100-Year Rainfall Return Period.

For the municipality of Sulat, with an area of 150.05 sq. km., 25.83% will experience flood levels of less 0.20 meters. 1.13% of the area will experience flood levels of 0.21 to 0.50 meters while 1.15%, 1.45%, 2.26% and 1.7% of the area will experience flood depths of 0.51 to 1 meter, 1.01 to 2 meters, 2.01 to 5 meters, and more than 5 meters respectively. Listed in Table 37 are the affected areas in Sulat in square kilometers by flood depth per barangay.

Table 37. Affected Areas in Sulat, Eastern Samar during 100-Year Rainfall Return Period.

Affected Area (sq. km.) by flood depth (in m.)	Areas of affected Barangays in Sulat (in sq.km.)								
	A-Et	Del Remedio	Kandalakit	Mabini	Maglipay	San Juan	San Mateo	Santo Niño	Santo Tomas
0.03-0.20	4.38	2.89	9.16	5.39	0.078	4.97	4.32	2.1	5.46
0.21-0.50	0.1	0.074	0.19	0.13	0.02	0.15	0.36	0.5	0.17
0.51-1.00	0.089	0.045	0.17	0.074	0.0056	0.17	0.46	0.56	0.15
1.01-2.00	0.11	0.042	0.23	0.074	0.002	0.19	0.53	0.8	0.19
2.01-5.00	0.7	0.051	0.4	0.15	0.0026	0.7	0.74	0.22	0.43
> 5.00	0.19	0.14	0.12	0.58	0	1.08	0.38	0.038	0.031

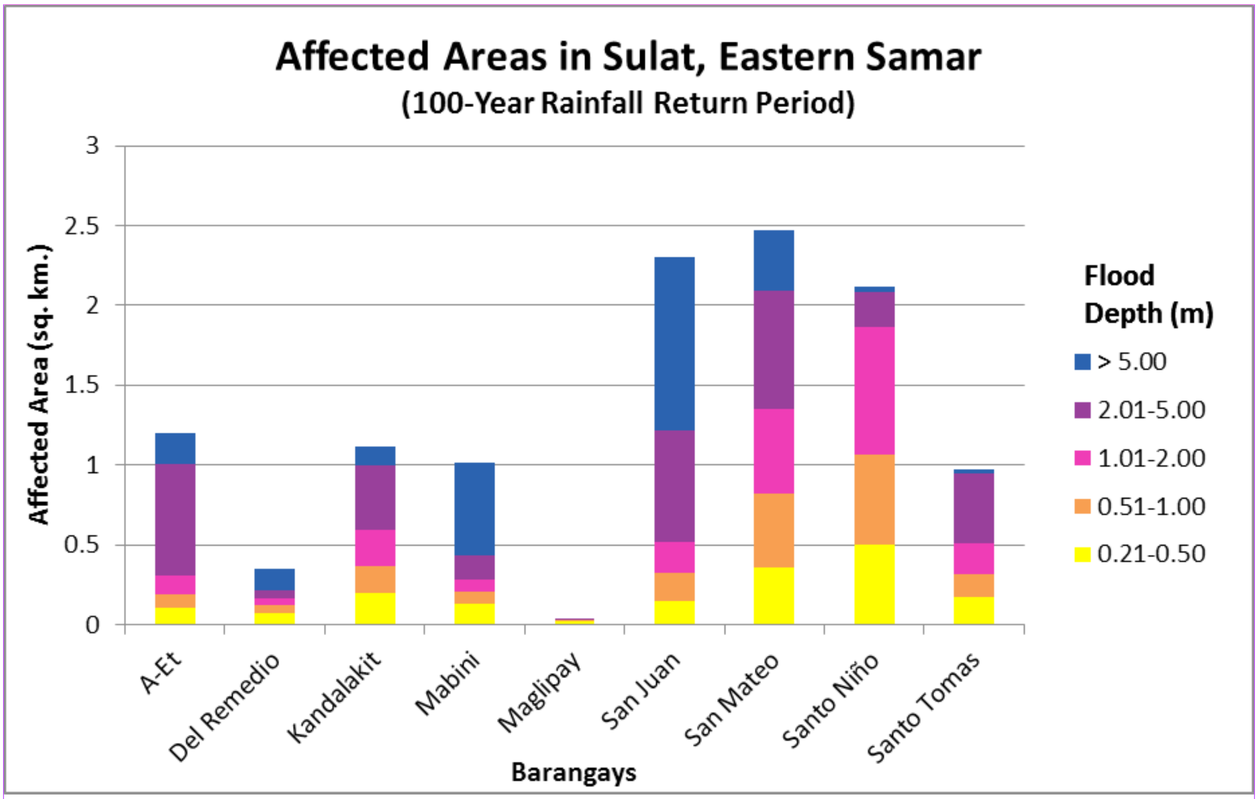

Figure 76. Affected Areas in Sulat, Eastern Samar during 100-Year Rainfall Return Period.

For the municipality of Taft, with an area of 230.27 sq. km., 1.07% will experience flood levels of less 0.20 meters. 0.029% of the area will experience flood levels of 0.21 to 0.50 meters while 0.022%, 0.021%, 0.031% and 0.014% of the area will experience flood depths of 0.51 to 1 meter, 1.01 to 2 meters, 2.01 to 5 meters and more than 5 meters respectively. Listed in Table 38 are the affected areas in square kilometres by flood depth per barangay.

Table 38. Affected Areas in Taft, Eastern Samar during 100-Year Rainfall Return Period.

Affected Area (sq. km.) by flood depth (in m.)	Areas of affected Barangays in Taft (in sq.km.)	
	Malinao	Mantang
0.03-0.20	1.17	1.3
0.21-0.50	0.036	0.032
0.51-1.00	0.023	0.027
1.01-2.00	0.021	0.026
2.01-5.00	0.045	0.026
> 5.00	0.0031	0.03

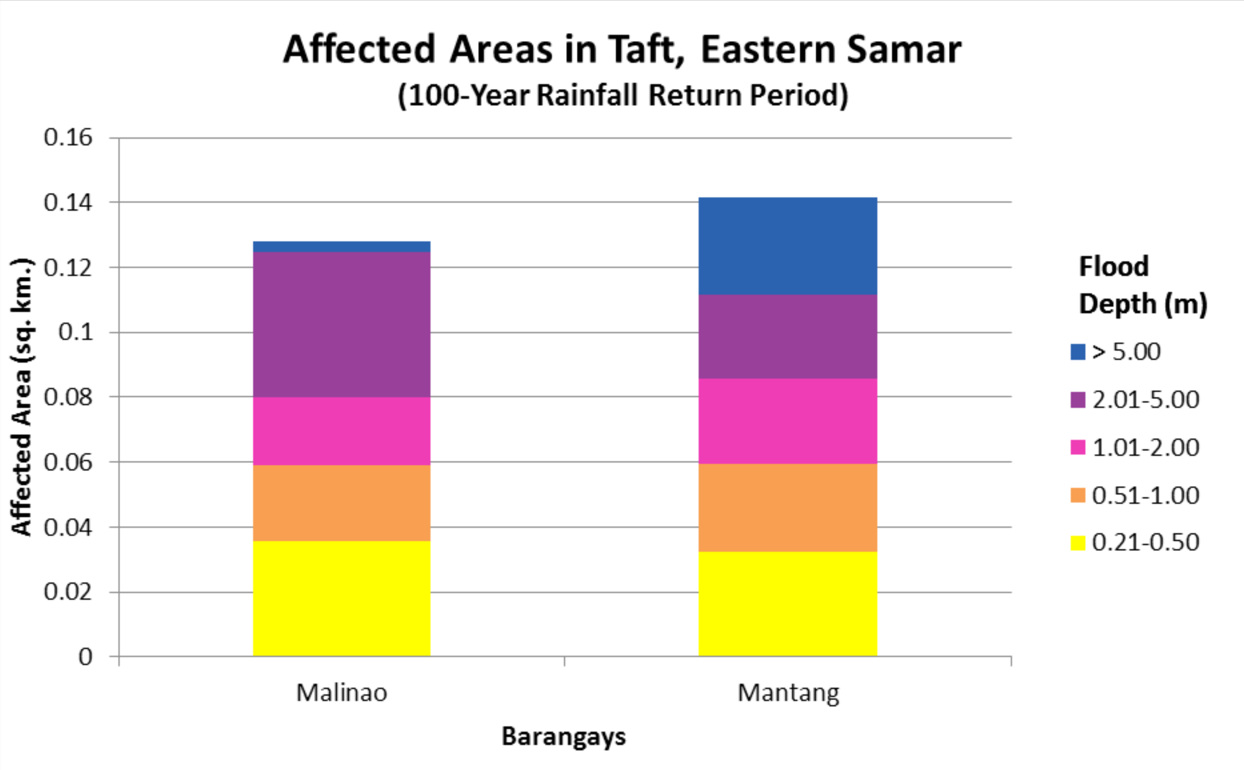

Figure 77. Affected Areas in Taft, Eastern Samar during 100-Year Rainfall Return Period.

Among the barangays in the municipality of San Julian, Nena is projected to have the highest percentage of area that will experience flood levels at 0.81%. Meanwhile, Putong posted the second highest percentage of area that may be affected by flood depths at 0.41%.

Among the barangays in the municipality of Sulat, Kandalakit is projected to have the highest percentage of area that will experience flood levels at 6.85%. Meanwhile, San Juan posted the second highest percentage of area that may be affected by flood depths at 4.84%.

Among the barangays in the municipality of Taft, Mantang is projected to have the highest percentage of area that will experience flood levels of at 0.62%. Meanwhile, Malinao posted the percentage of area that may be affected by flood depths of at 0.56%.

Moreover, the generated flood hazard maps for the Sulat Floodplain were used to assess the vulnerability of the educational and medical institutions in the floodplain. Using the flood depth units of PAGASA for hazard maps - “Low”, “Medium”, and “High” - the affected institutions were given their individual assessment for each Flood Hazard Scenario (5-year, 25-year, and 100-year).

Table 39. Area covered by each warning level with respect to the rainfall scenarios

Warning Level	Area Covered in sq. km		
	5 year	25 year	100 year
Low	1.69	1.77	1.77
Medium	2.94	2.76	2.93
High	4.79	6.41	7.26

Of the four (4) identified Education Institute in Sulat Flood plain, two schools were discovered exposed to Medium-level flooding for the 5- and 25-year scenarios. For the 100 year scenario, these 2 schools were assessed for High level flooding.

Only one medical institution was identified in Sulat Floodplain, namely Sto Niño Health Center. The institution was assessed to be exposed to the Medium level flooding during a 5, 25, and 100 year scenario.

5.11 Flood Validation

In order to check and validate the extent of flooding in different river systems, there is a need to perform validation survey work. Field personnel gather secondary data regarding flood occurrence in the area within the major river system in the Philippines.

From the flood depth maps produced by Phil-LiDAR 1 Program, multiple points representing the different flood depths for different scenarios were identified for validation.

The validation personnel will then go to the specified points identified in a river basin and will gather data regarding the actual flood level in each location. Data gathering can be done through a local DRRM office to obtain maps or situation reports about the past flooding events or interview some residents with knowledge of or have had experienced flooding in a particular area.

The actual data from the field were compared to the simulated data to assess the accuracy of the Flood Depth Maps produced and to improve on the results of the flood map. The points in the flood map versus its corresponding validation depths are shown in Figure 78.

The flood validation consists of 181 points randomly selected all over the Sulat flood plain Comparing it with the flood depth map of the nearest storm event, the map has an RMSE value of 0.67 m. Table 40 shows a contingency matrix of the comparison. The validation points are found in ANNEX 11.

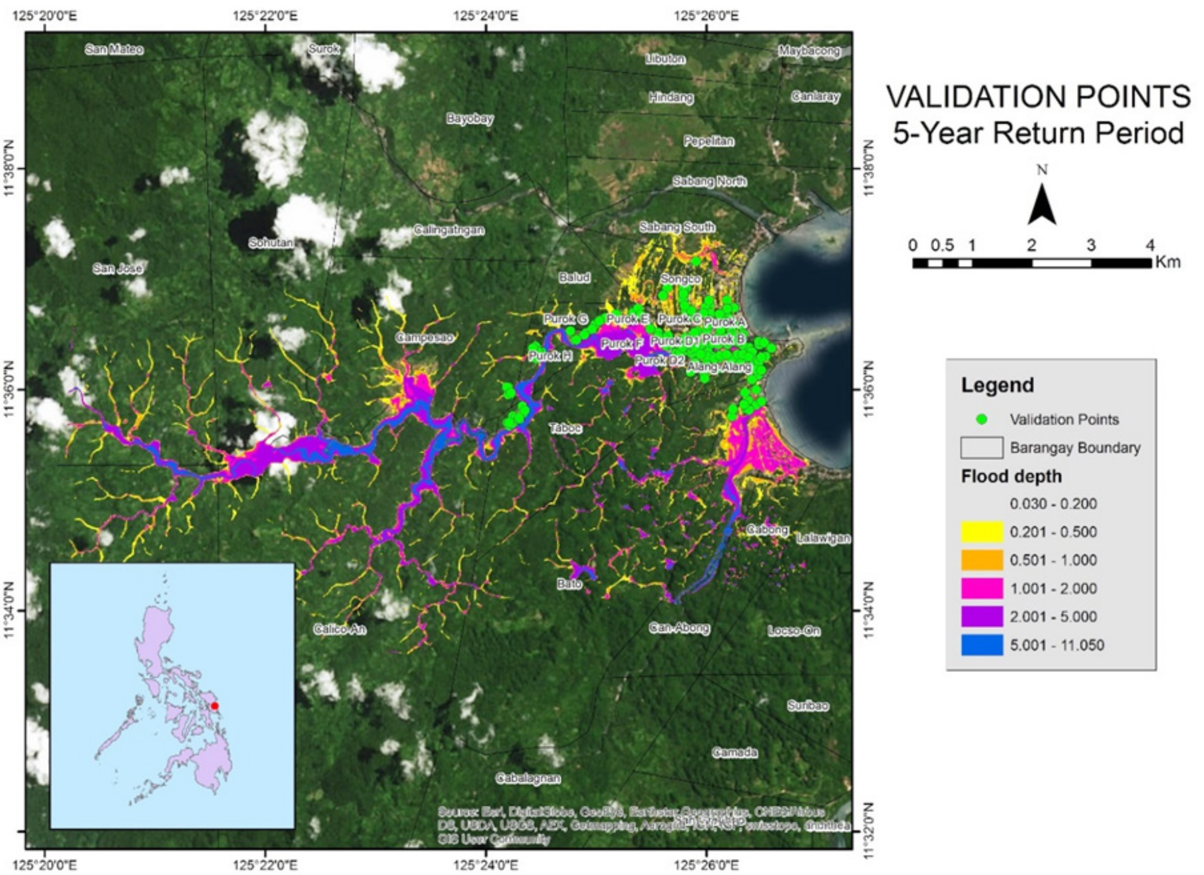

Figure 78. Validation Points for a 5-year Flood Depth Map of the Sulat Floodplain.

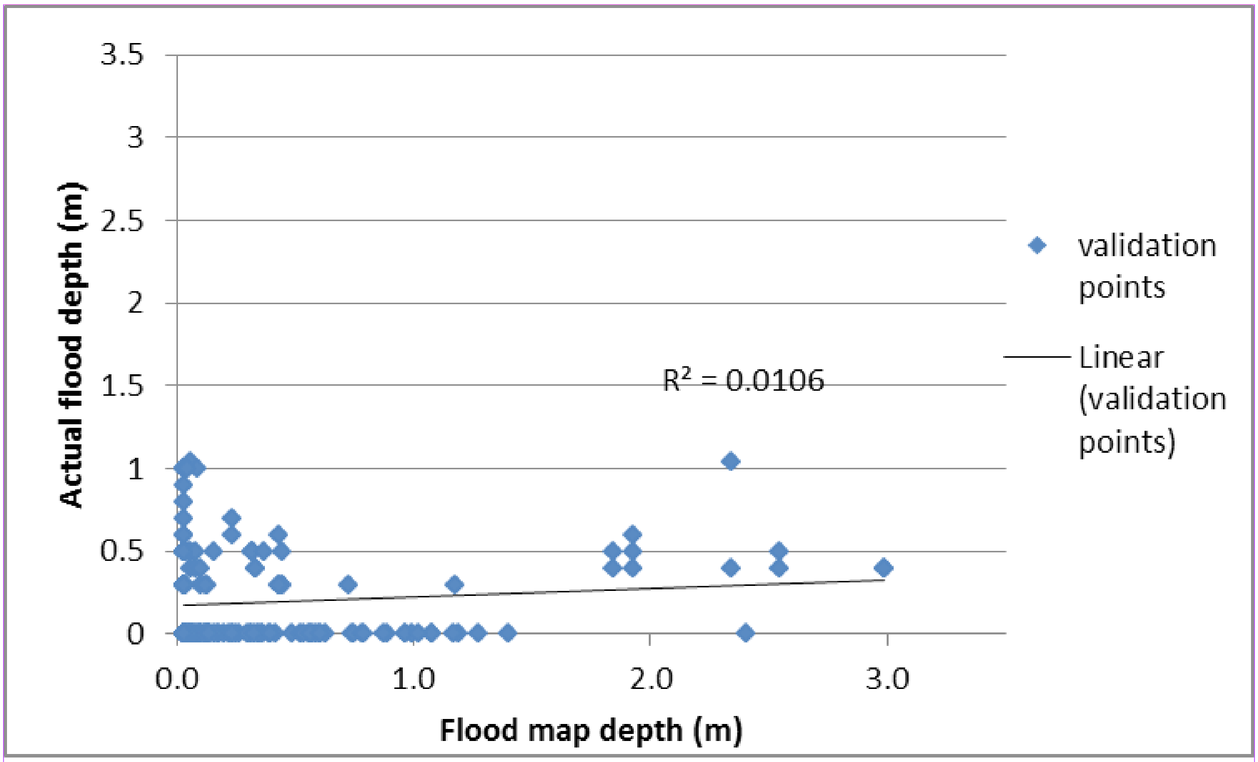

Figure 79. Flood Map depth versus Actual Flood Depth

Table 40. Actual Flood Depth versus Simulated Flood Depth at different levels in the Sulat River Basin.

SULAT BASIN		MODELED FLOOD DEPTH (m)						
		0-0.20	0.21-0.50	0.51-1.00	1.01-2.00	2.01-5.00	> 5.00	Total
Actual Flood Depth (m)	0-0.20	70	17	18	7	1	0	**113**
	0.21-0.50	28	11	1	5	5	0	**50**
	0.51-1.00	12	3	0	1	0	0	**16**
	1.01-2.00	1	0	0	0	1	0	**2**
	2.01-5.00	0	0	0	0	0	0	**0**
	> 5.00	0	0	0	0	0	0	**0**
	Total	**111**	**31**	**19**	**13**	**7**	**0**	**181**

On the whole, the overall accuracy generated by the flood model is estimated at 44.75%, with 81 points correctly matching the actual flood depths. In addition, there were 51 points estimated one level above and below the correct flood depths while there were 35 points and 14 points estimated two levels above and below, and three or more levels above and below the correct flood. A total of 56 points were overestimated while a total of 44 points were underestimated in the modelled flood depths of Sulat. Table 41 depicts the summary of the Accuracy Assessment in the Sulat River Basin Flood Depth Map.

Table 41. Summary of the Accuracy Assessment in the Sulat River Basin Survey.

	No. of Points	%
Correct	81	44.75
Overestimated	56	30.94
Underestimated	44	24.31
Total	**181**	**100**

REFERENCES

Ang M.O., Paringit E.C., et al. 2014. *DREAM Data Processing Component Manual.* Quezon City, Philippines: UP Training Center for Applied Geodesy and Photogrammetry.

Balicanta L.P., Paringit E.C., et al. 2014. *DREAM Data Validation Component Manual.* Quezon City, Philippines: UP Training Center for Applied Geodesy and Photogrammetry.

Lagmay A.F., Paringit E.C., et al. 2014. *DREAM Flood Modeling Component Manual.* Quezon City, Philippines: UP Training Center for Applied Geodesy and Photogrammetry.

Paringit E.C, Balicanta L.P., Ang, M.O., Sarmiento, C. 2017. *Flood Mapping of Rivers in the Philippines Using Airborne Lidar: Methods.* Quezon City, Philippines: UP Training Center for Applied Geodesy and Photogrammetry.

Sarmiento C., Paringit E.C., et al. 2014. *DREAM Data Acquisition Component Manual.* Quezon City, Philippines: UP Training Center for Applied Geodesy and Photogrammetry.

UP TCAGP 2016, *Acceptance and Evaluation of Synthetic Aperture Radar Digital Surface Model (SAR DSM) and Ground Control Points (GCP).* Quezon City, Philippines: UP Training Center for Applied Geodesy and Photogrammetry.

ANNEX

ANNEX 1. Technical Specifications of the LIDAR Sensors used in the Sulat Floodplain Survey

1. AQUARIUS SENSOR

Figure A-1.1 Aquarius Sensor

Table A-1.1 Parameters and Specifications of Aquarius Sensor

Parameter	Specification
Operational altitude	300-600 m AGL
Laser pulse repetition rate	33, 50. 70 kHz
Scan rate	0-70 Hz
Scan half-angle	0 to ± 25 ˚
Laser footprint on water surface	30-60 cm
Depth range	0 to > 10 m (for k < 0.1/m)
Topographic mode	
Operational altitude	300-2500
Range Capture	Up to 4 range measurements, including 1st, 2nd, 3rd, and last returns
Intensity capture	12-bit dynamic measurement range
Position and orientation system	POS AVTM 510 (OEM) includes embedded 72-channel GNSS receiver (GPS and GLONASS)
Data Storage	Ruggedized removable SSD hard disk (SATA III)
Power	28 V, 900 W, 35 A
Image capture	5 MP interline camera (standard); 60 MP full frame (optional)
Full waveform capture	12-bit Optech IWD-2 Intelligent Waveform Digitizer (optional)
Dimensions and weight	Sensor:250 x 430 x 320 mm; 30 kg; Control rack: 591 x 485 x 578 mm; 53 kg
Operating temperature	0-35˚C
Relative humidity	0-95% no-condensing

ANNEX 2. NAMRIA Certificate of Reference Points Used in the LiDAR Survey

1. SME-3139

Republic of the Philippines
Department of Environment and Natural Resources
NATIONAL MAPPING AND RESOURCE INFORMATION AUTHORITY

June 24, 2014

CERTIFICATION

To whom it may concern:

This is to certify that according to the records on file in this office, the requested survey information is as follows -

Province: **EASTERN SAMAR**
Station Name: **SME-3139**
Order: **4th**

Island: **VISAYAS**		Barangay: **SANTO NIÑO**
Municipality: **SULAT**		
	PRS92 Coordinates	
Latitude: **11° 50' 2.95701"**	Longitude: **125° 26' 3.02189"**	Ellipsoidal Hgt: **0.35600 m.**
	WGS84 Coordinates	
Latitude: **11° 49' 58.57713"**	Longitude: **125° 26' 8.12160"**	Ellipsoidal Hgt: **62.18500 m.**
	PTM Coordinates	
Northing: **1308628.152 m.**	Easting: **547309.911 m.**	Zone: **5**
	UTM Coordinates	
Northing: **1,309,289.26**	Easting: **765,219.59**	Zone: **51**

Location Description

SME-3139

From Tacloban City, travel about 70 Km. NE towards the junction of Buena Vista, Quinapondan. Then travel about 170 Km. NW pass Gen. Mc Arthur, Hernani, Llorente, Balangkayan, Maydolong, Borongan and San Julian pass Sulat proper towards Brgy. Sto. Niño until reaching a bridge near the Km. post 900 S-4. Station is located at the right side of the road about 1 m S of the bridge, about 100 m S of Km. post 900 S-4, about 500 m S of the brgy. basketball court. Mark is the head of a 4 in. copper nail centered on a 0.20 m x 0.20 m x 1.00 m concrete monument with inscriptions, "SME-3139, 2008, NAMRIA".

Requesting Party:	**Engr. Cruz**
Pupose:	**Reference**
OR Number:	**8796376 A**
T.N.:	**2014-1442**

For **RUEL DM. BELEN, MNSA**
Director, Mapping And Geodesy Branch

9 9 0 6 2 4 2 0 1 4 1 1 1 1 7 1 8

CERTIFICATION INTERNATIONAL ISO 9001:2008 · JAB ACCREDITED · CIP/4701/12/09/814

NAMRIA OFFICES:
Main : Lawton Avenue, Fort Bonifacio, 1634 Taguig City, Philippines Tel. No.: (632) 810-4831 to 41
Branch : 421 Barraca St. San Nicolas, 1010 Manila, Philippines, Tel. No. (632) 241-3494 to 98
www.namria.gov.ph

ISO 9001: 2008 CERTIFIED FOR MAPPING AND GEOSPATIAL INFORMATION MANAGEMENT

Figure A-2.1 SME-3139

ANNEX 3. Baseline Processing Reports of Control Points used in the LiDAR Survey

1. SE-16

SME-3139 - SE-16 (6:11:03 AM-11:04:02 AM) (S2)

Baseline observation:	SME-3139 --- SE-16 (B2)
Processed:	6/30/2014 5:42:19 PM
Solution type:	Fixed
Frequency used:	Dual Frequency (L1, L2)
Horizontal precision:	0.001 m
Vertical precision:	0.002 m
RMS:	0.000 m
Maximum PDOP:	3.434
Ephemeris used:	Broadcast
Antenna model:	Trimble Relative
Processing start time:	6/9/2014 6:11:10 AM (Local: UTC+8hr)
Processing stop time:	6/9/2014 11:04:02 AM (Local: UTC+8hr)
Processing duration:	04:52:52
Processing interval:	1 second

Vector Components (Mark to Mark)

From:	SME-3139				
Grid		Local		Global	
Easting	765219.591 m	Latitude	N11°50'02.95701"	Latitude	N11°49'58.57713"
Northing	1309289.260 m	Longitude	E125°26'03.02189"	Longitude	E125°26'08.12160"
Elevation	2.987 m	Height	0.356 m	Height	62.185 m

To:	SE-16				
Grid		Local		Global	
Easting	765219.942 m	Latitude	N11°50'03.05106"	Latitude	N11°49'58.67117"
Northing	1309292.154 m	Longitude	E125°26'03.03429"	Longitude	E125°26'08.13400"
Elevation	3.103 m	Height	0.472 m	Height	62.301 m

Vector					
ΔEasting	0.350 m	NS Fwd Azimuth	7°23'58"	ΔX	-0.028 m
ΔNorthing	2.894 m	Ellipsoid Dist.	2.914 m	ΔY	-0.608 m
ΔElevation	0.116 m	ΔHeight	0.116 m	ΔZ	2.852 m

Standard Errors

Vector errors:					
σ ΔEasting	0.000 m	σ NS fwd Azimuth	0°00'35"	σ ΔX	0.001 m
σ ΔNorthing	0.000 m	σ Ellipsoid Dist.	0.000 m	σ ΔY	0.001 m
σ ΔElevation	0.001 m	σ ΔHeight	0.001 m	σ ΔZ	0.000 m

ANNEX 4. The LiDAR Survey Team Composition

Table A-4.1 The LiDAR Survey Team Composition

Data Acquisition Component Sub-Team	Designation	Name	Agency / Affiliation
PHIL-LIDAR 1	Program Leader	ENRICO PARINGIT, D.ENG	UP-TCAGP
Data Acquisition Component Leader	Data Component Project Leader - I	ENGR. CZAR JAKIRI SARMIENTO	
		ENGR. LOUIE P. BALICANTA	
Survey Supervisor	Chief Science Research Specialist (CSRS)	ENGR. CHRISTOPHER CRUZ	
	Supervising Science Research Specialist (Supervising SRS)	LOVELY GRACIA ACUÑA	
		LOVELYN ASUNCION	
FIELD TEAM			
LiDAR Operation	Research Associate (RA)	PAULINE JOANNE ARCEO	UP-TCAGP
		MARY CATHERINE ELIZABETH BALIGUAS	
Ground Survey, Data Download and Transfer	RA	JERIEL PAUL ALAMBAN	
LiDAR Operation	Airborne Security	SSG. RAYMUND DOMINE	PHILIPPINE AIR FORCE (PAF)
	Pilot	CAPT. NEIL ACHILLES AGAWIN	ASIAN AEROSPACE CORPORATION (AAC)
		CAPT. JACKSON JAVIER	

ANNEX 5. Data Transfer Sheet for Sulat Floodplain

DATA TRANSFER SHEET
6/19/2014 (Samar - Leyte)

DATE	FLIGHT NO.	MISSION NAME	SENSOR	RAW LAS		LOGS	POS	RAW IMAGES	MISSION LOG FILE	RANGE	DIGITIZER	BASE STATION(S)		OPERATOR LOGS (OPLOG)	FLIGHT PLAN		SERVER LOCATION
				Output LAS	KML (swath)		MB	GB		GB		BASE STATION(S)	Base Info (.txt)		Actual	KML	
30-May-14	1520A	3BLK33VSS150A	Aquarius	NA	424/602	1.48	289	88.5	748	14	164	10.5	1KB	1KB	4	NA	X:\Airborne_Raw\1520A
31-May-14	1522A	3BLK33SS151A	Aquarius	NA	288	469KB	112	9.78/21	164/69	4.87	59.1	4.53	1KB	1KB	5	NA	X:\Airborne_Raw\1522A
1-Jun-14	1526A	3BLK33SSR152A	Aquarius	NA	456/784	1.68	277	119	403	15.5	204	8.36	1KB	1KB	6	NA	X:\Airborne_Raw\1526A
2-Jun-14	1530A	3BLK33RSQ153A	Aquarius	NA	353/605	1.48	254	30.9/80.2	555/246	15.6	165	7.88	1KB	1KB	3	NA	X:\Airborne_Raw\1530A
3-Jun-14	1534A	3BLK33QS154A	Aquarius	NA	1175	1.49	250	56.9/35.1	399/154	14.5	114/95.5	6.6	1KB	1KB	7	NA	X:\Airborne_Raw\1534A
7-Jun-14	1550A	3BLK33P158A	Aquarius	NA	657	1.03	199	52.9	na	10.8	149	7	1KB	1KB	3	NA	X:\Airborne_Raw\1550A
8-Jun-14	1554A	3BLK33PSM159A	Aquarius	NA	533/1012	1.78	257	99.8	695	14.5	27.2/59/32.2	16.4	1KB	1KB	3	NA	X:\Airborne_Raw\1554A
8-Jun-14	1556A	3BLK33MS159B	Aquarius	NA	982	1.52	291	97.2	477	15.9	216	16.4	1KB	1KB	5	NA	X:\Airborne_Raw\1556A
9-Jun-14	1558A	3BLK33J160A	Aquarius	NA	833	1.27	277	95.7	452	14.2	95.6/80.5	16.1	1KB	1KB	4	NA	X:\Airborne_Raw\1558A
9-Jun-14	1560A	3BLK33J	Aquarius	NA	1583	1.67	223	72.2	357	12.1	123	16.1	1KB	1KB	5	NA	X:\Airborne_Raw\1560A

Received from

Name O. JOAQUIN
Position DA
Signature

Received by

Name JOIDA PRIETO
Position SSRS
Signature
6/19/14

14-43

Figure A-5.1 Transfer Sheet for Sulat Floodplain - A

ANNEX 6. Flight logs for the flight missions

1. Flight Log for 1558A Mission

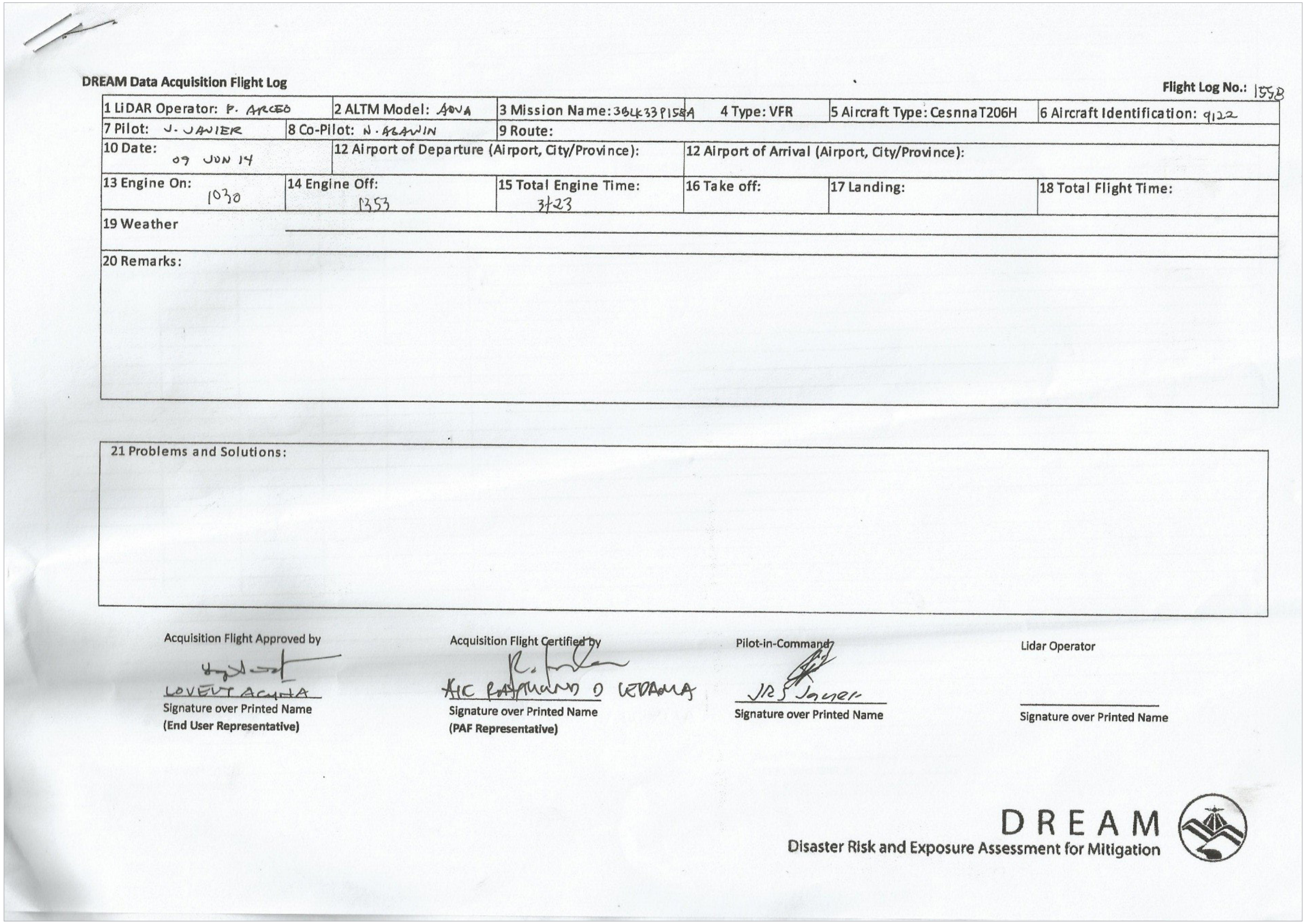

DREAM Data Acquisition Flight Log

Flight Log No.: 1558

1 LiDAR Operator: P. ARCEO	2 ALTM Model: AQUA	3 Mission Name: 3BLK33P158A	4 Type: VFR	5 Aircraft Type: Cesnna T206H	6 Aircraft Identification: 9122
7 Pilot: J. JAVIER	8 Co-Pilot: N. ABAWIN	9 Route:			
10 Date: 09 JUN 14	12 Airport of Departure (Airport, City/Province):		12 Airport of Arrival (Airport, City/Province):		
13 Engine On: 1030	14 Engine Off: 1353	15 Total Engine Time: 3+23	16 Take off:	17 Landing:	18 Total Flight Time:
19 Weather					
20 Remarks:					

21 Problems and Solutions:

Acquisition Flight Approved by	Acquisition Flight Certified by	Pilot-in-Command	Lidar Operator
LOVELYT ACUNA	A1C RAYMUND D CEDAMA	JR S Javier	
Signature over Printed Name (End User Representative)	Signature over Printed Name (PAF Representative)	Signature over Printed Name	Signature over Printed Name

DREAM
Disaster Risk and Exposure Assessment for Mitigation

Figure A-6.1 Flight Log for Mission 7320GC

2. Flight Log for 1560A Mission

PHIL-LiDAR 1 Data Acquisition Flight Log

Flight Log No.: 1560A

1 LiDAR Operator: C. BALIGUAS	2 ALTM Model: AQUA	3 Mission Name: 3BLK33JS 608	4 Type: VFR	5 Aircraft Type: Cesnna T206H	6 Aircraft Identification: 9122
7 Pilot: J JAVIER	8 Co-Pilot: N. AGAWIN	9 Route:			
10 Date: 09 JUNE 14	12 Airport of Departure (Airport, City/Province):		12 Airport of Arrival (Airport, City/Province):		
13 Engine On:	14 Engine Off:	15 Total Engine Time: 3+53	16 Take off:	17 Landing:	18 Total Flight Time:
19 Weather					

20 Flight Classification

20.a Billable
- ✓ Acquisition Flight
- o Ferry Flight
- o System Test Flight
- o Calibration Flight

20.b Non Billable
- o Aircraft Test Flight
- o AAC Admin Flight
- o Others: ____________

20.c Others
- o LiDAR System Maintenance
- o Aircraft Maintenance
- o Phil-LiDAR Admin Activities

21 Remarks

Mission completed over BLK33J

22 Problems and Solutions

- o Weather Problem
- o System Problem
- o Aircraft Problem
- o Pilot Problem
- o Others: ____________

Acquisition Flight Approved by	Acquisition Flight Certified by	Pilot-in-Command	LiDAR Operator	Aircraft Mechanic/ LiDAR Technician
Signature over Printed Name (End User Representative)	K. [signature] Signature over Printed Name (PAF Representative)	JR Javier Signature over Printed Name	[signature] Signature over Printed Name	Signature over Printed Name

Figure A-6.2 Flight Log for Mission 1560A

ANNEX 7. Flight status reports

Sulat Mission

June 9, 2014

Table A-7.1 Flight Status Report

Flight No	Area	Mission	Operator	Date Flown	Remarks
1558A	BLK33J	3BLK33J160A	PJ ARCEO	9 JUN 14	Completed 12 lines over BLK33J
1560A	BLK33J	3BLK33JS160B	MCE BALIGUAS	9 JUN 14	Mission completed over BLK33J

SWATH PER FLIGHT MISSION

Flight No. :	1558A
Area:	BLOCK 33J
Total Area:	115.55 sq. km.
Mission Name:	3BLK33J60A
Altitude:	500m
PRF:	50 kHz
SCF:	45 Hz
Lidar FOV:	22 deg
Sidelap:	30%

Figure A-7.1 Swath for Flight No. 1558A

Flight No. :	1560A
Area:	BLOCK 33J
Total Area:	105.37 sq. km.
Mission Name:	3BLK33JS60A
Altitude:	500m
PRF:	50 kHz
SCF:	45 Hz
Lidar FOV:	22 deg
Sidelap:	25%

Figure A-7.2 Swath for Flight No. 1560A

ANNEX 8. Mission Summary Reports

Table A-8.1 Mission Summary Report for Mission Blk33J

Flight Area	Samar-Leyte
Mission Name	**Blk33J**
Inclusive Flights	1560A, 1558A
Range data size	26.3 GB
POS	500 MB
Image	167.9 GB
Transfer date	June 19, 2014
Solution Status	
Number of Satellites (>6)	Yes
PDOP (<3)	Yes
Baseline Length (<30km)	No
Processing Mode (<=1)	No
Smoothed Performance Metrics (in cm)	
RMSE for North Position (<4.0 cm)	2.1
RMSE for East Position (<4.0 cm)	2.2
RMSE for Down Position (<8.0 cm)	3.1
Boresight correction stdev (<0.001deg)	0.000327
IMU attitude correction stdev (<0.001deg)	0.000898
GPS position stdev (<0.01m)	0.0098
Minimum % overlap (>25)	36.01%
Ave point cloud density per sq.m. (>2.0)	2.71
Elevation difference between strips (<0.20 m)	Yes
Number of 1km x 1km blocks	291
Maximum Height	248.48 m
Minimum Height	49.30 m
Classification (# of points)	
Ground	110,486,647
Low vegetation	51,277,620
Medium vegetation	61,095,498
High vegetation	151,119,077
Building	2,518,830
Orthophoto	Yes
Processed by	Engr. Jommer Medina, Engr. Edgardo Gubatanga, Engr. Gladys Mae Apat

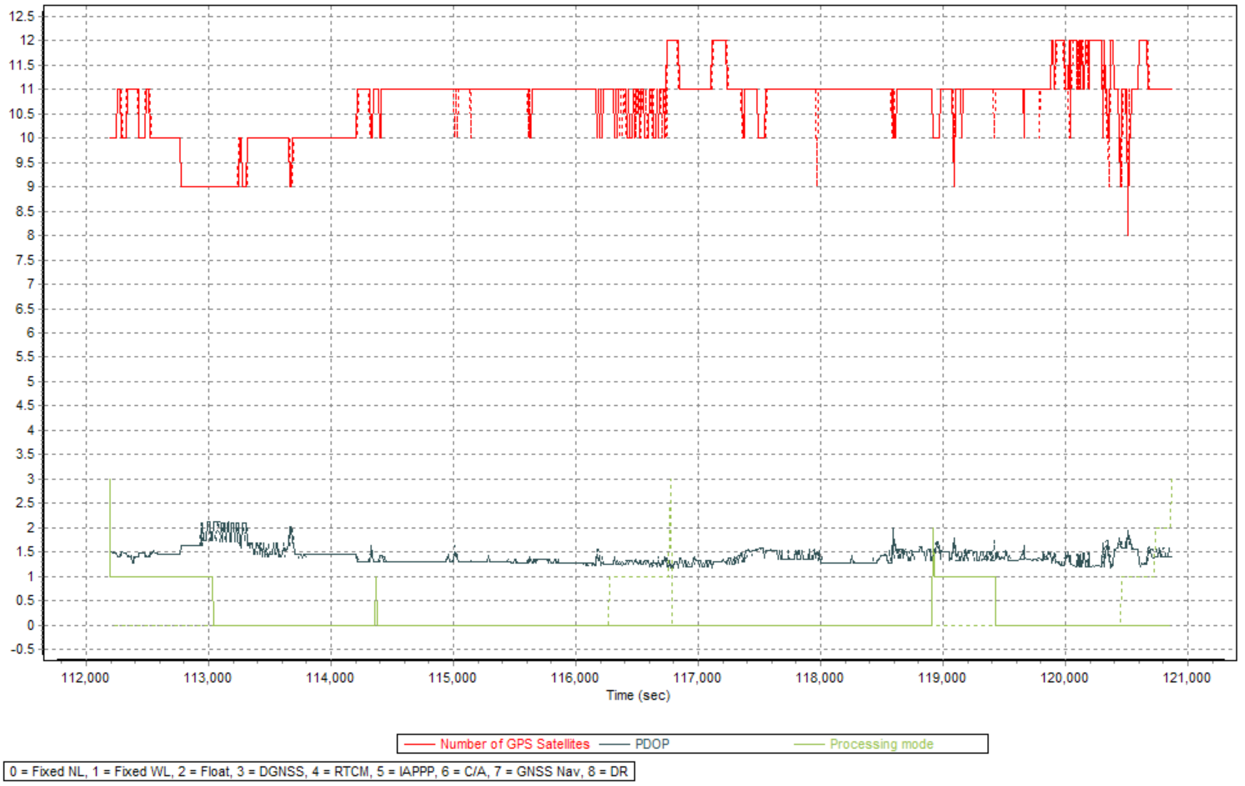

Figure A-8.1 Solution Status

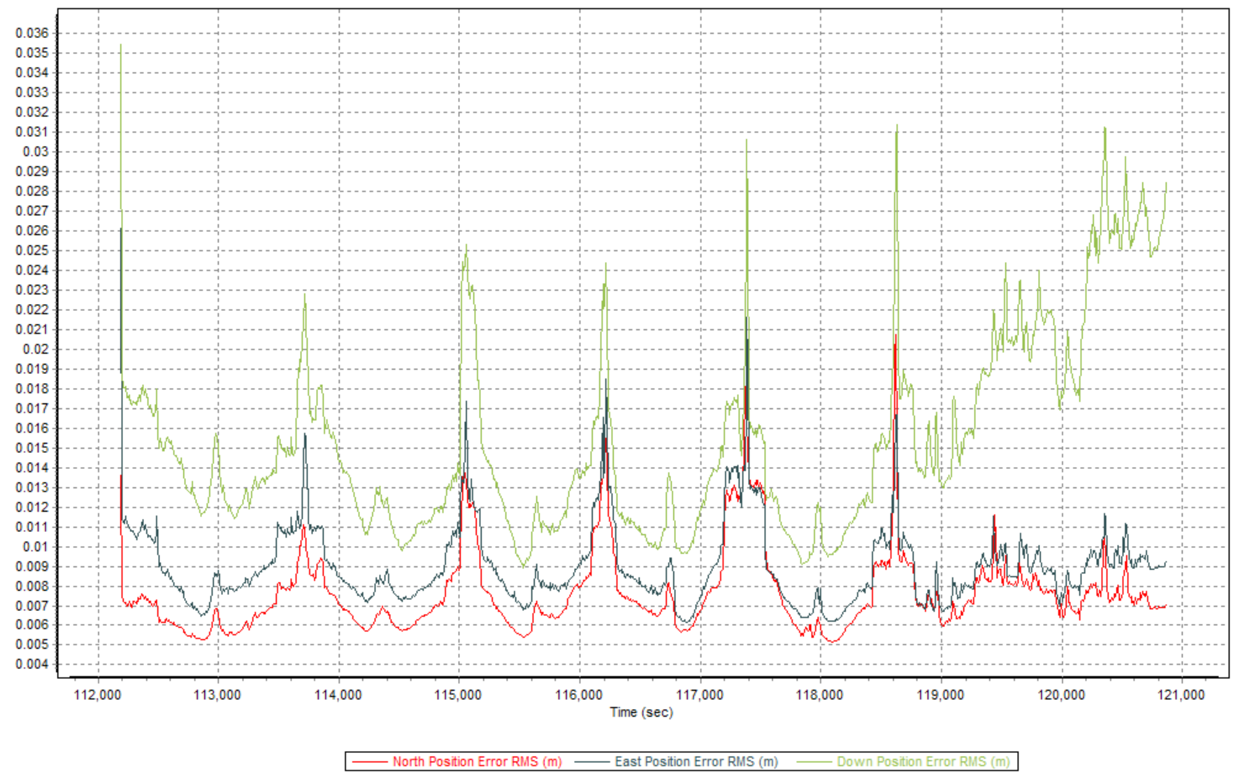

Figure A-8.2 Smoothed Performance Metric Parameters

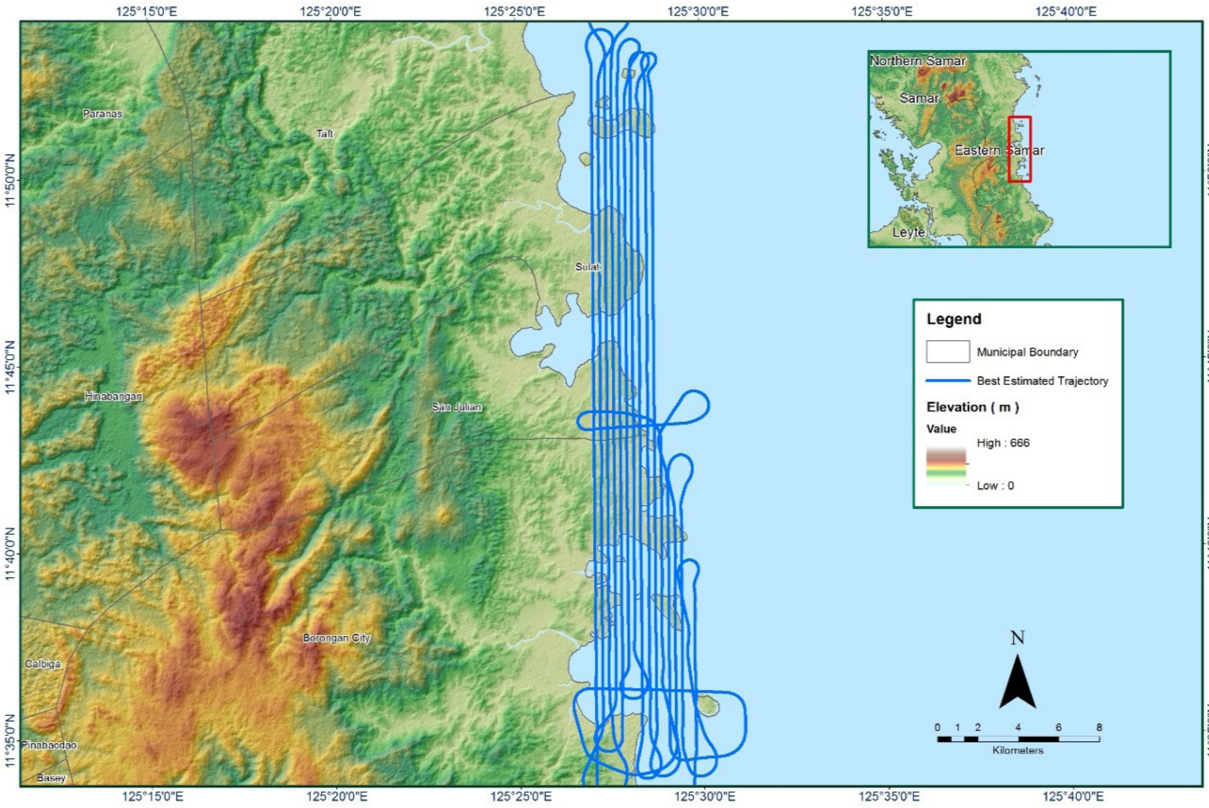

Figure A-8.3 Best Estimated Trajectory

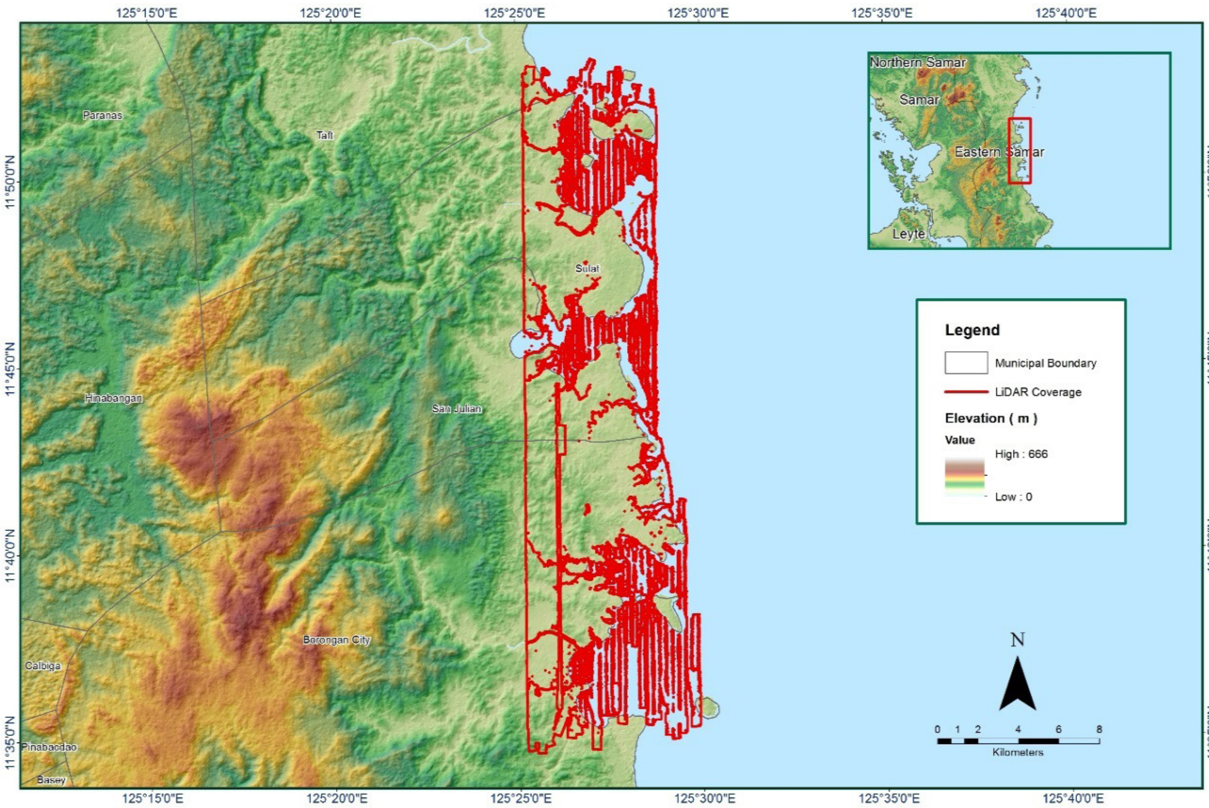

Figure A-8.4 Coverage of LiDAR data

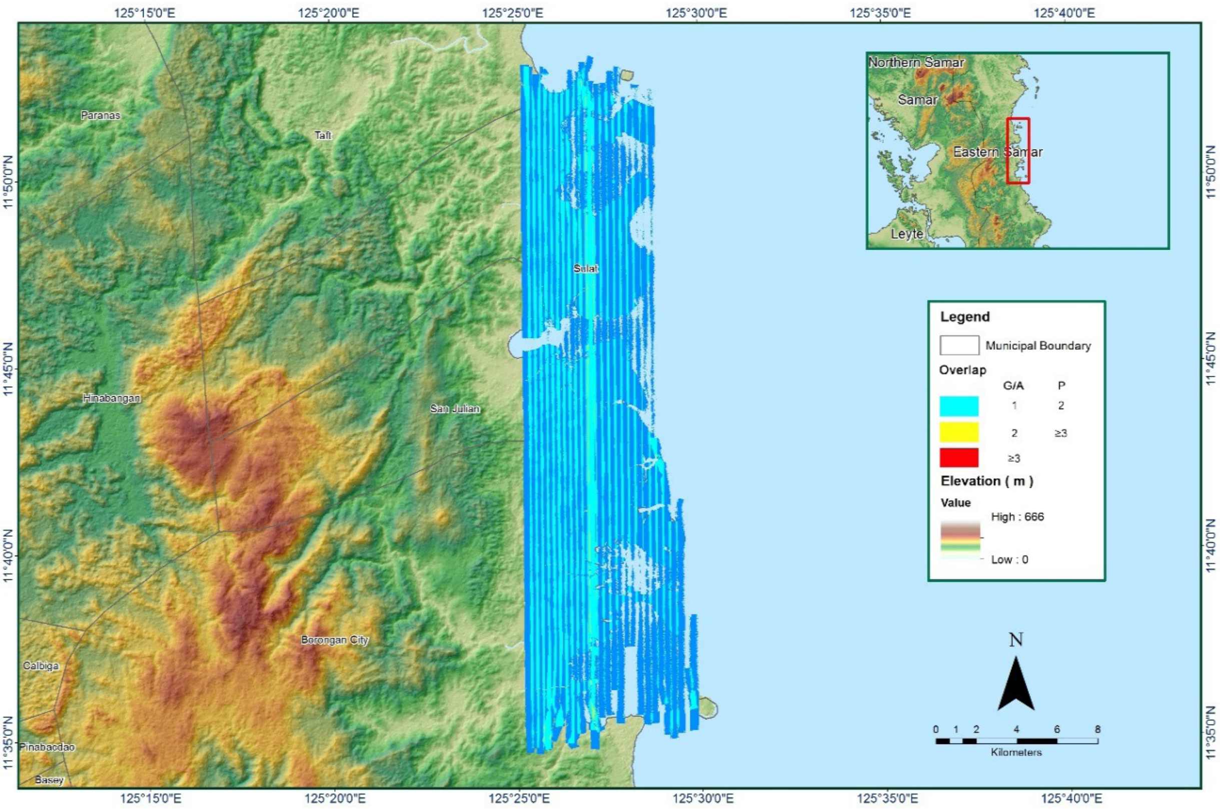

Figure A-8.5 Image of data overlap

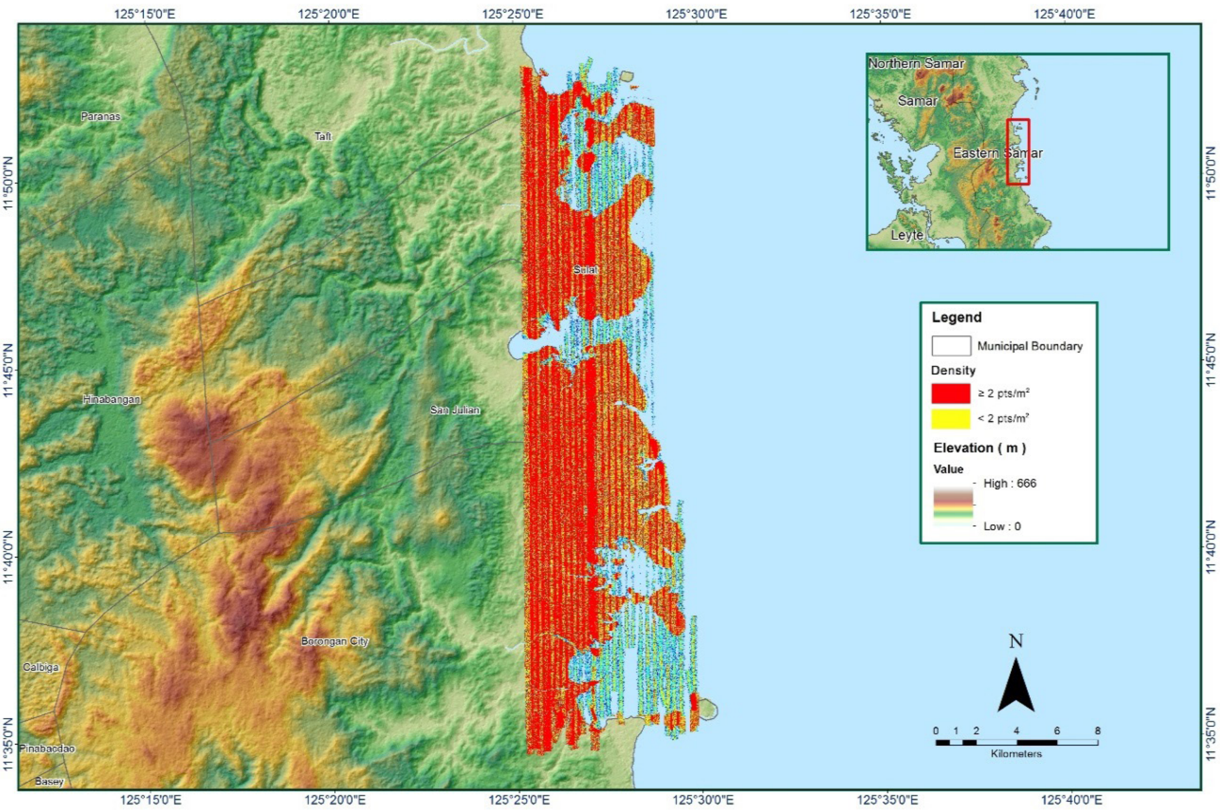

Figure A-8.6 Density map of merged LiDAR data

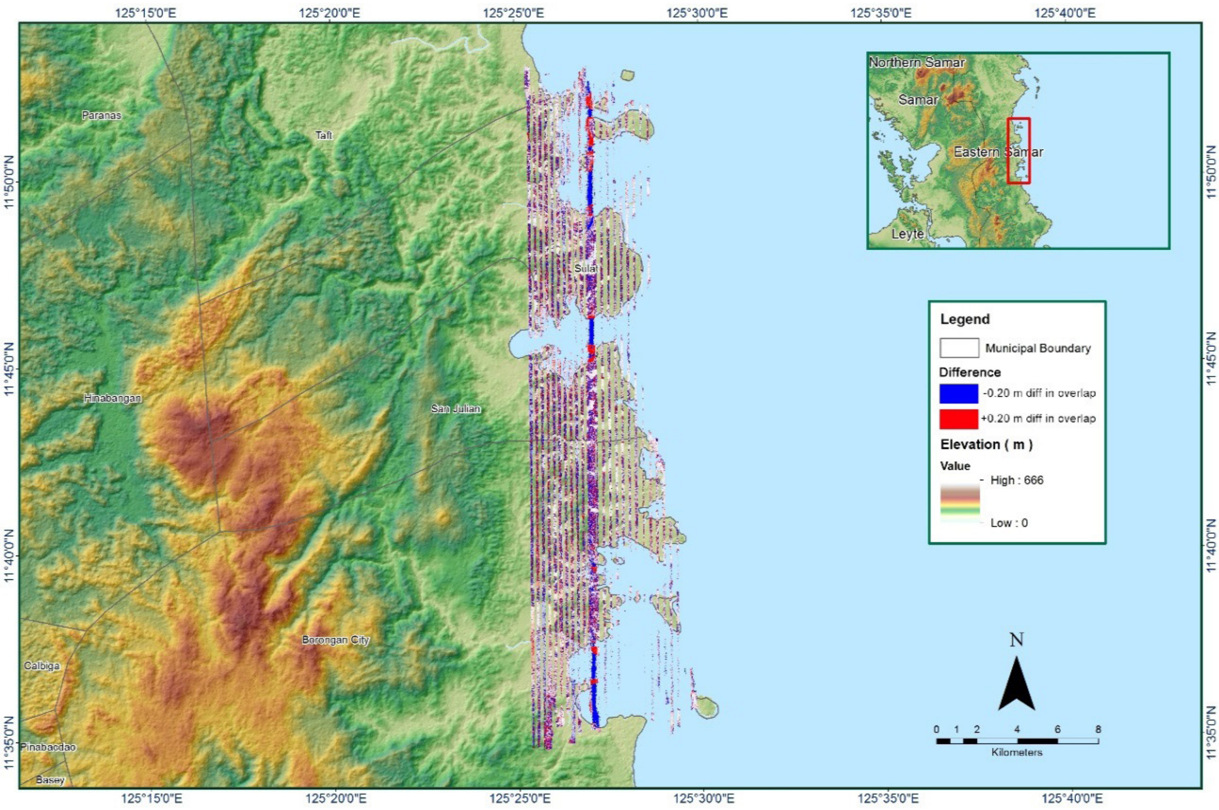

Figure A-8.7 Elevation difference between flight lines

ANNEX 9. Sulat Model Basin Parameters

Table A-9.1 Sulat Model Basin Parameters

Basin Number	SCS Curve Number Loss			Clark Unit Hydrograph Transform		Recession Baseflow				
	Initial Abstraction (mm)	Curve Number	Impervious (%)	Time of Concentration (HR)	Storage Coefficient (HR)	Initial Type	Initial Discharge (cms)	Recession Constant	Threshold Type	Ratio to Peak
W100	0.0016135	99	0	7.024965	0.07241	Discharge	7.80984	0.7	Ratio to Peak	0.3
W110	0.0057635	99	0	15.8745	0.163628	Discharge	12.8376	0.7	Ratio to Peak	0.3
W120	0.006752	99	0	4.649015	0.047918	Discharge	3.47805	0.7	Ratio to Peak	0.3
W130	0.001434	99	0	11.7553	0.12117	Discharge	9.0306	0.7	Ratio to Peak	0.3
W140	0.001752	99	0	7.615865	0.0785	Discharge	8.02008	0.7	Ratio to Peak	0.3
W150	0.009919	99	0	12.6293	0.130174	Discharge	9.9819	0.7	Ratio to Peak	0.3
W160	0.0080782	99	0	15.01285	0.154742	Discharge	12.8844	0.7	Ratio to Peak	0.3
W170	0.001017	99	0	5.5784	0.0575	Discharge	5.6376	0.7	Ratio to Peak	0.3
W180	0.0018285	99	0	7.328015	0.075532	Discharge	9.5202	0.7	Ratio to Peak	0.3

ANNEX 10. Sulat Model Reach Parameters

Table A-10.1 Sulat Model Reach Parameters

Reach Number	Muskingum Cunge Channel Routing						
	Time Step Method	Length (m)	Slope	Manning's n	Shape	Width	Side Slope
R10	Automatic Fixed Interval	2561.1	0.0200445	0.04	Trapezoid	15.706	1
R20	Automatic Fixed Interval	4601.7	0.01	0.04	Trapezoid	25.252	1
R30	Automatic Fixed Interval	6846.2	0.0146860	0.04	Trapezoid	18.758	1
R70	Automatic Fixed Interval	5896.1	0.0112919	0.04	Trapezoid	19.566	1

ANNEX 11. Sulat Field Validation Points

Table A-11.1 Sulat Field Validation Points

Point Number	Validation Coordinates		Model Var (m)	Validation Points (m)	Error (m)	Event/Date	Rain Return/ Scenario
	Lat	Long					
1	11.84077	125.4378	0.058	0.4	0.34	Ruby/December 6, 2014	5-year
2	11.84077	125.4378	0.058	1.04	0.98	Low Pressure/January 10, 2017	2-year
3	11.84027	125.438	0.058	0.5	0.44	Ruby/December 6, 2014	5-year
4	11.83982	125.4379	0.031	1	0.97	Ruby/December 6, 2014	5-year
5	11.83969	125.4371	0.03	1	0.97	Ruby/December 6, 2014	5-year
6	11.83922	125.4379	0.03	0.5	0.47	Ruby/December 6, 2014	5-year
7	11.83922	125.4379	0.03	0.7	0.67	Low Pressure/January 10, 2017	2-year
8	11.83862	125.4374	0.319	0.5	0.18		
9	11.83808	125.4372	0.448	0.5	0.05	Yolanda/November 8, 2013	5-year
10	11.83808	125.4372	0.448	0.3	-0.15	Ruby/December 6, 2014	5-year
11	11.83808	125.4372	0.448	0.3	-0.15	Low Pressure/January 10, 2017	2-year
12	11.83785	125.4373	0.031	0.5	0.47		
13	11.83753	125.4369	0.433	0.6	0.17	Yolanda/November 8, 2013	5-year
14	11.83753	125.4369	0.433	0.3	-0.13	Ruby/December 6, 2014	5-year
15	11.83753	125.4369	0.433	0.3	-0.13	Low Pressure/January 10, 2017	2-year
16	11.83794	125.4367	0.056	0.5	0.44		
17	11.83709	125.4368	0.391	0	-0.39		
18	11.83704	125.4365	0.138	0	-0.14		
19	11.83667	125.4366	0.49	0	-0.49		
20	11.83645	125.4367	0.03	0	-0.03		
21	11.83619	125.4366	0.03	0	-0.03		
22	11.83575	125.4367	0.032	0	-0.03		
23	11.83521	125.4359	0.059	0	-0.06		
24	11.83503	125.436	0.361	0	-0.36		
25	11.83495	125.4363	0.176	0	-0.18		
26	11.8345	125.4364	0.073	0	-0.07		
27	11.83448	125.436	0.03	0	-0.03		
28	11.83445	125.4355	0.132	0	-0.13		
29	11.83458	125.4346	0.068	0	-0.07		
30	11.83406	125.4361	0.079	0	-0.08		
31	11.83389	125.4358	0.03	0	-0.03		
32	11.8335	125.4357	0.03	0	-0.03		

Point Number	Validation Coordinates		Model Var (m)	Validation Points (m)	Error (m)	Event/Date	Rain Return/ Scenario
	Lat	Long					
33	11.83321	125.4356	0.03	0	-0.03		
34	11.83227	125.4352	0.03	0	-0.03		
35	11.83118	125.4346	0.03	0.5	0.47		
36	11.83095	125.4345	0.03	0.5	0.47		
37	11.83027	125.4343	0.031	0.5	0.47		
38	11.83006	125.4342	0.03	0.5	0.47		
39	11.82946	125.4339	0.316	0.5	0.18		
40	11.82897	125.4339	0.264	0	-0.26		
41	11.82571	125.435	0.032	0	-0.03		
42	11.82409	125.4357	0.03	0	-0.03		
43	11.82196	125.4353	0.74	0	-0.74		
44	11.82144	125.4356	0.03	0	-0.03		
45	11.8216	125.4361	0.03	0	-0.03		
46	11.82099	125.4359	0.559	0	-0.56		
47	11.82003	125.4371	0.031	0	-0.03		
48	11.81971	125.4372	0.09	0	-0.09		
49	11.81936	125.4381	0.129	0.3	0.17		
50	11.81956	125.4389	0.73	0.3	-0.43		
51	11.81944	125.4395	0.03	0.3	0.27		
52	11.81916	125.4402	0.039	0	-0.04		
53	11.81265	125.4302	0.032	0.3	0.27	Yolanda/November 8, 2013	5-year
54	11.8136	125.4297	0.03	0.3	0.27	Yolanda/November 8, 2013	5-year
55	11.81691	125.4235	0.083	0.4	0.32	Ruby/December 6, 2014	5-year
56	11.81691	125.4235	0.083	0.5	0.42	Low Pressure/January 10, 2017	2-year
57	11.81589	125.4209	1.842	0.4	-1.44	Ruby/December 6, 2014	5-year
58	11.81589	125.4209	1.842	0.5	-1.34	Low Pressure/January 10, 2017	2-year
59	11.81631	125.4207	2.403	0	-2.4		
60	11.82033	125.42	2.545	0.4	-2.15	Ruby/December 6, 2014	5-year
61	11.82033	125.42	2.545	0.5	-2.05	Low Pressure/January 10, 2017	2-year
62	11.82324	125.4277	0.03	0	-0.03		
63	11.82401	125.4347	0.887	0	-0.89		
64	11.82336	125.4219	0.603	0	-0.6		
65	11.82265	125.4228	0.876	0	-0.88		
66	11.82338	125.4209	1.274	0	-1.27		
67	11.82414	125.4223	0.031	0	-0.03		
68	11.83374	125.4345	0.067	0	-0.07		

Point Number	Validation Coordinates		Model Var (m)	Validation Points (m)	Error (m)	Event/Date	Rain Return/ Scenario
	Lat	Long					
69	11.81614	125.4199	0.335	0.4	0.06	Ruby/December 6, 2014	5-year
70	11.81614	125.4199	0.335	0.4	0.06	Low Pressure/January 10, 2017	2-year
71	11.82844	125.4328	1.077	0	-1.08		
72	11.82916	125.4334	0.996	0	-1		
73	11.8344	125.4325	0.233	0	-0.23		
74	11.83623	125.4362	0.246	0	-0.25		
75	11.83725	125.4365	0.137	0	-0.14		
76	11.83823	125.4371	0.198	0	-0.2		
77	11.84034	125.4374	0.031	1	0.97	Ruby/December 6, 2014	5-year
78	11.84096	125.4381	0.233	0.7	0.47	Yolanda/November 8, 2013	5-year
79	11.84096	125.4381	0.233	0.6	0.37	Ruby/December 6, 2014	5-year
80	11.81709	125.4229	0.03	0	-0.03		
81	11.81954	125.4368	0.121	0	-0.12		
82	11.8192	125.4377	0.031	0	-0.03		
83	11.82111	125.4365	1.188	0	-1.19		
84	11.82151	125.4352	0.34	0	-0.34		
85	11.82268	125.4359	0.031	0	-0.03		
86	11.8275	125.4338	0.03	0	-0.03		
87	11.83173	125.4349	0.418	0	-0.42		
88	11.83395	125.4351	0.03	0	-0.03		
89	11.83473	125.435	0.314	0	-0.31		
90	11.83318	125.4361	0.031	0	-0.03		
91	11.83484	125.4367	0.05	0	-0.05		
92	11.83666	125.4369	0.122	0	-0.12		
93	11.83445	125.4349	0.095	0	-0.09		
94	11.83329	125.4351	0.965	0	-0.96		
95	11.8359	125.4364	0.03	0	-0.03		
96	11.82345	125.4214	0.963	0	-0.96		
97	11.82372	125.4226	0.103	0	-0.1		
98	11.83363	125.4353	0.589	0	-0.59		
99	11.83432	125.4358	0.036	0	-0.04		
100	11.82836	125.4344	0.134	0	-0.13		
101	11.83751	125.4372	0.031	0	-0.03		
102	11.83821	125.4369	0.031	0.6	0.57		5-year
103	11.83821	125.4369	0.031	0.3	0.27		5-year
104	11.83821	125.4369	0.031	0.3	0.27		2-year
105	11.83652	125.4364	0.361	0	-0.36		

Point Number	Validation Coordinates		Model Var (m)	Validation Points (m)	Error (m)	Event/Date	Rain Return/ Scenario
	Lat	Long					
106	11.83421	125.4345	0.218	0	-0.22		
107	11.83497	125.4347	0.03	0	-0.03		
108	11.83297	125.4354	0.349	0	-0.35		
109	11.8297	125.4346	0.14	0	-0.14		
110	11.82259	125.4262	0.03	0	-0.03		
111	11.82107	125.4355	0.571	0	-0.57		
112	11.83625	125.4368	0.03	0	-0.03		
113	11.83781	125.437	0.319	0.5	0.18		
114	11.84149	125.4379	0.03	0.8	0.77	Yolanda/November 8, 2013	5-year
115	11.84149	125.4379	0.03	0.5	0.47	Ruby/December 6, 2014	5-year
116	11.84177	125.4381	0.03	0.9	0.87	Yolanda/November 8, 2013	5-year
117	11.84177	125.4381	0.03	0.5	0.47	Ruby/December 6, 2014	5-year
118	11.83938	125.4375	0.032	0	-0.03		
119	11.81792	125.4199	2.345	0.4	-1.95	Ruby/December 6, 2014	5-year
120	11.81792	125.4199	2.345	1.04	-1.31	Low Pressure/January 10, 2017	2-year
121	11.8196	125.4386	1.177	0.3	-0.88		
122	11.82383	125.4222	0.052	0	-0.05		
123	11.8143	125.4528	Not Covered On Map	0.1		Ruby/December 6, 2014	5-year
124	11.81419	125.4524	Not Covered On Map	0.1		Ruby/December 6, 2014	5-year
125	11.81382	125.4523	Not Covered On Map	0.1		Ruby/December 6, 2014	5-year
126	11.81382	125.4523	Not Covered On Map	0.1		Yolanda/November 8, 2013	5-year
127	11.81582	125.4542	Not Covered On Map	0.2		Yolanda/November 8, 2013	5-year
128	11.8169	125.4459	Not Covered On Map	0			
129	11.81801	125.4436	Not Covered On Map	0			
130	11.81754	125.4439	Not Covered On Map	0			

Point Number	Validation Coordinates		Model Var (m)	Validation Points (m)	Error (m)	Event/Date	Rain Return/ Scenario
	Lat	Long					
131	11.81683	125.4425	Not Covered On Map	0			
132	11.81951	125.4399	0.043	0	-0.04		
133	11.81916	125.4397	0.031	0	-0.03		
134	11.82041	125.4372	0.03	0	-0.03		
135	11.82244	125.4353	1.079	0	-1.08		
136	11.83453	125.4354	0.309	0	-0.31		
137	11.83608	125.4365	0.172	0	-0.17		
138	11.83696	125.4366	0.297	0	-0.3		
139	11.83765	125.4367	0.16	0.5	0.34		
140	11.82344	125.4216	0.745	0	-0.75		
141	11.83374	125.4356	0.327	0	-0.33		
142	11.8344	125.4352	0.52	0	-0.52		
143	11.83433	125.4364	0.03	0	-0.03		
144	11.8384	125.4374	0.03	0.6	0.57	Yolanda/November 8, 2013	5-year
145	11.8384	125.4374	0.03	0.3	0.27	Ruby/December 6, 2014	5-year
146	11.8384	125.4374	0.03	0.3	0.27	Low Pressure/January 10, 2017	2-year
147	11.83981	125.4382	0.045	1	0.95	Ruby/December 6, 2014	5-year
148	11.81843	125.42	1.925	0.4	-1.52	Ruby/December 6, 2014	5-year
149	11.81843	125.42	1.925	0.5	-1.42	Yolanda/November 8, 2013	5-year
150	11.81843	125.42	1.925	0.6	-1.32	Low Pressure/January 10, 2017	2-year
151	11.81633	125.4209	2.984	0.4	-2.58	Ruby/December 6, 2014	5-year
152	11.81633	125.4209	2.984	0.4	-2.58	Low Pressure/January 10, 2017	2-year
153	11.82369	125.4211	0.786	0	-0.79		
154	11.82312	125.4221	0.792	0	-0.79		
155	11.82389	125.4225	0.105	0	-0.1		
156	11.83368	125.4361	0.105	0	-0.1		
157	11.83321	125.4358	0.03	0	-0.03		
158	11.83452	125.4351	0.238	0	-0.24		
159	11.83685	125.4369	0.103	0.3	0.2	Ruby/December 6, 2014	5-year
160	11.83685	125.4369	0.103	0.4	0.3	Yolanda/November 8, 2013	5-year
161	11.83148	125.4346	1.401	0	-1.4		
162	11.82354	125.4219	0.535	0	-0.54		
163	11.83417	125.436	0.03	0	-0.03		
164	11.83414	125.4363	0.03	0	-0.03		

Point Number	Validation Coordinates		Model Var (m)	Validation Points (m)	Error (m)	Event/Date	Rain Return/ Scenario
	Lat	Long					
165	11.83511	125.4362	0.399	0	-0.4		
166	11.84009	125.4376	0.041	1	0.96	Ruby/December 6, 2014	5-year
167	11.83431	125.4333	0.032	0	-0.03		
168	11.83868	125.4378	0.03	0.5	0.47		
169	11.8353	125.4366	0.03	0	-0.03		
170	11.81317	125.4298	0.037	0.3	0.26	Yolanda/November 8, 2013	5-year
171	11.82361	125.4208	1.023	0	-1.02		
172	11.84048	125.4379	0.087	1	0.91	Ruby/December 6, 2014	5-year
173	11.83718	125.437	0.03	0	-0.03		
174	11.8117	125.4518	Not Covered On Map	0			
175	11.81028	125.4506	Not Covered On Map	0			
176	11.81124	125.4508	Not Covered On Map	0			
177	11.83392	125.4363	0.069	0	-0.07		
178	11.82146	125.4359	1.168	0	-1.17		
179	11.83349	125.4355	0.628	0	-0.63		
180	11.83484	125.4364	0.03	0	-0.03		
181	11.83467	125.4353	0.563	0	-0.56		
182	11.83063	125.4344	0.122	0.3	0.18	Yolanda/November 8, 2013	5-year
183	11.8217	125.4355	0.604	0	-0.6		
184	11.81955	125.4374	0.115	0	-0.12		
185	11.81751	125.4449	Not Covered On Map	0			
186	11.81644	125.4465	Not Covered On Map	0			
187	11.82359	125.4362	0.159	0	-0.16		
188	11.83367	125.4358	0.03	0	-0.03		
189	11.83957	125.438	0.048	1	0.95	Ruby/December 6, 2014	5-year
190	11.81944	125.4376	0.054	0	-0.05		
191	11.83909	125.4376	0.371	0.5	0.13		
192	11.83594	125.4367	0.032	0	-0.03		
193	11.83388	125.4362	0.03	0	-0.03		
194	11.81975	125.4369	0.14	0	-0.14		
195	11.81949	125.4392	0.03	0.3	0.27		

ANNEX 12. Educational Institutions affected by flooding in Sulat Flood Plain

Table A-12.1 Educational Institutions in Sulat, Eastern Samar affected by flooding in Sulat Flood Plain

EASTERN SAMAR				
SULAT				
Building Name	Barangay	Rainfall Scenario		
		5-year	25-year	100-year
Hamorawon Day Care Center	San Juan	Medium	Medium	High
Hamorawon Elementary School	San Juan	Medium	Medium	High
Sto. Niño Elementary School	Santo Niño			
Sto. Niño National High School	Santo Niño			

ANNEX 13. Medical Institutions affected by flooding in Sulat Flood Plain

Table A-13.1 Medical Institutions in Sulat, Eastern Samar affected by flooding in Sulat Flood Plain

EASTERN SAMAR				
SULAT				
Building Name	Barangay	Rainfall Scenario		
		5-year	25-year	100-year
Sto. Niño Health Center	Santo Niño	Medium	Medium	Medium

HAZARD MAPPING OF THE PHILIPPINES USING LIDAR (PHIL-LIDAR 1)

LIDAR SURVEYS AND FLOOD MAPPING OF SULAT RIVER

UP Training Center for Applied Geodesy and Photogrammetry (TCAGP)
College of Engineering
University of the Philippines – Diliman
Quezon City
1101 PHILIPPINES